

Estimation of Illuminance for Automated Monitoring of Indoor Space using Wireless Sensor Network

Thesis submitted by

ARIJIT GHOSH

Doctor of Philosophy (Engineering)

Department of Electrical Engineering
Faculty Council of Engineering & Technology
Jadavpur University
Kolkata, India

2023

Estimation of Illuminance for Automated Monitoring of Indoor Space using Wireless Sensor Network

Thesis submitted by

ARIJIT GHOSH

Doctor of Philosophy (Engineering)

Under the supervision of

Dr. Palash Kumar Kundu
Professor

Department of Electrical Engineering
Faculty Council of Engineering & Technology
Jadavpur University
Kolkata, India

&

Dr. Gautam Sarkar
Professor

Department of Electrical Engineering
Faculty Council of Engineering & Technology
Jadavpur University
Kolkata, India

2023

1. Title of the thesis:

Estimation of Illuminance for Automated Monitoring of Indoor Space using Wireless Sensor Network

2. Name, Designation & Institution of the Supervisors:

Dr. Palash Kumar Kundu, Professor, Electrical Engineering Department, Jadavpur University

Dr. Gautam Sarkar, Professor, Electrical Engineering Department, Jadavpur University

3. List of Publications:

Journal Publications:

[1] A. Ghosh, P. K. Kundu, and G. Sarkar, "Design and real-time implementation of cloud based indoor illumination monitoring system," *Journal of The Institution of Engineers (India): Series B*, vol. 101, no. 3, pp. 223-227, 2020.

[2] A. Ghosh, P. K. Kundu, and G. Sarkar, "Internet of human centric lighting: a brief overview on Indian aspects," *Science and Culture Journal*, vol. 86(11-12):350-356, Nov-Dec, 2020, pp. 350-356.

[3] A. Ghosh, P. Satvaya, P. K. Kundu, and G. Sarkar, "Machine Learning Based Illuminance Estimation from RGB Sensor in a Wireless Network," *Wireless Personal Communications-Springer* (2022), <https://doi.org/10.1007/s11277-022-09639-5>.

[4] A. Ghosh, P. Satvaya, P. K. Kundu, and G. Sarkar, "Calibration of RGB Sensor for Estimation of Real-Time Correlated Colour Temperature using Machine Learning Regression Techniques," *Optik-Elsevier* (2022), <https://doi.org/10.1016/j.ijleo.2022.168954>.

[5] A. Ghosh, P. K. Kundu, and G. Sarkar, "Similarity Detection of Illuminance Images using Eigenface Method," *Journal of The Institution of Engineers (India): Series B-Springer* (2022), <https://doi.org/10.1007/s40031-022-00750-6>.

[6] A. Ghosh, P. K. Kundu, and G. Sarkar, "Object Detection Using Computer Vision Methods on Real-Time Lux Sensor Data," *Journal of The Institution of Engineers (India): Series B-Springer* (2022), <https://doi.org/10.1007/s40031-022-00756-0>.

[7] A. Ghosh, P. K. Kundu, and G. Sarkar, "Impact of Light on Human Health - A Brief Review," *Science and Culture Journal*, vol. 88(5-6):160-167, May-June, 2022, pp. 160-167, https://doi.org/10.36094/sc.v88.2022.Impact_of_Light_on_Human_Health.Ghosh.

Conference Publications:

[8] A. Ghosh, P. K. Kundu, and G. Sarkar, "Automated lux measurement for lighting design in indoor space using mobile sensor," *Proceedings of IEEE International Conference on Applied Signal Processing (ASPCON-2018)*, pp. 106–109, 2018, India.

[9] A. Ghosh, P. K. Kundu, and G. Sarkar, "Computer Vision based Obstacle Identification using Real-Time Illumination Sensor Data," *Proceedings of 2nd IEEE International Conference on Control, Measurement and Instrumentation (CMI-2021)*, pp. 190–195, 2021, India.

[10] A. Ghosh, P. K. Kundu, and G. Sarkar, "Classification of Illuminance Images using Eigenface Technique," *Proceedings of Springer International Conference on Industrial Instrumentation and Control (ICI2C-2021)*, pp. 77-85, 2021, India.

4. List of Patents: Nil

5. List of Presentations in National/International/Conferences/Workshops:

[1] A. Ghosh, P. K. Kundu, and G. Sarkar, "Automated lux measurement for lighting design in indoor space using mobile sensor," *Proceedings of IEEE International Conference on Applied Signal Processing (ASPCON-2018)*, pp. 106–109, 2018, India.

[2] A. Ghosh, P. K. Kundu, and G. Sarkar, "Computer Vision based Obstacle Identification using Real-Time Illumination Sensor Data," *Proceedings of 2nd IEEE International Conference on Control, Measurement and Instrumentation (CMI-2021)*, pp. 190–195, 2021, India.

[3] A. Ghosh, P. K. Kundu, and G. Sarkar, "Classification of Illuminance Images using Eigenface Technique," *Proceedings of Springer International Conference on Industrial Instrumentation and Control (ICI2C-2021)*, pp. 77-85, 2021, India.

“Statement of Originality”

I Arijit Ghosh registered on 28.05.2019 do hereby declare that this thesis entitled “Estimation of Illuminance for Automated Monitoring of Indoor Space using Wireless Sensor Network” contains literature survey and original research work done by the undersigned candidate as part of Doctoral studies.

All information in this thesis have been obtained and presented in accordance with existing academic rules and ethical conduct. I declare that, as required by these rules and conduct, I have fully cited and referred all materials and results that are not original to this work.

I also declare that I have checked this thesis as per the “Policy on Anti Plagiarism, Jadavpur University, 2019”, and the level of similarity as checked by iThenticate software is 6%.

Signature of Candidate: *Arijit Ghosh*.

Date: *22.03.2023*.

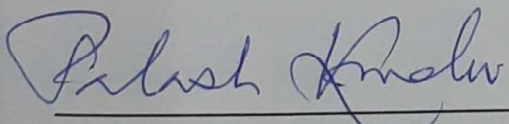
Certified by Supervisor(s):

- Prakash Kishor*
Professor
Electrical Engineering Department
JADAVPUR UNIVERSITY
Kolkata - 700 032
- Gautam Sarkar*

Prof. Gautam Sarkar
Electrical Engineering Department
Jadavpur University
Kolkata, INDIA

CERTIFICATE FROM THE SUPERVISORS

This is to certify that the thesis entitled "Estimation of Illuminance for Automated Monitoring of Indoor Space using Wireless Sensor Network", submitted by Shri Arijit Ghosh, who got his name registered on 28.05.2019 for the award of Ph.D. (Engg.) degree of Jadavpur University is absolutely based upon his own work under the supervision of Dr. Palash Kumar Kundu and Dr. Gautam Sarkar and that neither his thesis nor any part of the thesis has been submitted for any degree/diploma or any other academic award anywhere before.



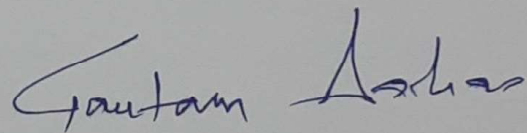
Dr. Palash Kumar Kundu

Professor

Dept. of Electrical Engineering
Faculty Council of Engineering
and Technology
Jadavpur University
Kolkata, India

Professor

Electrical Engineering Department
JADAVPUR UNIVERSITY
Kolkata - 700 032



Dr. Gautam Sarkar

Professor

Dept. of Electrical Engineering
Faculty Council of Engineering
and Technology
Jadavpur University
Kolkata, India

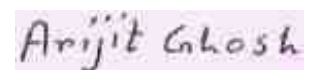
Prof. Gautam Sarkar
Electrical Engineering Department
Jadavpur University
Kolkata, INDIA

ACKNOWLEDGEMENT

I would like to express my most sincere gratitude to my research supervisors, Dr. Palash Kumar Kundu, Professor, Dept. of Electrical Engineering, Jadavpur University and Dr. Gautam Sarkar, Professor, Dept. of Electrical Engineering, Jadavpur University for providing me with the opportunity to carry out this research study under their kind supervision. I am grateful to them for their vision, patience, immense knowledge and relentless motivation that have continued to inspire me. Their persistent guidance and mentorship have assisted me even while preparing this thesis. I would also like to extend my heartfelt thanks to them for their fellow feeling and empathy during the crisis time; and most importantly, the faith with which they have entrusted me with the research opportunity throughout the tenure. It was really a great privilege and honour to carry out this research work under their blessed guidance.

I am grateful to the Head of the Department of Electrical Engineering, Jadavpur University for providing all the possible facilities towards this work. I would also like to thank the rest of the faculty members and the research advisory committee members for their insightful comments and encouragement, as well as for the relevant questions that have compelled me to widen my research perspectives.

Finally, and most importantly, I am extremely indebted to my parents, for their love, prayers and sacrifices that have all helped to carry out this study; especially the inspiration from my father has been enormous. My mother has given her unequivocal support throughout, as always, for which my mere expression of thanks likewise does not suffice. I am most thankful to my wife for her patience, admiration, and continuous support. I am also thankful to my little son for his nice understanding and my in-laws, other family members, friends and colleagues for their inspiration and encouragement in this endeavour.



Arijit Ghosh
(Index No. 86/19/E)
Jadavpur University
2023

Dedicated

To

My Family

Table of Contents

Abstract

List of Figures and Tables

List of Symbols and Acronyms

Chapter	Title	Page No.
1	General Introduction	1-12
	1.1 Introduction	1
	1.1.1 Photoreceptors of Human Eye	2
	1.2 Research Background	5
	1.3 Problem Identification	6
	1.4 Novelty of Work	8
	1.5 Scope of Work	9
	1.6 Organization of Thesis	11
	Chapter Summary	12
2	Basics of Lighting Technology	13-28
	2.1 Introduction	13
	2.2 Categories of Lighting	14
	2.2.1 Natural Light Sources	14
	2.2.2 Artificial Light Sources	15
	2.3 Artificial Lighting Technology	15
	2.3.1 Incandescent Lamps	16
	2.3.2 Compact Fluorescent Lamps (CFL)	17
	2.3.3 Fluorescent Lamps	17
	2.3.4 Halogen Lamps	17
	2.3.5 High Intensity Discharge (HID) Lamps	18
	2.3.6 Light Emitting Diode (LED) Lamps	18
	2.4 Physiological Effects of Light	19
	2.4.1 Visual Impacts of Lighting	19
	2.4.1.1 Visual performance	20
	2.4.2 Biological Impacts of Lighting	21
	2.4.2.1 Light and Body Rhythms	21

Chapter	Title	Page No.
	2.4.3 Radiant Energy Absorption Effect	21
	2.4.3.1 Photochemistry	22
	2.4.3.2 Photobiology	22
	2.5 Psychological Effects of Light	22
	2.6 Human Centric Lighting (HCL)	23
	2.6.1 Lighting for Mankind: HCL	24
	2.6.2 Applications of HCL in Indian aspects	25
	2.7 Purpose of Illuminance Monitoring	27
	2.8 Limitation of Existing Illuminance Measurement Methods	27
	Chapter Summary	28
3	Estimation of Sensor Data using Computational Intelligence Techniques	29-64
	3.1 Introduction	29
	3.2 Objective of this Study	31
	3.3 Related Works	32
	3.4 Overview of Regression Analysis	35
	3.4.1 Polynomial Regression (PR)	35
	3.4.2 Support Vector Machine Regression (SVMR)	37
	3.4.3 General Regression Neural Network (GRNN)	38
	3.4.4 Gaussian Process Regression (GPR)	40
	3.4.5 Performance criteria	41
	3.5 Experimental Set-Up for Estimation of Illuminance from Lux Sensor Data	42
	3.5.1 Results and Discussions	46
	3.6 Experimental Set-Up for Estimation of Illuminance and Correlated Colour Temperature from RGB Sensor Data	52
	3.6.1 Results and Discussions	54
	Chapter Summary	64
4	Automated Indoor Illuminance Monitoring System	65-91
	4.1 Introduction	65
	4.2 Objective of this Study	66
	4.3 Related Literatures	66
	4.4 Indoor Illuminance Monitoring System using Lux Sensor	67

Chapter	Title	Page No.
	4.4.1 Experimental Framework	69
	4.4.2 Results and Discussions	71
	4.5 Obstacle Detection using Computer Vision Methods	74
	4.5.1 Proposed Methodology	74
	4.5.2 Results and Discussions	80
	4.6 Indoor Illuminance and Correlated Colour Temperature Monitoring System using RGB Sensor	82
	4.6.1 Experimental Framework	85
	4.6.2 Results and Discussions	86
	Chapter Summary	91
5	Classification of Illuminance Images	92-113
	5.1 Introduction	92
	5.2 Objective of this Study	93
	5.3 Related Works	94
	5.4 Proposed Methodology	96
	5.4.1 Principal Component Analysis (PCA)	96
	5.4.2 Eigenface Method	98
	5.4.2.1 Eigenface Calculation Procedure	98
	5.4.3 Histogram Method	100
	5.4.3.1 Histogram Intersection Method	100
	5.4.3.2 Histogram Distance Method	102
	5.5 Experimental Set-Up	103
	5.5.1 Client-Server System	103
	5.5.2 Transformation to the Image Domain	104
	5.6 Results and Discussions	104
	Chapter Summary	113
6	Conclusion and Future Scope	114-121
	6.1 Conclusion	114
	6.1.1 Social Impacts of Study	117
	6.1.2 Economic Impacts of Study	117
	6.1.3 Environmental Impacts of Study	118
	6.2 Future Prospects of Research Work	118
	Chapter Summary	121
	List of References	122-140

Abstract

The rising demand for improving the quality of life requires for increase in system complexity. Nowadays, the physical objects are connected to a network which can be wired or wireless in nature and can be accessed through the internet and is known as 'Internet of Things'. The objects contain embedded technology by which it can interact with the external environment. The sensor values obtained from the connected objects can be displayed, recorded for future use and may be transmitted to a remote location for similar applications or for any other purpose. A concept named Internet of Human Centric Lighting has been conceived theoretically in this study by which the installed lighting systems can be monitored and administered by smart internet enabled gadgets for stimulating our work efficiency and relaxation at night to reinforce the natural circadian rhythm for a better living environment.

Illuminance and Correlated Colour Temperature (CCT) measurement are salient features to evaluate the quality of lighting in an indoor space. This is required in situations where the daylight is not sufficient enough and compensatory lighting arrangement is to be installed as we spend most of our quality time in the indoors. The real-time acquired data or imported data from a dataset is trained using regression methods to formulate the sensor model. Then, it needs to be validated using the testing dataset to find out the efficacy of those techniques relying on their generalization capability. Regression analysis is done for prediction of sensor values and qualitative as well as quantitative performance evaluation of them is performed with respect to a standard reference meter. A lux sensor was intended to be calibrated using machine learning based regression techniques for estimation of illuminance data in terms of a pre-calibrated lux meter. For acquisition of sensor data, a lux sensor was interfaced with a wireless microcontroller that served as the client unit. At the same elevation, just beside to the sensing platform, a standard lux meter was placed and data from the reference lux meter were also noted. The client unit transmitted the lux information to a server computer in presence of a wireless router. Now, using the captured lux data from both the sensor and from the reference lux meter, machine learning based regression techniques were applied to develop the sensor model and predict the actual lux value. After successful execution of this experiment, the same technique was applied for estimation of both illuminance and CCT values from RGB sensor data with reference to a standard chroma meter. For capturing of data, RGB sensor and wifi enabled microcontroller together functions as the client platform

in an indoor wireless network. A calibrated chroma meter was utilized to sense the illuminance and CCT values for each RGB reading. The client unit transmitted the RGB values to a computer system, which served as server unit under the influence of a wireless router. The captured data have been used to train and validate the system using various types of regression techniques. Conversion of RGB values into lux and CCT data or periodic calibration were not required at the client terminal. Only, the sensed values were transmitted in a wireless network to server computer for conversion into illuminance and CCT values using the formulated regression model. Finally, from the estimated sensor values, corrective measures and preventive actions can be designed such that the parameters never fall below a certain threshold limit. Moreover, the maintenance personnel may become alert about the situation as and when it arrives.

In this research work, we also propose to develop an IoT based illuminance monitoring system which may enable the users to measure lux values at multi-positional indoor space using mobile sensors and store them in a cloud server wireless network. The sensing unit was designed by the integration of a lux sensor for capturing the illuminance values and IR transceiver was used for position detection. The sensors were interfaced with embedded microcontroller having on-chip wifi device and the designed system was placed over a RF controlled car. The car when moved through a selected indoor space, gathered positional lux information at certain time interval and store them on a cloud server using wireless mobile sensor network. These values were used to generate a lux map that was compared with the benchmark data and the result of comparison was considered to be an intelligent information for modification of any faulty illumination system. A similar type of system was also developed by the interfacing of RGB sensor with IR transceiver and this unit was mounted above a RF operated remote car to capture positional RGB data at certain duration. Now, using the formulated model obtained during machine learning based sensor calibration, the RGB information was converted into lux as well as CCT values and the positional lux and CCT data were saved in a cloud server using similar wireless mobile sensor network, as before. These values can further be utilized for development of an intelligent sensor data monitoring platform similar to the previous case-study.

During conduction of our earlier experiments in the selected indoor space, it was observed that the illuminance values declined suddenly and it was presumed to be a concern with the installed lighting system. After inspection by the maintenance section and detailed analysis of the issue, it was detected that the shadow of an object was the reason behind it. Various methods were studied and finally some edge detection techniques were utilized to find a

solution to the persisting problem. A comparative performance analysis has been conducted in this real-time experimental platform to find out the most preferred solution. A lux-map was initially developed along X-Y coordinate locations for the entire selected space from acquired real-time positional lux data. Then, they were converted into images and Canny, Prewitt, Sobel, and LOG type computer vision techniques were applied to detect the possible position and shape of the object at the indoor space.

Furthermore, another study was conducted to classify the illuminance images after acquisition from a lux sensor that was interfaced with wifi-enabled microcontroller. The experimentation set-up was placed over the roof of a remote operated car in a client-server wireless mobile sensor network configuration. The illuminance data thus gathered were converted into images that were analysed using PCA-eigenface technique, histogram based intersection method, and histogram based euclidean distance technique for evaluation of its illuminance class in comparison with the standard lux images. The feature value was detected for both training and testing image to find out the proximity of neighbouring pixels between training and testing images in PCA-eigenface technique. Similarly, histograms are represented as frequency dispersal of pixel intensity values. While the training stage was conducted, image histograms were formed and stored in the database. During the testing stage, histogram of a test image was matched with each training stage histogram either by means of histogram similarity analysis technique that computed their overlapping region or by the help of Euclidean distance between them.

Finally, the social, economic, and environmental aspects of the conducted research work have been described and the study concludes with identification of its future perspectives.

List of Figures

Figure No.	Caption	Page No.
1.1	Types of human vision	3
1.2	Circadian efficiency function $C-\lambda$ curve along visual spectrum	4
2.1	Light Spectrum	16
2.2	Spectral Eye Sensitivity (SES) Curve for Cone Cells and Rod Cells (dotted)	20
3.1	SVMR architecture	37
3.2	GRNN architecture	39
3.3	Block diagram of proposed system using BH-1750	44
3.4	Hardware set-up of experimentation unit using BH-1750	45
3.5	Block diagram of experimentation unit using BH-1750	45
3.6	Real-time picture of standard lux meter	46
3.7	Illumination training dataset for BH-1750	47
3.8	Illumination testing dataset for BH-1750	47
3.9	Illumination dataset with added random noise for BH-1750	48
3.10	Illuminance computation chart of different MLR techniques using BH-1750	50
3.11	PAE chart of different MLR techniques for lux estimation using BH-1750	50
3.12	Block diagram of proposed system using TCS 34725	53
3.13	Real-time picture of experimentation unit using TCS 34725	53
3.14	Block diagram of experimentation unit using TCS 34725	54
3.15	Real-time picture of standard chroma meter	55
3.16	Training Dataset Diagram for TCS 34725	55
3.17	Validation Dataset Diagram for TCS 34725	55
3.18	Sensor Dataset for Illumination Measurement with added random noise for TCS 34725	56
3.19	Sensor Dataset for CCT Measurement with added random noise for TCS 34725	56

Figure No.	Caption	Page No.
3.20	Illuminance computation chart of different MLR techniques using TCS 34725	57
3.21	PAE analysis chart of different MLR techniques for lux estimation using TCS 34725	57
3.22	CCT computation chart of different MLR techniques using TCS 34725	60
3.23	PAE analysis chart of different MLR techniques for CCT estimation using TCS 34725	60
4.1	Online illuminance monitoring system using BH-1750	68
4.2	Block diagram of online illuminance monitoring system using BH-1750	68
4.3	Directional movement of car to measure lux	70
4.4	Remote with circuit connected car using BH-1750	72
4.5	3-D illuminance map for BH-1750	72
4.6	Difference illuminance map with respect to standard illumination map for BH-1750	73
4.7	Ratio map between measured lux to reference lux for BH-1750	73
4.8(a)	Canny type edge detection kernels	75
4.8(b)	Prewitt type edge detection kernels	77
4.8(c)	Sobel type edge detection kernels	78
4.8(d)	LOG type edge detection kernels	79
4.9(a)	Response for Canny type edge detection technique	81
4.9(b)	Response for Prewitt type edge detection technique	81
4.9(c)	Response for Sobel type edge detection technique	81
4.9(d)	Response for LOG type edge detection technique	81
4.10	Online illuminance and CCT monitoring system using TCS 34725	83
4.11	Block diagram of online illuminance and CCT monitoring system using TCS 34725	83
4.12	Remote with circuit connected car	87
4.13	RGB Colour Data with reference to X-Y Coordinate Location	87

Figure No.	Caption	Page No.
4.14	3-D illuminance map for TCS 34725	88
4.15	Difference illumination map with respect to standard illuminance map for TCS 34725	88
4.16	Ratio map between measured lux to reference lux for TCS 34725	89
4.17	3-D CCT map for TCS 34725	89
5.1	Eigenface image recognition technique flowchart	100
5.2	Sensor data acquisition terminal	103
5.3	Experimental unit for data acquisition	103
5.4(a)	Grade-I Training Image No.-I	105
5.4(b)	Grade-I Training Image No.-II	105
5.4(c)	Grade-I Training Image No.-III	105
5.4(d)	Grade-II Training Image No.-I	105
5.4(e)	Grade-II Training Image No.-II	105
5.4(f)	Grade-II Training Image No.-III	105
5.4(g)	Grade-III Training Image No.-I	106
5.4(h)	Grade-III Training Image No.-II	106
5.4(i)	Grade-III Training Image No.-III	106
5.5(a)	Grade-I Testing Image No.-I	106
5.5(b)	Grade-I Testing Image No.-II	106
5.5(c)	Grade-I Testing Image No.-III	106
5.5(d)	Grade-II Testing Image No.-I	106
5.5(e)	Grade-II Testing Image No.-II	106
5.5(f)	Grade-II Testing Image No.-III	106
5.5(g)	Grade-III Testing Image No.-I	106
5.5(h)	Grade-III Testing Image No.-II	106
5.5(i)	Grade-III Testing Image No.-III	106
5.6(a)	Histogram of Grade-I Test Image-I and Training Image-I	108
5.6(b)	Histogram of Grade-I Test Image-I and Training Image-II	108
5.6(c)	Histogram of Grade-I Test Image-I and Training Image-III	108

Figure No.	Caption	Page No.
5.6(d)	Histogram of Grade-I Test Image-II and Training Image-I	108
5.6(e)	Histogram of Grade-I Test Image-II and Training Image-II	108
5.6(f)	Histogram of Grade-I Test Image-II and Training Image-III	108
5.6(g)	Histogram of Grade-I Test Image-III and Training Image-I	108
5.6(h)	Histogram of Grade-I Test Image-III and Training Image-II	108
5.6(i)	Histogram of Grade-I Test Image-III and Training Image-III	108
5.7(a)	Histogram of Grade-II Test Image-I and Training Image-I	109
5.7(b)	Histogram of Grade-II Test Image-I and Training Image-II	109
5.7(c)	Histogram of Grade-II Test Image-I and Training Image-III	109
5.7(d)	Histogram of Grade-II Test Image-II and Training Image-I	109
5.7(e)	Histogram of Grade-II Test Image-II and Training Image-II	109
5.7(f)	Histogram of Grade-II Test Image-II and Training Image-III	109
5.7(g)	Histogram of Grade-II Test Image-III and Training Image-I	109
5.7(h)	Histogram of Grade-II Test Image-III and Training Image-II	109
5.7(i)	Histogram of Grade-II Test Image-III and Training Image-III	109
5.8(a)	Histogram of Grade-III Test Image-I and Training Image-I	110
5.8(b)	Histogram of Grade-III Test Image-I and Training Image-II	110
5.8(c)	Histogram of Grade-III Test Image-I and Training Image-III	110
5.8(d)	Histogram of Grade-III Test Image-II and Training Image-I	110
5.8(e)	Histogram of Grade-III Test Image-II and Training Image-II	110
5.8(f)	Histogram of Grade-III Test Image-II and Training Image-III	110
5.8(g)	Histogram of Grade-III Test Image-III and Training Image-I	110
5.8(h)	Histogram of Grade-III Test Image-III and Training Image-II	110
5.8(i)	Histogram of Grade-III Test Image-III and Training Image-III	110

List of Tables

Table No.	Caption	Page No.
2.1	Features of HCL system	25
3.1	Evaluation of Performance Indices for Illuminance Estimation using BH-1750	51
3.2	Evaluation of Performance Indices for Lux Estimation using TCS 34725	59
3.3	Evaluation of Performance Indices for CCT Estimation using TCS 34725	61
4.1	Quantitative Performance Analysis of different Edge Detection Techniques	81
5.1	Performance Evaluation using PCA-Eigenface Method	107
5.2	Performance Evaluation using Histogram Intersection Method	111
5.3	Performance Evaluation using Histogram Distance Method	112

Chapter 1

General Introduction

1.1 Introduction

Monitoring is the act of observation of system behaviour and simultaneously ensuring that certain properties are maintained. These properties may either be quantitative in nature if the observed behaviour is measurable or it may be qualitative if the observations are in line with the expectations. Thus, proper monitoring gives fruitful insight for better sensing and control of the system of interest. Monitoring can further be segmented into manual monitoring, which requires intervention of human beings while the data is actually acquired. On the other hand, automated monitoring provides us with the flexibility of sensing any parameter without direct manual involvement. If the sensing architecture is established properly, then sensing may be mechanized. After sensing, the information is to be processed for amplification and filtering and only then it may be stored in smaller memory devices or larger memory space for further investigation. Significant developments in the server and network technologies together with increase in the number of connected physical objects and remote devices have enhanced the deployment of intelligent services. These are grouped under a new paradigm concept, popularly known as Internet of Things (IoT). According to a Cisco report in 2008, the number of things connected to the internet exceeded the world population. It was estimated that by 2020, approximately 50 billion devices will be connected over the internet which is almost 8

devices per people with reference to the projected population [1-2]. The reason for development of IoT is very much related to the factors categorically may be mentioned hereinafter: Moore's Law and Koomey's Law. Moore's Law states that the number of transistors used to develop an IC doubles in every two years. This law enables the researchers to develop even more powerful devices without increasing the chip size. Whereas, Koomey's Law suggests that the number of computations per KWh nearly doubles in every 1.5 years. After combining the aforesaid laws, it can be inferred that same amount of computations can be done on a smaller chip with lesser energy consumptions gradually [3]. Kevin Ashton highlighted this as the potential reason for the development of smaller, powerful yet energy efficient devices while addressing a presentation at Proctor and Gamble in 1999. IoT involves 'Things' or popularly known as sensors which are used to sense objects of the physical world, store them, access from there if required and process them to operate the device for which it has been designed from any corner of the world via 'Internet'. The communication between two devices (virtual or physical) may be direct type like Bluetooth or ZigBee; it may also be with or without the help of a gateway like wifi or GSM. Based on the risk-return analysis, IoT may be used in some specific domain for a plethora of applications. So far, only the sensors have been categorized as the 'Things'. Simultaneously, the actuators connected over 'internet' using internet protocol (IP) at the network layer may also be considered as the 'Things'.

1.1.1 Photoreceptors of Human Eye

There are three types of photoreceptor cells in human retina, known as ganglion cells, rod cells and cone cells. Ganglion cells and nerve fibres transmit visual information towards brain for circadian rhythm and pupillary reflex action. Rod cells are abundant in nature and light sensitive than cone cells. Human retina comprises of about 120 million rod cells and 6 million cone cells. Rod cells are sensible for vision at low levels (scotopic vision). But, they are not responsible for colour vision and have low spatial acuity, which is because everything is in grayscale at night. On the other side, cone cells are sensible at high light levels (photopic vision) and are used for colour vision. The light level where both the rod and cone cells are functional is known as mesopic vision. Fig. 1.1 describes all the aforesaid types of vision interms of luminance (cd/m^2).

As most of the information from environment is perceived from our eyes, hence its effect is enormous. Already discussed earlier, there are two parts of retina: cones are responsible

for colour perception and rods are for brightness perception. The visual impression traverses through ganglion cells and optical nerve to emerge at the occipital lobe visual centre.

Circadian rhythm (circa = about, diem/dies = day) refers to the biological processes repeating in our body. Circadian entrainment is the ability to affect our biological clock in forward or reverse direction by endogenous or exogenous processes. The effect of light is influenced by melatonin, which is a photoreceptor in human eye comprising of intrinsically photosensitive retinal ganglion cells (ipRGCs) covering retina like web and is connected with suprachiasmatic nucleus (SCN) directly which acts as the primary clock for circadian rhythms through secretion of melatonin and cortisol hormones [4-9].

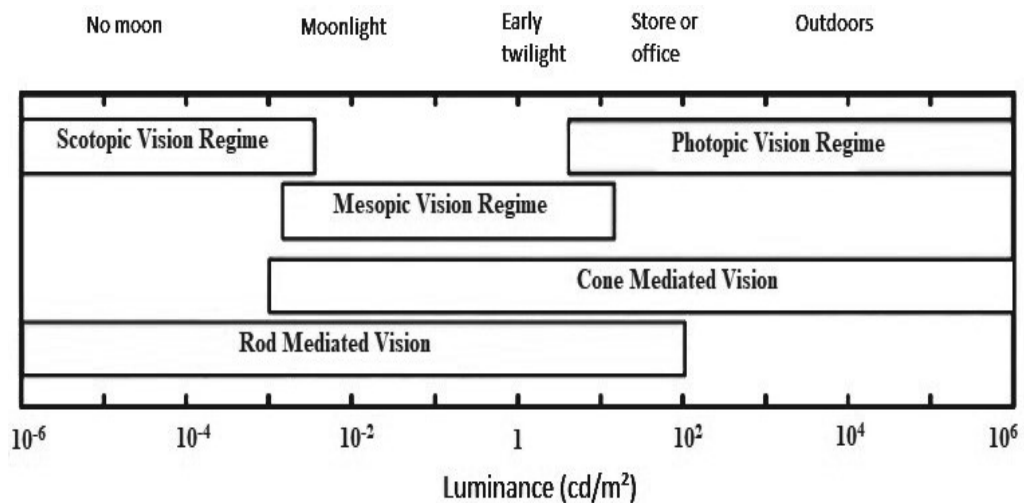


Fig. 1.1 Types of human vision

Melatonin or the sleep hormone is produced from the pineal gland to tell the body when it is night for sleep. Its production may get hampered by the stimulation of high intensity light and it gives rise to the production of activity hormone named cortisol, leading to poor sleep, indigestion, reduced concentration as well as performance. If the disturbance sustains for a large amount of time it may lead to cardiovascular diseases, obesity, diabetes or even cancer. Even though exercise, social gatherings, scheduled diets can reduce the impact but still it cannot nullify the biological clock disruption from occurring. This may further lead towards reduced activity, emotional break down and depression. Length and quality of sleep is equally important as it increases attention level, has direct impact on memory, reduced sleep and performance upgradation [10-14]. The circadian efficiency function $C-\lambda$ curve interms of wavelength along the entire visual spectrum is shown in Fig. 1.2.

The spectral distribution of light varies throughout the day with short wavelength light during the day and large wavelength light at night. In the morning with shorter wavelength, the melatonin production is blocked which helps us to wake-up. If the reversal occurs, then our sleep will be disrupted and throughout the day we may feel sleepy. Apart from the colour, the intensity also has direct effect on the alertness of people. As human beings have evolved from natural light to artificial light sources, the combined impact of the composition and variation in terms of intensity and colour provides the best functioning model for the people under influence of light. It has been observed in some studies that blue light is required in the morning for waking up, increasing concentration during the day and better sleep in the following night, whereas, red light is required in the afternoon to keep people activated without hampering the ability to sleep at night. That is why it is not recommended to use mobile phones at night, as light emitted from mobile screen increases the production of melatonin and disrupts our sleep pattern.

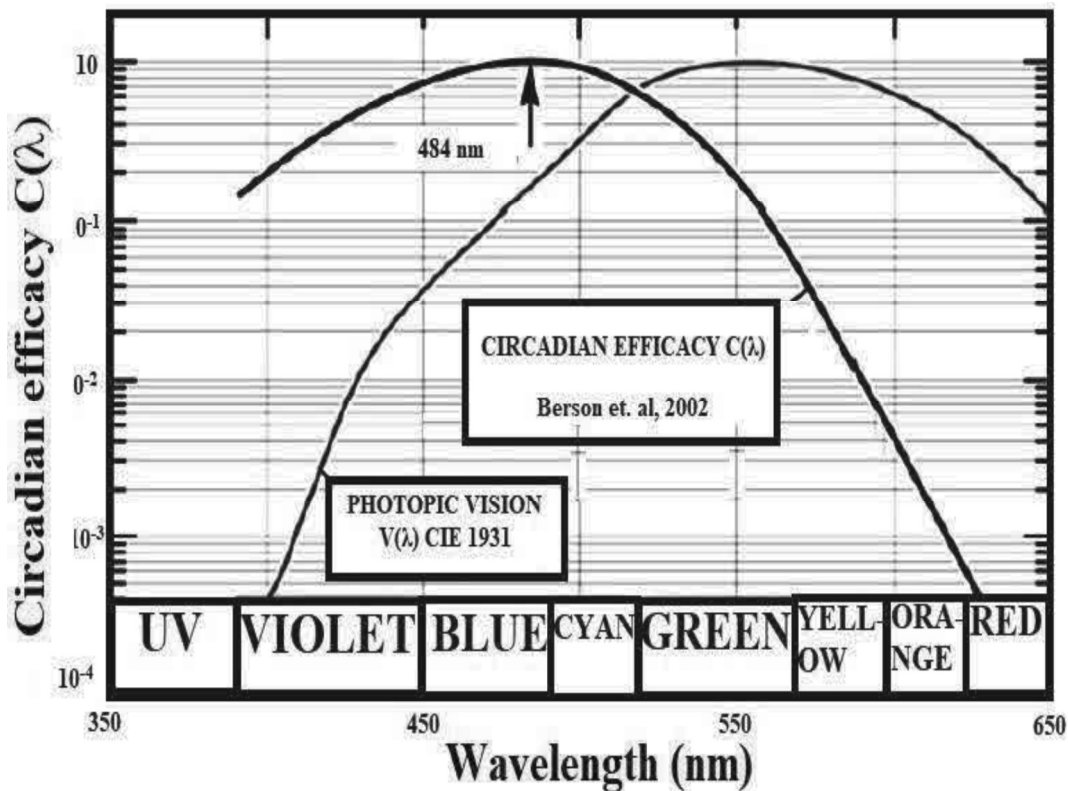


Fig. 1.2 Circadian efficiency function $C-\lambda$ curve along visual spectrum

Moreover, it has been observed in other studies that too much exposure towards blue light in evening increases the risk of depression. Dynamic colour lighting on the other hand

mimics sunlighting pattern using software driven control link for colour and intensity adjustment of artificial light for a healthy life. It leads to visual ergonomics (protect from glare and flickers with proper contrast and reasonable Colour Rendering Index or CRI). Dynamic lighting system is usually developed using modern day LEDs providing low energy consumption, larger lifetime, lesser heat radiation, and wider colour spectrum. Although this type of lighting system suffers from voltage sensitivity i.e. with the voltage change its lifetime reduces considerably. Simultaneously, cost per lumen will also be increased [15].

1.2 Research Background

This section provides some background information about the study. Light has a positive role to play in the visual performance and in the lighting environment. The lighting arrangement should be designed to maximize the amount of sunlight inflow and requires minimal subjection to artificial light such that the physical and mental health of all the concerned are in better condition. Exposure to sunlight has considerable impact on the physical and psychological health of a human being. Artificial lights with appropriate illumination level sometimes have a progressive effect on our stress level and mood. Lights also have a significant role in the secretion of cortisol (stress) and melatonin (sleep) hormone. The cortisol hormone level remains high throughout the day and keeps us active. It minimizes to the lowest value at midnight and prepares us for the next day's activity. But, if the cortisol levels increase beyond a threshold limit, the human body becomes exhausted and inefficient. In contrast, the melatonin hormone remains low during the daytime to reduce drowsiness. It rises at night giving us a sound sleep. It has been observed that dimmed to bright light transformation elevates secretion of cortisol hormone and suppresses melatonin hormone secretion, whereas, bright to dimmed light transformation increases secretion of melatonin hormone and reduces secretion of cortisol hormone. Hence, lighting levels at the workplace and inside our house are to be fixed keeping this in mind.

The impending health risk of illuminating sources is provided by the accessibility of subjection data for public and professional vulnerability due to the stress of emission from different types of lamps [16]. Nowadays, the MH luminaries and even the CFL technology has been replaced by LEDs with minimal operational expenses. If LED technology is used, the electricity consumption is reduced to a large extent, although, the capital

investment may be on the higher side. Although, prolonged UV and IR radiation causes lesions in cornea leading to cataract and even towards retinopathy. It is well known that lighting plays a significant role in our daily activities. As we all spend the major portion of work-time in the indoor space under the influence of artificial lighting, hence, their contributions towards health cannot be written-off. The researchers continue their study of lighting on circadian rhythms and contribution of modern day lighting technology for human life development both in the workplace as well as in our home.

In this study, estimation of illuminance for an automated lux monitoring system suitable to collect sensor values from an indoor space using wireless sensor network is proposed. The proposed system is functionally differentiated from a conventional wireless sensor network system in terms of the fact that here the sensors are not attached over the selected indoor space in a distributed manner, rather, there is an embedded system incorporating of a single sensor connected with a microcontroller in a server-client wireless configuration network. The illumination values (in lux), which is an important parameter for understanding the light level; serve as the variable of interest in this study. Illuminance is defined as the luminous flux received at each unit area by any point on the surface that is subjected to incident light. The sensor data acquisition unit is mounted over a remote car and thus it is made mobile in nature. It does not require making approximations about the possible sensor values amongst the locations where it is not positioned; the mobile sensing unit can approach those locations as well to acquire the sensor data. The designed mobile system is developed with the hardware components readily available at the market, thus making the system easy to build and cost-efficient at the same time. The sensors have been calibrated using machine learning techniques and the proposed system has been successfully applied in several applications.

1.3 Problem Identification

Traditional wireless sensor network systems have the sensors attached in the selected space. Now the sensors can be connected in a wired network as part of the system, however, the capital investments in these systems seem to be on the higher side. The sensors may also be connected in a wireless network and the initial investment in those cases can be a little lesser but the lifetime of these sensor systems are fixed due to the limited tenure of a battery. Moreover, the wireless network establishment cost as well as the maintenance cost makes the project expense sometimes higher than the wired network

set-up cost. In any case, the sensor transmit data at periodic intervals to a local computer and depending upon the transmitted values certain intelligence is required to be applied at times. However, the sensor networks drive the systems connected successfully and can be utilized for detection of any diagnostic system anomalies. Although the sensor systems consume very less amount of power, still the overall energy consumption will ultimately increase if the system is connected permanently. However, it cannot be denied that in the developing nations, people spend majority of their life under the influence of artificial lights, hence, the productivity will enhance if the health and comfort of the workers are intact. The modern day systems should optimize the factor of power consumption with health and comfort. The sensor driven systems should maintain the optimal sensor values within a selected space where human intervention may also be available, as and when required. Unlike larger commercial or industrial spaces, this degree of maintainability is impossible particularly at the smaller personal or commercial space where there is an infrastructural constraint. The sensor systems are not only expensive but also they are inaccessible at times. Also, as the sensors are attached to a particular location in a network, hence, their capability in detecting faults and system performance entirely depends upon the place where they are physically placed. With the increase in number of fixed sensors, the fault detection capability becomes upgraded but with an enhanced capital expenditure as well as operating expenses. Furthermore, it will bring disparity amongst people within the same selected space. Hence, an automated mobile sensor system can mitigate the challenge successfully.

On the other hand, calibration of the required sensor can sometimes become an uphill task. A calibrated reference meter may not be readily available due to its high cost. Therefore, if the sensors can be calibrated prior to its application and if the calibrated sensor model is embedded within the measurement process, then separate calibration may not be required. The application will also become smooth and trustworthy. This method can be helpful for finding the grade of light level within an indoor space from the acquired sensor data directly and simultaneously maintaining a desired level of accuracy. During the data acquisition process, if the mobile sensor system encounters with any static obstacle, it can be found out from the captured sensor values by suitable edge detection techniques within a satisfactory grade of accuracy.

There are available methods to detect the quality of illuminance in a selected space using costly cameras and because of its high price it is not available always for the researchers.

Also, sometimes, the measurement process does not provide the flexibility of capturing an image. In those situations, it will become helpful, if the data is acquired by mobile sensors, followed by conversion of the sensor values into images and finally by suitable image processing algorithms they are used to detect about the level of illuminance within the selected indoor space.

1.4 Novelty of Work

The primary contributions of the thesis are as follow:

- Calibration of a lux sensor to estimate the illumination values with reference to a pre-calibrated lux meter using machine learning regression techniques. Moreover, calibration of a RGB sensor to estimate the illumination and correlated colour temperature values with respect to a standard chroma meter using machine learning regression techniques. Apply the generated sensor model in a measurement process.
- Development of an automated indoor space illumination monitoring system using server-client wireless sensor network. The sensor data acquisition system is placed over the roof of a remote operated car, which is considered as the client unit. While the car traverses through the selected indoor space, it transmits the positional illuminance data from the client unit to the server unit, which is a PC/laptop. From the captured illumination values, find out the presence of a static obstacle using popular edge detection algorithms.
- Detection of similarity level of lux images from a real-time captured illumination dataset using server-client wireless network arrangement. An illuminance sensor is interfaced with a wireless microcontroller, which is considered to be the client terminal. This entire system is kept at the top of a remote car; while traversing through the selected floor space, it acquires lux values of that place, transmit and save them in a computer system, which is considered as the server terminal, where, each data is converted into a grayscale lux image. Now, when a test image arrives, they are compared for resemblance with a training image using PCA-eigenface method and histogram technique by calculating their pixel proximities. Moreover, a comparative performance assessment has also been executed for the selected techniques.

1.5 Scope of Work

The thesis is aimed for estimation of illuminance for an automated lux monitoring of indoor space using the concept of wireless sensor network. The quality of lighting in terms of technological variation is generally described here including their perceptions as obtained from different studies. This observation is subjected to change depending upon the region of data collection with the temperament of the persons in that geographical region. However, this study is not a comparative analysis for finding out the best lighting technology.

First and foremost scope for consideration is to the fact that there should be ample space available for the mobile sensing system to traverse through the entire selected indoor space. Otherwise, the proposed experimental unit cannot move within the designated area and the investigational analysis cannot be executed at all.

The calibration of sensors is largely based on the adopted methodology and also it depend on the number of observations undertaken. Accuracy of the formulated equations or the obtained models are directly correlated with them. Hence, the number of observations are required to be quite large and repeatable under various lighting conditions. In this thesis, the number of observations is although sufficient enough to establish the precision of a model but it cannot claim to be a conclusive one. Depending upon the variations in the lighting technology as well as in the number of observations, there is always a chance of further upgradation. Moreover, the techniques that have been selected are used for similar type of sensor calibration related applications but as per the knowledge available, they have not been used yet for calibration of a lux sensor or a RGB sensor for lighting related applications.

We have studied the performance of different type of sensors available through their datasheets. Finally, in this study, the data within an indoor space were captured using two different type of sensors and it was noticed that they were providing a desirable amount of accuracy. Moreover, they were cost-efficient as well. However, it is upon the decision of the user to finally select the model of a sensor. Using their expertise and priority of selection, the user may select any other model.

The captured illuminance has been segmented into certain types based on the choice of the user. If the numbers of segments are high, more precise illumination grade may be decided upon by the user or by the lighting designer. Moreover, if there is binary gradation with

small variation in illumination values, the acquired readings may not be segmented properly. Anyhow, there is no uniform standard available in the market as per our knowledge to decide upon the segmentation of lighting quality.

There are several parameters that largely correlate with the visual appearance of lighting. Some of them may be identifiable and out of them only a few of them are quantifiable. The quantity and/or quality of the doors, windows, walls and other interior space are quite responsible to create a praiseworthy lighting environment. No attempt was made to find out their contribution in the collected lux values. Here, the individual or combined contribution of all other parameters have not been taken under consideration as the sensor was pre-calibrated prior to its application in a similar lighting environment. Moreover, the calibrated sensor was also applied for acquisition of illuminance values in the selected indoor space. Hence, the contribution of other factors as a whole that can influence the illumination values have been assumed to be included into the system.

The impact of several lighting parameters that supports or stimulates the well-being of human beings relating to their physical or psychological health have only been studied based on the available literatures but is not explained nor included in this thesis. A suitable lighting environment is supportive for any work and contributes in every aspect as we spend a major portion of our daily routine within the indoors in most of the cases. Whereas, if the lighting environment is not suitable for the jobs that we require to execute in the indoors it becomes detrimental to our usual routine. Although, the consideration of the factors affecting the visual, mental or energy dependent parameters have been excluded in this study.

In this thesis, the sensor data are acquired at a suitable sampling rate and the accuracy of the sensor values are largely dependent on it. Moreover, the transmitted sensor data are saved in a particular cloud platform. Although, it cannot be denied that the factors are not conclusive and there may be provision of further refinement if any other factors or any other type of model is selected.

The experiments were conducted under the influence of a wireless router. If the router is not available then mobile hotspot may also serve the purpose. However, if the range is beyond the threshold limit then other sort of mechanisms are required to be formulated.

Hence, it can be concluded that the designed cost-effective system can become an efficient model and can handle the acquisition, processing and classification of illumination sensor data if a certain degree of imprecision may be tolerated.

1.6 Organization of Thesis

This chapter (Chapter-1) deals with the general introduction related to the field of illuminance monitoring. It starts with the photoreceptors of human eye, followed by discussion on the biological impact of light. Then, the background of this research and idea behind formulation of the research problem is discussed. The originality of the thesis as well as the scope of this research is also mentioned separately. The chapter ends with the discussion on the thesis organization.

The remaining chapters are outlined as follows. Chapter 2 gives an overview about the basics of lighting technology. The different types of light sources that are available is discussed in this chapter followed by the various lighting technologies that are available have also been mentioned in a nutshell. Then, the physiological impacts (visual impact, other biological impacts) of lighting are mentioned. The psychological effects of lighting have also been discussed. The concept of human centric lighting along with their probable implications and applications particularly in Indian context has been elaborated thereafter. The chapter ends with discussion on the purpose of illumination monitoring and also refers the limitations of the existing illuminance measurement methods.

Chapter 3 indicates the calibration technique adopted for estimation of illuminance inside the selected indoor space using computational intelligence. In this study, a master-slave based configuration was adopted for acquisition of sensor values. The machine learning based regression techniques applied to this study for calibration of both lux sensor and RGB sensor are well-accepted methods and popularly applied for several applications. However, their usage for calibration in lighting applications is somewhat not found in earlier literatures. If manual calibration was done instead of the adopted methodology, it would appear to be more time-consuming considering the range of the sensors. However, here the sensor data was required to be collected over the entire sensor range only for a limited number of observations and based on the acquired data suitable machine learning based regression techniques were applied to find out a suitable model that can be used to find out the sensor data for any input value.

Chapter 4 describes the method of sensor data acquisition within a selected indoor space by suitable placement of the sensor after interfacing it with a microcontroller in a wireless network. Mobile hotspot system can serve the purpose as well if the network connection is properly available. From the acquired illumination sensor data, presence of an obstacle

can be estimated using edge detection techniques that are popularly used in similar application studies. In this chapter, the sensor data acquisition system has been developed using two different type of sensors. The initial system was developed using an illumination sensor to capture the lux readings directly. On the other hand, the second system was developed using RGB sensor that was also used to compute the illuminance values and transmit to the server system in a client-server wireless communication network.

Chapter 5 discusses on classification of illuminance images depending upon the requirement. If sensor data processing may not give a better understanding on the captured data then segmentation of lux images using PCA-eigenface method, histogram based intersection and histogram based euclidean distance method can help in gradation of the illumination images captured within the room. A comparative performance analysis amongst them has also been executed. Here, the data are primarily acquired and converted into an image. Only after then they are required to be segmented using popular techniques like PCA based eigenface method, image histogram intersection technique, and histogram based euclidean distance method that are used in our case-study. The performance comparison gives an idea about the efficacy of the considered techniques for illuminance image classification related problems.

Finally, Chapter 6 presents the conclusions of conducted study and outlines the orientation towards future research work in this domain.

Chapter Summary:

This chapter depicts a general introduction of the conducted research work. The photoreceptors of human eye and the biological impact of a lighting arrangement have been discussed. It also describes the background information of the study, basis of problem formulation, and originality of the carried out work. Moreover, the chapter is concluded by indicating the scope of this study and organization of the thesis. The next chapter deals with discussion on different categories of light sources. Moreover, the physiological and psychological impacts of light on human health are also explored with mentioning of Human Centric Lighting in the next chapter.

Basics of Lighting Technology

2.1 Introduction

Light is considered to be the nucleus for human beings and it functions as the physical as well as psychological influencer [17-19]. Renowned physicist, J.C. Maxwell, defined light as an electromagnetic wave (visible range from 400 to 780 nm for an adult human eye) passing through space that covers a wide range, from radio waves having higher wavelength with wave shaped behaviour, down to x-rays with very less wavelength wherein the behaviour of electromagnetic radiation is particle shaped. Similar to the electromagnetic radiation, the light waves also impede amongst others; bends slowly while passing through an edge and likely to be directionally polarized. These features permit light to be refined by wavelength or escalated coherently when subjected to a laser beam [20]. In the study of radiometry, the proliferating wave-front of light is modelled since it propagates in the form of tiny wave particle namely, photon. Recent studies demonstrate that there is a correlation between light and its impact on human health. Light not only provides mere visual particulars rather constitutes a dominant modulator of circadian entrainment and various non-visual features including the state of attentiveness and analytical performance [21].

2.2 Categories of Lighting

There are two categories of light, namely, natural light sources and artificial light sources. They have been briefly discussed herein below.

2.2.1 Natural Light Sources

As per the Illuminating Engineering Society (IES), “Day light refers to the art and practice of admitting sunlight beam, diffuse skylight, and reflected light from the exterior into a building to facilitate lighting requirements and energy saving through the use of electric lighting controls” [22]. In comparison with natural light, the artificial sources have no restriction to provide uninterrupted light although the intensity fluctuations are unpredictable. There are two concepts, viz., Correlated Colour Temperature (CCT) and Colour Rendering Index (CRI). A high valued CRI of light source transliterates to an object colour nearer to its natural colour, seen under daylight and having same colour temperature [23]. The sun is capable of generating a wide spectrum of light having ample wavelength (CRI=100) [24] for recognition of almost every colour. Natural light enhances productivity; however, if daylight is unavailable for a larger period of time, it can result into mood swing and even depression. Natural light provides an uninterrupted renewable spectrum with varying brightness levels. If natural light sources are available, then, it can eliminate requirement of electrical energy and decreases the emission of CO₂. These sources of light can be obtained either from an object or from other live species. Amongst the plethora of available natural sources the sun, some stars, lightning, jelly-fish, fire-fly, etc. are noteworthy. Natural light is nothing but a combination of the luminous behaviour of sunlight from direct type solar radiation and also skylight captured from diffuse type solar radiation. Almost upto 20th century, it was the sole source for illuminating a building but due to convenience, it is now replaced by electrical lighting. But, off late, due to energy preservation and environment related concerns, daylighting has emerged to the forefront again. Latest studies have indicated that there is a perfect correlation between the health performance and work efficacy with the lighting conditions. Daylight interacts by the help of our skin during photosynthesis and generates Vitamin D that instigates absorption of calcium and thus our bones get strengthened. There are other visual and non-visual effects of natural light that makes this study worth mentioning.

2.2.2 Artificial Light Sources

The idea of flame oriented lamps introduced first as artificial light at night (ALAN)–time environment gets priority demand matching with the population intensification as well as need of technological demand which extends to electric powered lamps at the grass-root levels for producing artificial lights. This derives from diversity of sources namely, incandescent and luminescence lamps. Luminescence lamps can further be classified into discharge/fluorescence lamps (FL) and solid state lighting devices (SSL) respectively [25-27]. ALAN upsets natural light patterns that take the form of two principles [28]. Primarily, lights are fixed in public places at different urban centers and marine sites with immense demographic diversity [29]. Secondly, ALAN is introduced as light spectrum unlike natural sources e.g., sunlight, moonlight and star-light [28]. Next, comes the era of high intensity discharge light and light emitting diode (LED). Thus, in time, the dominance technology tends to vary in a heterogeneous manner satisfying local conditions. There is a tendency to use white light source. However, coloured LEDs are used in the sense of performing architectural and beautiful spectrums [30].

2.3 Artificial Lighting Technology

Human beings are familiar with natural light source (sun) providing varied intensity and Correlated Colour Temperature (CCT). Eventually, we learnt to make use of fire providing low CCT with reddish glow. Next, we looked for some artificial sources of light as most of our time is spent at indoors where sunlight is sparsely available. Initially, incandescent bulb was discovered which is considered under primitive lighting technology with reddish glow (CCT around 2700K). Then, came fluorescent lamp with blue light similar to the colour composition of the outdoor light. Both of these technologies have their advantages and disadvantages. The latest technology to create light with various character types is Light Emitting Diodes (LEDs) using semiconductor based light source to emit light when activated. When appropriate amount of voltage is applied to its leads, electrons will recombine within device holes to release energy in form of photons. The colour of light emitted by it corresponds to the energy of photon determined by the band gap of semiconductor. The wavelength may vary from red (700 nm approx.) to violet (400 nm). Also, some LED sources can transmit infrared energy (830 nm). It emits light from an area lesser than 1 mm² and in the process increase the risk of glare which is minimized by limiting

the light source luminance or by increasing background luminance surrounding the light source. The entire light spectrum is depicted in Fig. 2.1.

Generally, LEDs use 100% of the electrical energy to produce light in comparison with the incandescent bulbs which convert 80% into heat and 20% into light. With such integration of LED based intelligent systems, spectral distribution and lighting dynamics can be properly adjusted to develop an environment which is stimulated and at the same time relaxing for production yield, as well as healthy well-being.

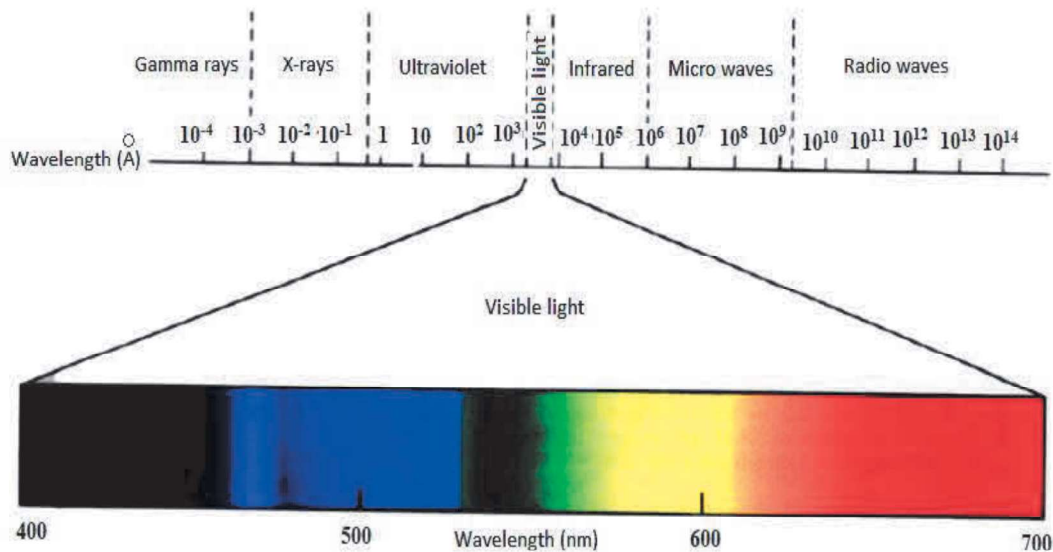


Fig. 2.1 Light Spectrum

2.3.1 Incandescent Lamps

Incandescent light bulbs were conventionally found in most of the households and in companies until recent times but not used now at least in this part of the world. This type of lamp was constructed using a very thin wire and the entire arrangement is sealed within a glass bulb such that it emits light as and when electricity passes through it. The advantage of this type of lamp is that it is cost-efficient, creates soothing warm lighting effect, does not require any additional arrangement to operate and it may also be dimmed by some special procedure, if required. However, the limitation of this type of light source is that it can convert only around five percent of the consumed electricity into light while the remaining part is radiated as heat energy. Although this type of bulb is energy efficient with reference to some of its counterparts but as it is minimally luminous, hence, everyone is driving towards more energy efficient substitutes and that is why they are neither produced nor sold in bulk quantity as done before [31].

2.3.2 Compact Fluorescent Lamps (CFL)

As the incandescent lamps are not energy efficient and hence, not produced or promoted in most of the countries, therefore the manufacturers came up with energy efficient alternates. Amongst them, until recently most popularly used in households and companies to replace the incandescent lamps were CFL. The advantage of this type of lamp is that it lasts for a larger time period and it is energy efficient as well for production of similar amount of light. They were developed by a type of fluorescent lamps with in-built electronic ballast and starting arrangement. These lamps were available with wide variety, correlated colour temperature (CCT), colour rendering index (CRI), and cost. All the types of these lamps are however not dimmable nor they allow for fast switching and as it contains a certain level of mercury, hence, they are replaced by other alternatives but until recently they were very much popular and widely accepted [31].

2.3.3 Fluorescent Lamps

These lamps produce a very large amount of artificial light than most of the other variants and functions similar to the earlier variant, i.e. CFL but the ballast is excluded from the main lamp. The glass made tube is occupied with minimal amount of mercury with gas. The glass conduit is coated with fine phosphor coating and the spout terminals are considered to be as electrodes. If electricity passes between the terminals, the mercury vapour emanates UV radiation. While the radiation passes through the phosphor coating, visible light is emitted with a colour that changes with various phosphor mixes. Thus, they are available with different CRI as well as CCT values. These lamps save a large amount of energy and at the same time they last for a larger period of time. Moreover, the brightness of these lamps is controllable [31].

2.3.4 Halogen Lamps

These types of lamps possess more luminous intensity values than that of incandescent lamps. These lamps are used to fix the reference CRI value as because they devise a wider colour spectrum range. Due to this reason, they are popularly applied for spot lighting, exhibition lighting, and in other similar lighting applications. These lamps have a very high lifespan because of which they are used for dimming control lighting as well as in human-centric lighting [31].

2.3.5 High Intensity Discharge (HID) Lamps

This category of lamps is comprised of sodium vapour lamps, mercury vapour lamps and finally metal halide lamps. These discharge type of lamps necessitate superior type of ballast and distinct type and power rating dependent fixtures. Prior to turn on, these lamps require a warm-up time as well as cool-down time post turn-off. However, these lamps can remain active for larger time periods and are widely popular for outdoor lighting applications. Amongst the other types, sodium vapour lights are highly energy efficient but have smaller CRI and limited lifespan. Mercury vapour variant has high CRI but suffers from least efficacy amongst all other types. Metal halide lamps have similar CRI to that of mercury vapour but its efficacy is much higher than others and even higher than fluorescent lamps [31].

2.3.6 Light Emitting Diode (LED) Lamps

These type of lamps are widely popular nowadays, particularly, in this part of the world and have slowly replaced the other variants in most of the applications and the governments are also endorsing them in terms of providing subsidies to the manufacturers such that their price remains affordable to the citizens because they are highly energy efficient with compact dimensions to fit in any configuration and simultaneously providing with a satisfactory level of CCT value. Moreover, with LED bulbs, the CRI value is not only within acceptable limit but most importantly, the lighting eminence is almost nearer to the daylight level and that is why they are highly recommended in modern day applications with adequate arrangement.

The semiconductor crystals are electrically excited to produce the light of LEDs in n-conducting space having a plethora of electrons and also in p-conducting space having a deficiency of electrons and the intermediate space is known as the p-n depletion layer. Here, light is produced to the crystal with bright lumination flux that allows heat sensitive materials-regardless of display windows, malls, VIP palaces, corridors and showrooms, even streets or highways. LEDs emit nearly monochromatic radiation having multi-dominance colour of wavelengths viz., red, orange, yellow, green, indigo, violet and blue. It almost contains neither ultra-violet (UV) nor infrared (IR) radiation. Hence, they can be employed on food industry and on the illumination of sensitive art museum works.

The light from LEDs, at present, continues to grow in demand that exceeds the values of halogen and filament lamps. It has an extended lifetime that results in a paradigm shift with respect to the design and development of lighting. In case of interior decoration, headlights of

two to four wheelers and even in traffic indicators, LEDs have very fast changed the orientation of the lighting model and established components of the general lighting concepts [31-32].

2.4 Physiological Effects of Light

Already, we have discussed earlier about light as an electromagnetic wave. Sir Isaac Newton separated visual light to its individual colour components by advancing it through a glass prism. It is an established fact that sunlight comprises of an electromagnetic energy spectrum that was referred as photons by Sir Albert Einstein. Apart from the colour, energy level of a photon inversely depends on its wavelength. Various studies exhibited that a highly energized photon of 290 nm wavelength possess the ability to trigger Vitamin D reaction on skin or stimulate hormones for secretion from endocrine glands are formed deeply in brain. The vacuum UV spectrum from the Sun radiates to terrestrial environment and can result in numerous pathological conditions. Human beings require UV wavelength to generate Vitamin D₃, even, at lower concentration, it increases risk for heart failure, stroke and sometimes develop cardiac anomalies. Photobiology analysts have proved that blood pressure, as well as serum cholesterol levels, get minimized significantly post-exposure. Incidentally, day lighting has a natural healing effect to the external world.

2.4.1 Visual Impacts of Lighting

The visual effects regulate the sensory receptors in the retina, cones, and rods of the eye. Light after reaching those cells initiates a chemical action. A chemical, namely, activated rhodopsin is formulated that produces electrical impulses into the nerves and connect the photoreceptor cells at the cortex region of brain to be explicated as “vision”. The rods function in extreme lower level lighting condition that do not allow colour vision. On the other hand, cone is liable for sharpness as well as detailed colour vision. The spectral sensitivity of human eye determines the probability of a photon at a certain wavelength to be absorbed and its possibility to be converted to a neural signal depend upon varying wavelength of light for a certain level of intensity. The aforesaid statement is described using Figure 2.2: spectral eye sensitivity curve V_{λ} represents for cone system forms the basis of all lighting units known as the photopic system, whereas, V_{λ}' illustrates the rod system named as the scotopic system. It can be observed from the figure that the eye is neither sensitive to

extreme blue light nor to extreme red light, but possesses optimum sensitivity for green-yellow light.

The photoreceptor cells in the eye retina were initially detected in the year 2002 by Berson et al. [33] which regulate the biological impacts. While light reaches those cells, a chemical reaction takes place (photo pigment melanopsin) and it produces electrical impulses [34-35]. The cells possess their nerve connections for locating in the brain termed as suprachiasmatic nucleus (SCN), also known as the biological clock of brain and to that of pineal gland. We will primarily discuss on visual performance, then gradually possess to biological effects of light.

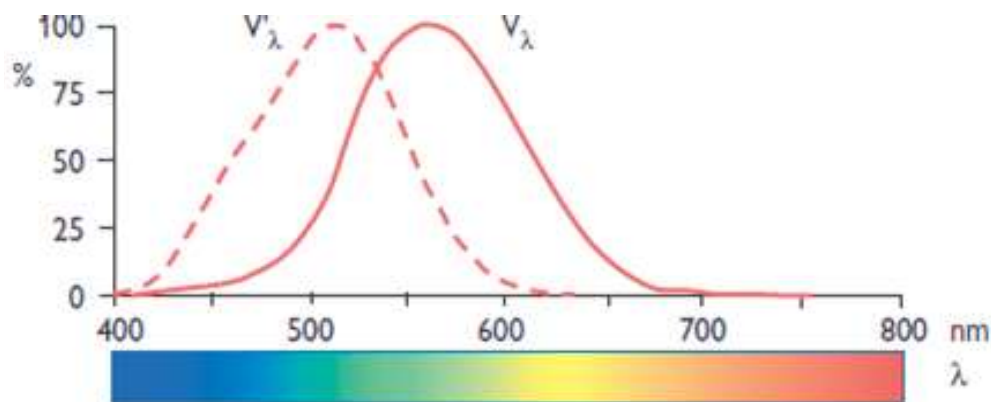


Fig. 2.2 Spectral Eye Sensitivity (SES) Curve for Cone Cells and Rod Cells (dotted)

2.4.1.1 Visual performance

The visual performance not only depends upon the quality of lighting but also on 'seeing ability' of the observer with respect to age and lens power of eyes. One such is ageing effect on the deterioration of transmission on the lens of eye which means that the transmittance has become lower for the person of interest. It further means that lesser amount of blue light is disseminated. Many studies predict the influence of lighting quality on visual performance in a comparatively strenuous job (like industrial office task or machine task) or an onerous job (like colour inspection or fine assembling). All the jobs indicate enhancement of visual performance with improvement of lighting quality. An escalation in visual performance improves the work performance, which is dependent on visual component of the job and reflects in higher threshold with fewer errors.

Apart from visual effect, lights also have significant impact on the environment as well as it has its notion at the workspace [36]. Today, a lot of emphasis is given on the layout of interior design of the workplace. Efficient lighting design can brace up the interior depiction, whereas, a poor lighting design can decline or sometimes shatter the impact of design. Over

and above, restricted surface brightness puts a limit on the orientation of the physical space viz. ceiling, wall and floor. Glare and lighting reflections are also unacceptable as it senses the luminosity of the visual spectra which turns out to be appreciably higher than the adapted eye brightness level. It can eventually lead towards reduced visual performance followed by stress and discomfort to human eye.

2.4.2 Biological Impacts of Lighting

The eye as a vision organ has photoreceptor cells connected to the brain, which deals with various health problems. Most importantly, it is associated with the control of circadian rhythm and management of few major hormones through light-dark rhythms having dominance over alertness and good health.

2.4.2.1 Light and Body Rhythms

Light transmits signals through photoreceptor cells and neurotransmitters for regulating the biological clock of a diversified biological process. Cortisol (known as stress hormone) and melatonin (called as sleep hormone) have a significant contribution for attention and nap. Cortisol enhances the blood sugar and gives us the energy and improves the immunity system. But during escalation of cortisol extent beyond a certain limit, the body turns out to be fatigued and incompetent. The cortisol amount rises at the day to prepare our body for the daily routine. They stay over same for the whole day with sufficient activities, falling to minimal level during midnight. In contrast, the level of melatonin hormone (sleep) minimizes at the day and reduce drowsiness. It enhances only during darkness and permits satisfactory level (as cortisol reaches its minimal value). In case of a healthy person, the rhythms are not disrupted extensively and it is continued everyday.

Normally, morning light synchronizes our biological entrainment with the earth's 24-hour revolving rhythm, in absence of which it would be free-running causing deviation in body temperature as well as in the cortisol and melatonin level fixed by the environmental clock [37]. Absence of this light-dark rotational rhythm, results in lack of attentiveness, drowsiness during daytime and even insomnia. In case of rotating shifts, workers mostly face these traits at least for two days after their change of schedule due to similar rationale [38].

2.4.3 Radiant Energy Absorption Effect

The optical radiation has a large impact that is required to be monitored. More simply, it is said that radiant energy is required to be transmitted to the material of interest for observation

of the effect. Radiant energy due to heat is transformed into kinetic energy in terms of molecular motion. In all cases, temperature is enhanced i.e., photochemical impression is thus developed. The radiant energy (in Joule) is absorbed at unit time with certain volume which determines the temperature increase and is termed as absorption power (J/s) or absorption factor (watt/m^3), it determines how quickly it cools the environment [39]. The main mechanisms for the absorbed radiant energy to take place are as follow:

2.4.3.1 Photochemistry

The radiant energy can be subsequently utilized in photochemical reaction. This radiant energy emanates as discrete “quanta” or photon that shall be equal to the excitation energy. Ultra Violet (UV) radiation is photochemically active (means photons convey the utmost energy) and is absorbed in eyes and in organic molecules over diverse processes [40]. Light is photo-chemically agile in our eyes; ocular perception is initiated with photo-isomerism of opsin proteins. Although, Infrared (IR) radiation is heat arbitrated and incapable of transmitting the valence electrons to upper energy stages, hence, it initiates photochemical reaction. Few eye tissues absorb light and decrease retina exposure, otherwise, light induces oxidative pressure impairment known as photo-chemical and photo-dynamic damage [41]. UV and IR radiation cause lesions in cornea as well as in the lens of eye although it is repairable. Prolonged UV exposure due to sunlight causes cataract over eye lens. Anyhow, the damages are not for interim or enduring exposure to lighting devices. Retinopathy is normally irremediable and permanent [39].

2.4.3.2 Photobiology

Here, optical radiation penetrates through our skin or eye, exposure and irradiance are the frequently used photo-biologic metric to enumerate the transmission of radiant energy to human body. Light penetrates through the skin and the body gets pain reflex sensation. Generally, artificial lights intensely do not cause burns but instigates chemical reactions towards detrimental intensities. Our eye retina is specifically endangered to lesser radiation wavelengths (e.g. blue light) and its vulnerability surges with age. Blue light has been found to have a pronounced effect than white light or other colours that are commonly in use [39].

2.5 Psychological Effects of Light

Küller and Wetterberg studied the EEG pattern of people in laboratory turned into an office environment, at times with a comparatively higher illuminance level as well as with a lower

illuminance level [42]. The EEG at the upper illuminance level turns out to be indicating drowsiness, which means that intense light influences the central nervous system. In this regard, delta waves are high-amplitude but slowest waves and are associated with sleep or non-aroused condition. They are normally found in infants or in younger children, however, if it is present in an adult one should understand that the person is stressed, unable to think properly and is also having learning issues.

Some investigations indicate higher illumination levels to deal with lethargy, and result in higher awareness levels [43-45]. In January, daylight permeation is not at adequate level, while in May, it is sufficient enough to cause any considerable level of stress. An investigation depicts that artificial interior lights having adequate illumination level in winter have a progressive consequence on temperament and vitality [46].

2.6 Human Centric Lighting (HCL)

Light has an impact on our biological and emotional well-being apart from its visual demands. Thus, while designing the concept of lighting, when human beings are the focus of attention, it is known as Human Centric Lighting (HCL). A recent European study revealed that in a factory of 750 workforces, with the introduction of HCL at 2000 lx, the electricity expense was enhanced from \$47,000 to \$60,000 i.e. by \$13,000 but productivity was also increased by 4.5 percentage level. Moreover, one percent lesser casualties were observed due to the rise in alertness which finally resulted in one percent fewer sick days and improved staff retention. A similar study was conducted in an educational institution in Europe amongst 1000 students and 80 teachers. The installation of HCL system enhanced the power consumption from \$8,900 to \$12,240 i.e. to the tune of \$3,340. However, the cognitive performance of some pupils increased upto fifteen percent with ten percent reduced healthcare and educational costs; amongst them 5.3 percent students were suffering from attention deficit hyperactivity disorder (ADHD). The report further assessed extra educational cost per ADHD pupil at \$6,670 but inspite of that it saved around \$667 per student per year. Moreover, it resulted in eighteen percent decrease of mental disorderness amongst staffs and reduction of 12 sick days due to stress and finally the attrition rate was reduced upto 2 years. The study further predicted a realistic market penetration for HCL to be two percent for residential use, five percent for repetitive industrial tasks, ten percent for education sector, thirteen percent in official jobs, and upto twenty percent in medical sector by 2020 [47].

2.6.1 Lighting for Mankind: HCL

The earth's natural light as received from the sun comprises of low light levels with lower CCT during the day, medium light levels at medium CCT at afternoon, low light levels at low CCT during evening and very low light levels at medium CCT under moonlight. The light levels and CCTs dynamic changes govern our twenty four hour internal clock and controls the secretion of different hormones produced inside our body. Dopamine hormone secretion controls our pleasure, alertness, and muscular coordination. Serotonin is secreted for carbohydrate cravings and impulse control, another hormone familiar as cortisol is secreted for stress response. At night, melatonin hormone however happens to secrete to allow deep sleep and refresh our body. This entire cycle is known as circadian rhythm of human body. If the hormones are not secreted properly then it disrupts the rhythm causing discomfort towards our body.

HCL is comparatively an emerging term which uses to indicate those lighting systems having positive circadian impacts and in the process minimizes light pollution. It takes into account the integration of visual, biological as well as emotional aspects in comparison to its traditional counterparts. Good lighting is not about turning on/off but to adjust its intensity primarily. Its composition can be varied to create a dynamic lighting environment for better living index than energy consumption and/or cost reduction. HCL is not only focussed on circadian entrainment but also to optimize the utility of light in terms of individual, societal and environmental phenomena. The functional and aesthetically pleasant lighting system has a positive effect on cognitive performances including higher concentration, sustained attention, and increase in the speed of work with higher accuracy and minimal time, fatigue and error rate with enhanced memory functions, emotional quotient (EQ) as well as on chronobiological system. Thus, this newly developed lighting technology is focussed to ensure the static goal which is right light at right place. In terms of designing HCL systems, the following considerations are to be kept in mind: illuminance level, spatial brightness distribution, occurrence and character of shadows and reflections, glare and lastly upon experience of the colour of light [48-49].

The global market worth is around \$849 million USD in 2019 with \$395 million USD or forty six percent of the global revenue is from Europe alone, while North America contributes \$238.3 million USD or twenty eight percent of the global revenue and APAC has a share of \$181.7 million USD or twenty one percent of this rapidly growing space. It is expected that it will reach around \$3.5 billion by 2024, having a 32.75 percent compound

annual growth rate (CAGR) over the next 5 years with the companies bringing in innovative products and services to materialize the growth estimation [50].

2.6.2 Applications of HCL in Indian aspects

Lighting affects human body in any of the following three ways:

- a. Visual system
- b. Circadian system
- c. Psychological system

Although the visual impacts are measurable but still now the non-visual impacts of HCL such as emotional stability cannot be measured as it is a subjective issue and varies from person to person. However, ‘biophilia hypothesis’ based research affirms that people feel wellbeing when kept closer to the nature. Thus during design, the lighting pattern needs to be dynamic in terms of circadian requirements and emotional responses with suitable light levels at required CCT as mentioned below in Table 2.1:

Table 2.1: Features of HCL system

Time	Lighting feature
Morning	Lighting should be warm amber during early morning, then to light amber and finally towards white light.
Noon	Lighting should change from white to cool white.
Supper	Lighting should change from cool white to white and finally to warm amber again.
Night	Lighting should adapt to various shades of blue throughout the night.

Lighting for visual acuity or decorative purpose only is nowadays no longer acceptable. The previous trends of energy efficient lighting have been shifted towards human centric energy efficient lighting approach. Hence, lighting should be such that it is friendlier to the circadian clock [51-52]. HCL is considered to be applicable mostly in indoor lighting conditions where the lux levels are within 1000 lux and having CCT from 3000K-6500 K. In outdoor lighting conditions when eye is sensitive to lower lux levels under mesopic condition, safety and vision become the most important factor.

Mindtree’s Network Operations center in Bangalore is developed keeping HCL in mind. However, a collective effort is required from all the stakeholders to give its entry just like daily dosage of tea or coffee [53]. HCL systems are installed in schools with sufficient

brightness and blue enriched to keep teachers and pupils calm, concentrated and alert during school hours. In commercial workplaces, HCL makes the office environment more natural and comfortable to increase the productivity yet maintaining the job satisfaction of workers. In healthcare sector, HCL is incorporated with cooler CCTs to make the staffs less fatigue, alert, provide them with better performance, precision as well as increased safety during shifts and warmer CCTs where patients are kept for comfort as they rest and recover from illness or stress due to modern lifestyle. HCL systems can add their benefits into hospitality and wellness sector as well to help visitors feel more comfortable, reduce jet-lag, and make rooms more elegant, ease of control with lower energy consumption, heat generation, operational expenditures and maintenance requirements. Systems which are installed in India use LEDs in their solutions providing larger lifetime with high CRI, zero maintenance, ease of installation and controllable through RF remote while conforming to IEC standards.

Under the Smart City scheme from Government of India, total 10459.2 crores of money has been released upto March 2018 to convert one city into a smart city which estimates an impact on 9,96,30,069 urban population. Out of 100 winning proposals, the total project cost under this scheme is 2,05,018 crores. Total area based development cost is 1,64,204 crores and total pan-city solution cost is 38,914 crores [54]. Under this scheme, if HCL based LED luminaries can be installed, their impacts can be investigated. India's LED market is projected to grow from \$ 918.70 million in 2016 to \$ 3,758.74 million in 2020, i.e. at a CAGR of 24.66 percent. According to a study, 2.54 billion smart lighting units will be installed by 2020 and smart lighting solutions are set to become the most frequently used home automation feature [55-56].

Presently, HCL is in nascent stage in India but opportunities galore as the scope for enhancement is huge due to its population and developing economy. The government of India launched a scheme named 'Domestic Efficient Lighting Programme (DELDP)' in 2015 which was renamed as 'Unnat Jyoti by Affordable LEDs for All' (UJALA) by which people could buy affordable LED bulbs instead of incandescent bulbs or CFLs, and mercury tubelights by which 25 crore households are benefitted as on date [57]. Street Lighting National Programme (SLNP) was launched by Energy Efficiency Services Limited (EESL) by which more than 21 lakh street lights were installed across 23 states and union territories. 230 million LED bulbs, 8 lakh energy efficient fans, and 203 million LED tubelights were also mounted that helped in saving 32 billion kWh of electricity annually and have reduced consumption of 19 million tonnes of coal which is equivalent to an annual reduction of 25 million tonnes of CO₂ and is further equivalent to 600 million trees over a period of ten years.

Consumers under this scheme saved around 124 billion INR annually on their electricity bills. This further led to increase in production of LED bulbs nationally and thus the price of the lights was naturally reduced by leaps and bounds [58]. The projection of the present central government's Make in India initiative has been instrumental in stimulating the smart HCL systems demand in this part of the globe. It is aimed at enhancing vision, well-being and performance by serving in-depth knowledge to evoke particular human biological responses [59]. According to a research made under Make in India initiative, it has been observed that about 25-30 people migrate per minute from rural areas in search of better livelihood and developed lifestyles. With this momentum, it is estimated that 843 million people will live in urban areas by 2050. Moreover, cities with human centric design approach will evolve from being smart towards responsive, thus, the citizens will move from the centre of attention towards the center of action [60].

2.7 Purpose of Illuminance Monitoring

The monitoring of illuminance is important for identification of the potential hazards and evaluation of the associated risk present in the workplace to ensure optimum efficacy with improved work environment and enhanced satisfaction of the employees or workers. Adequate lighting refers to the fact that the internal lighting level provides an illuminance that is sufficient enough for the jobs undertaken maintaining human-health, well-being and uplifting their safety at the workplaces to lead a prosperous life. Inadequate lighting level leads toward strain in the eyes i.e. the standard of vision starts degrading, fatigueness, headaches, eye irritation, stress and even glare. Whereas quality lighting should reduce accidents, decrease wastage of products, boost employee productivity, cuts down energy consumption bill, improves the health of the labourers; downgrade the possibility of injury and it should also enhance work performance for the persons of interest. However, the age and eye-condition of any person have a huge impact on the required illuminance level for conducting any specific task.

2.8 Limitation of Existing Illuminance Measurement Methods

While the literature survey was conducted, no automated system was found to be existing that was able to give positional lux measurement along the entire indoor space. It was also explored that as of now, almost everyone requiring measurement of illuminance, use

handheld lux meters that increases measurement time for a large space and simultaneously it becomes tedious to hold the instrument over a larger period of time. Over and above, if the space selected is quite large then the measurement time will be considerably high. Price range of handheld lux meters varies from about \$20 to \$400 and higher, depending upon the accuracy and precision with the high priced models offering better specifications. However, in a developing country like, India, even the low priced model seems to be very much costly. Whereas, if an illumination sensor with spectral response close to human eye is bought from the market and calibrated in terms of a reference meter, it serves the purpose. Moreover, present day available light meters only give digital readout of lux values whereas quality of lighting depends also on various other parameters. For that purpose separate multivariate, portable, costly meters may be required for measurement of those parameters and at times it may not be easily available. On the other hand, if RGB or similar sensor can be calibrated by the help of a Chroma meter or related type of reference instrument, then it can be properly used even in multiple applications as and when required.

Chapter Summary

The chapter starts with discussion on natural and artificial light sources. Also, the physiological and psychological as well as image and non-image related effects of lighting have been discussed here. A comparatively new concept namely, Human Centric Lighting and its possible implications, particularly, in-terms of the Indian scenario have also been mentioned in this chapter. The chapter ends with discussion on the purpose of illumination monitoring in context of this study. Lastly, it refer some shortcomings of the present day available methods for measurement of illuminance. Before going to the thrust area of the conducted study, a brief discussion on the aforesaid particulars were of utmost importance as a preliminary concept required for the experimental phases of the research work. The next chapter deals with comparative performance assessment of various types of machine learning regression methods for estimation of lux using illumination sensor and RGB sensor data before using it in any application. These techniques will eliminate the requirement of a pre-calibrated reference meter that may not be feasible in each case study considering its financial implication and other relevant parameters.

Estimation of Sensor Data using Computational Intelligence Techniques

3.1 Introduction

In the measurement process, sensors are chosen based on numerous parameters, like quality, cost, usability, etc. to name a few. With the paradigm shift in terms of smart sensing and remote connectivity, new age systems should not only sense the parameters of interest using high end sensing technologies, simultaneously provide more insights to the acquired data and enable higher productivity. In this new era of Industry 4.0, intelligent embedded systems should adapt themselves taking into account the changing needs as per the situation demand. The challenge remains in not only selecting accurate systems to give proper measurement data repeatedly but also predicting the output suitably using different types of regressive techniques in a simulated environment platform [61]. Lighting is considered as a necessary parameter nowadays to add comfort to our daily life. The illuminance observed from a light sensor is contributed by the light sources as well as the light reflected from the objects residing in an indoor environment [62]. Sensors acquire information about the lighting quality, after that the captured information is processed and then only it can be converted into usable electrical output. Illumination measurement is required for several purposes depending upon the precision, reliability, portability, and last but not the least is the application area.

Apart from the physical properties of the system under consideration, data estimation may also be done using statistical methods. Regression analysis is a universally accepted technique for modelling the statistical correlation between the input and output variables of any system as well as to formulate their associative equation. This technique has found its applications in every sphere of engineering applications intended for data analysis, estimation, prediction, and sometimes even for control purpose. The regression method that uses a single independent variable and if the relationship with the dependent variable is linear in nature, then it is known as univariate regression technique. On the other hand, if there is more than one independent variable and one dependent variable, then it is termed as multivariate regression technique. Autoregressive properties of the acquired data enable us to consider more separable values and complete the series.

Selection of appropriate source of light is immensely important not only in our residence but also in the office to improve the quality of life. Analysis of the light sources in both pre-installation and post-installation stage is equally significant as it is directly related to our well-being, work-ability and emotional stability. Illuminance, measured in lux, is an important parameter of monitoring the light level reflected from a definite point on a given surface. Light also plays an integral role for interpretation of colour, hence, it is essential to look for its characterization models. The objects reflect light from the surface and photoreceptors present in retina absorb and generate the perception of colour. Measurement of Correlated Colour Temperature (CCT) represent colour in Kelvin (K), which is the temperature of a black body radiator. It shows almost the same chromaticity as the analysed source of light [63]. The illuminance and CCT of installed luminaries at the indoor space have a significant influence on the visual performance, physiological as well as psychological parameters of human body. Artificial light sources with accurate lux and CCT values following the recommendations' of International Commission on Illumination (CIE) can be applied to prevent the adverse effects on human health by proper secretion of melatonin and glutamate for sleeping quality management, wound-healing, cosmetology, and hair regeneration [64-68].

The goal of this research finding is to develop an intelligent, cost-effective lighting solution with superior performance in different lighting environment. Hence, the selected system will be such that it can acquire data from a sensor and produce the response within a satisfactory level of accuracy by mimicking the performance of a standard and calibrated reference meter.

3.2 Objective of this Study

The novelty of this study is mentioned herein below:

- i. To achieve the performance of a standard and calibrated lux meter easily by the application of a cost-effective, real-time, embedded illumination measuring system using different regression techniques over full scale measurement range.
- ii. To compare feasibility analysis of various regression methods e.g. Polynomial Regression (PR), Support Vector Machine Regression (SVMR), General Regression Neural Network (GRNN), and Gaussian Process Regression (GPR) for prediction of unknown illuminance value.
- iii. Evaluation of performance indices like, R-squared (R^2), mean absolute error (MAE), and root mean square error (RMSE) for each of the aforesaid techniques and finding out the best applicable method on the acquired dataset.

In this study, regression analysis is done for prediction of sensor values and qualitative as well as quantitative performance evaluation of them is performed with respect to a standard chroma meter. For capturing of data, the sensor and wifi enabled microcontroller together function as the client platform in an indoor wireless network. Initially, a pre-calibrated reference meter is required to sense the illuminance values at every instant. The client unit transmits the sensor values to a computer system, which acts as a server unit under the influence of wireless router. The captured data are used to train and validate the system using four types of regression techniques to find the best possible solution at the server end. Conversion of sensor values into lux data or periodic calibration is not required at the client end. Only, the sensed values are transmitted in a wireless network to server computer for conversion into illuminance values using regression techniques. Finally, from the predicted values, corrective measures and preventive actions can be designed such that the parameters never fall below a certain threshold limit. Moreover, the maintenance personnel may become alert on the situation as and when it arrives.

The novelty of this experimental work is listed below:

- a. We have thoroughly studied the performance of illumination and RGB sensor for prediction of illuminance and CCT values using machine learning regression (MLR) methods in a wireless client-server network system.
- b. A detailed comparative study is done to evaluate the performance metrics for illumination and CCT measurement.

The objective of this study can be summarized as:

- i. State-of-the-art technique for acquisition of illumination and RGB sensor values in a wireless client-server indoor network.
- ii. Four different types of regression analysis have been done for prediction of lux and CCT data with respect to a standard and pre-calibrated meter.
- iii. Performance assessment of the machine learning based regression techniques and finding out the most suitable model for the selected sensor.

The present research findings are aimed to develop an intelligent yet energy-efficient lighting solution with longer lifetime and superior performance in static as well as dynamic lighting environment. The next section gives a brief theoretical overview of regression models considered in this study followed by the proposed experimental set-up. The comparative analysis for prediction of illuminance and CCT values using four types of machine learning techniques are described henceforth and the study ends with a conclusion.

3.3 Related Works

Visible light is defined as a part of wavelength spectrum perceived by human eye. Appropriate levels of lux measurement is required in all spheres of human activity nowadays starting from field work, normal reading, relaxation as well as psychological impacts [69]. The simplest method of lux measurement uses light dependent resistors (LDRs) which can be used with satisfactory limit of accuracy and is shown in [70]. Nowadays all photodiodes and phototransistors comprise of an epoxy filter which improves the relative spectral sensitivity to be closer to that of human eye within visible range [71]. Some sensors offer high gain, temperature stability, linear output replaceable phototransistor facility [72], some offers pre-calibration [73], whereas some others offer computer interface to measure relative light intensity [74]. The photopic luminosity function describes average sensitivity of human eye under suitable lighting condition, whereas, the scotopic density function describes average brightness perception of human eye in less-light condition. Depending upon the operating parameters, measurement range, applications, lighting conditions, cost, communication interface and several other factors various lux sensors are available in the market and it is the responsibility of the user to select the appropriate sensor for a particular application [75-78]. An autoregressive statistical regression method and support vector regression has been proposed in [79-81]. A distributed lighting system to control the illumination of multiple networked luminaries is proposed in [82] which use recursive calibration procedure to track

the gain change in illumination. Fourier transform based data analysis for pattern recognition of smart sensors is proposed for indoor air quality monitoring in [83]. Wireless Sensor Network (WSN) based intelligent lighting system have been developed in [84-85] with adaptive illumination control, indoor positioning and energy usage information services. Another system using WSN is proposed in [86] with two weeks of training data using daylight and artificial light piecewise linear model has predicted illuminance at seven monitoring stations with quite high accuracy. Whereas, SVM based regression model has predicted daylight illuminance with lesser accuracy. A daylight estimator model using least square regularization is proposed in [87]. The light sensor data are collected from office environment to compute dimming level and minimize power consumption in various lighting conditions. Also, a similar model using iterative centralized lighting control is proposed in [88] considering the fact that the sensors are co-located with the luminaries.

In short, there are various sensors available in the market with their individual specifications based on several parameters and cost. It entirely depends upon the user to select which type of sensors they are intending to use in their application.

Light level monitoring is very much popular nowadays in street-light control systems for minimization of energy consumption, and to increase the life period of installed luminaries. It also reduces carbon emission, prevents pollution due to light and thus improves human comfort [89-90]. The evaluation of human wellbeing and impact of productivity on energy management of buildings are gradually becoming an important research area after taking into account various human-centric parameters [91-92]. A Wireless Sensor Network (WSN) based Multi-Input Multi-Output (MIMO) system was proposed in [93]. The system comprised of energy-efficient Cluster Head (CH) identification using hybrid copula and distributed gradient descent algorithm for location optimization. Not only for outdoor light level monitoring, indoor light level monitoring is also equally important as we spend most of our quality time in the indoors. This is required in situations when the daylight is insufficient and compensatory lighting arrangement is to be installed [94]. Hence, selection of proper sensors and controllers are essential nowadays. The sensors should be accurate, precise with high resolution and are calibrated for the entire measurement range depending upon the application. The role of a controller is nothing less as it integrates the entire process to create a hassle-free lighting environment. If the controller output for each sensor value is known, then a system can be designed for prediction using machine learning regression algorithms. Primarily, the real-time acquired data or imported data from a dataset is trained using regression methods to find out the training model. Then, the formulated model needs to be

validated using the testing dataset to find out the efficacy of those techniques relying on their generalization capability [95-98].

Measurement of multiple parameters using a single sensor can be more beneficial as it gives indication of more than a single parameter with respect to the change of a measurand. Multifunction optoelectronic sensors are due to this reason gaining momentum in several application domains [99]. In this regard, calibration of RGB sensor using the equation provided by McCamy for measurement of CCT was presented in [100]. Polynomial fitting technique was used in [101] for measurement of illuminance from RGB sensor using I2C (inter integrated circuit) communication mode. CCT measurement system using PIC microcontroller was shown in [102] where the system was calibrated by the help of a spectrometer. A real-time LED based energy efficient lux and colour temperature sensing and actuation system was installed in [103] for maintaining the cultural heritage in a WSN (wireless sensor network) framework. However, the main drawback of this design was that all the designed systems available in the literatures mostly used wired network to estimate the sensor values and sometimes they are not calibrated properly with respect to a reference meter over the entire measurement range. Also, there was hardly any mechanism available to predict or understand a faulty situation before it was actually experienced while the literature survey was conducted.

In a nutshell, all the systems developed so far monitor a single parameter with certain degree of accuracy in a wireless sensor network. But there are limited literatures on remote multiple parameters monitoring system for either corrective or preventive maintenance. Moreover, detailed comparative analysis for prediction of multiple parameters using machine learning regression models are not observed widely. Hence, this idea came into our mind and is integrated in this study.

3.4 Overview of Regression Analysis

This section covers a brief theoretical background of the following regression techniques in this experimental study: Polynomial Regression (PR), Support Vector Machine Regression (SVMR), General Regression Neural Network (GRNN), and Gaussian Process Regression (GPR).

3.4.1 Polynomial Regression (PR)

This technique [104-107] aims to formulate a mathematical model between input variables and output variable. The independent antecedent variable 'x' is related to dependent consequent variable 'y'. The developed regression model containing multiple input variables is called a polynomial regression model (PRM). In an experiment containing n observations for input and output variables, the PRM can be represented by the following equations:

$y_i = \beta_0 + \beta_1 X_{i1} + \beta_2 X_{i2} + \dots + \beta_p X_{ip} + \varepsilon_i$ (for $i=1, 2, \dots, n$) and p is the number of input variables. Where, y_i (for $i=1, 2, \dots, n$) represents the observation or predictor variable and x_j (for $j = 1, 2, \dots, p$) are the regressor variables or independent variables.

The linear model comprising of n equations can be represented in matrix form as:

$$Y = \beta x + \varepsilon \quad (3.1)$$

$$\text{where, } Y = \begin{bmatrix} y_1 \\ y_2 \\ \dots \\ y_n \end{bmatrix}, X = \begin{bmatrix} 1 & x_{11} & x_{1p} \\ 1 & x_{21} & x_{2p} \\ \dots & \dots & \dots \\ 1 & x_{n1} & x_{np} \end{bmatrix}, \beta = \begin{bmatrix} \beta_0 \\ \beta_1 \\ \dots \\ \beta_p \end{bmatrix} \text{ and } \varepsilon = \begin{bmatrix} \varepsilon_1 \\ \varepsilon_2 \\ \dots \\ \varepsilon_n \end{bmatrix}$$

Normally, Y (n x 1) is a vector which represent observations, X (n x p) is a vector expressing independent variables matrix; β (p x 1) is the regression coefficient vector and ε is (n x 1) the residual vector.

The best curve-fitting line for the response values is obtained by squaring the sum of deviations and minimizing them from each data point to the line obtained in least-square model. The deviations are first squared and then summed, so the positive and negative data cancels out. $\beta_0, \beta_1, \dots, \beta_p$ are the regression coefficients estimated by least square method as follows.

$$L = \sum_{i=1}^n \varepsilon_i^2 = \sum_{i=1}^n (y_i - \beta_0 - \sum_{j=1}^p \beta_j x_{ij})^2 \quad (3.2)$$

For minimization of L with respect to $\beta_0, \beta_1, \dots, \beta_p$, the least square estimator must satisfy :

$$\frac{\partial L}{\partial \beta_0}(\beta_0, \beta_1, \dots, \beta_p) = -2 \sum_{i=1}^n (y_i - \beta_0 - \sum_{j=1}^p \beta_j x_{ij}) = 0$$

$$\frac{\partial L}{\partial \beta_j}(\beta_0, \beta_1, \dots, \beta_p) = -2 \sum_{i=1}^n (y_i - \beta_0 - \sum_{j=1}^p \beta_j x_{ij}) x_{ij} = 0 \quad (\text{for } j=1, 2, \dots, p)$$

Set of $(p+1)$ linear equations are formed for each of the unknown regression coefficients.

$$\text{In terms of matrix representation, } L = \sum_{i=1}^n \varepsilon_i^2 = (Y - \beta X)^T (Y - \beta X) \quad (3.3)$$

$$\text{Least square estimator: } \beta = (X^T \cdot X)^{-1} X^T \cdot Y = 0 \quad (3.4)$$

Solutions for the normal equations are termed as regression coefficients of the least square estimators.

The estimator of the variance σ^2 may be computed by: $s^2 = \frac{\sum_{i=1}^n e_i^2}{n - p - 1}$, also known as the mean squared error (MSE).

Overall quality of regression model fitness with reference to quantity is termed as regression coefficient which is defined by:

$$r^2 = \frac{SS_{x,y}^2}{SS_{x,x} SS_{y,y}} \quad (3.5)$$

$$\text{where, } S_{x,x} = \sum_{i=1}^n (x_i - \bar{x})^2, S_{y,y} = \sum_{i=1}^n (y_i - \bar{y})^2 \text{ and } S_{x,y} = \sum_{i=1}^n (x_i - \bar{x}) \cdot (y_i - \bar{y})$$

For calibration purpose, regressor variables (x) are assumed as values obtained from sensor and output variable (y) as values obtained from standard meter having high accuracy. Applying PRM, the regression coefficients for a) linear regression, b) 2nd order polynomial regression, and c) 3rd order polynomial regression $[\beta_0, \beta_1]$, $[\beta_0, \beta_1, \beta_2]$ and $[\beta_0, \beta_1, \beta_2, \beta_3]$ are computed.

Pseudo-code for Polynomial Regression

1. **Input:** Read the order of polynomial, o .
 2. **Input:** Read the number of data points, d .
 3. If $d < o + 1$, print the output that regression is not possible,
else, if, $d \geq o + 1$, then continue the process.
 4. Compute the normal equation elements in terms of augmented matrix.
 5. Solve the co-efficients $a_0, a_1, a_2, \dots, a_o$ of augmented matrix using elimination method.
 6. **Output:** Print the values of the co-efficients.
 7. **End**
-

3.4.2 Support Vector Machine Regression (SVMR)

It is a type of supervised learning technique [108-115] using linear or non-linear kernel function depending upon the applications. The training sometimes become time-consuming for large dataset and various strategies are adopted to accelerate the training speed of SVM. Sequential Minimal Optimization (SMO) is one such training procedure to eliminate the requirement of other quadratic iterative optimizer and reach optimal analytic solution. The SVMR architecture is represented using Fig. 3.1.

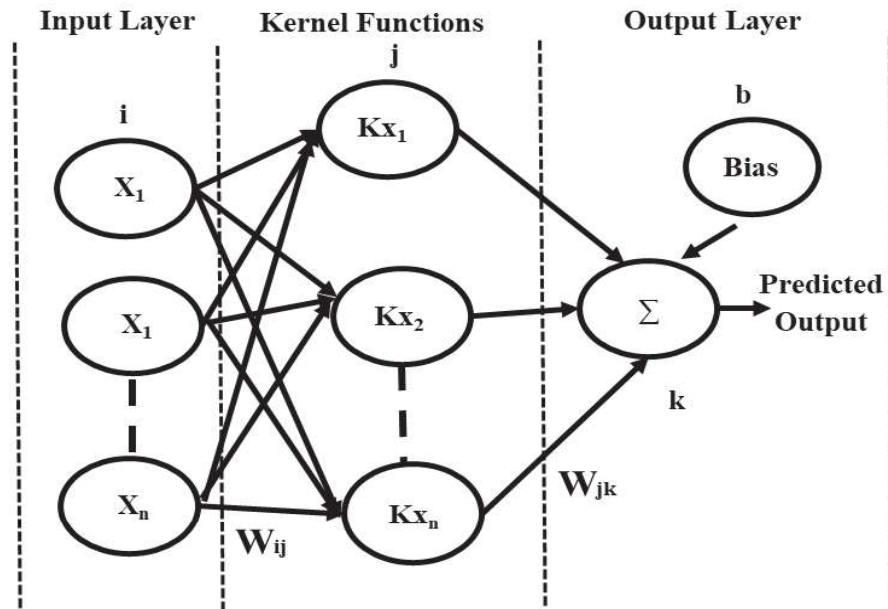


Fig. 3.1 SVMR architecture

For dataset $D = \{(x_1, y_1), \dots, (x_i, y_i)\}$, $x_i \in \mathbb{R}^n$, $y_i \in \mathbb{R}$, $i = 1, \dots, n$

Here, x_i is n -dimensional input vector, y_i represents output sample, n is the number of sample.

For SVMR with linear kernel, the function is formulated as

$$f(x) = w\varphi(x) + b, \quad (3.6)$$

$\varphi(x)$ is mapped vector, w is regression weight vector, and b is regression bias. These are obtained by solving and minimizing the quadratic equation.

$$\text{Loss function, } L = C \sum_{i=1}^n \xi_i + 0.5 \|w\|^2 \quad (3.7)$$

$$\text{such that, } y_i(w^T \varphi(x) + b) \geq 1 - \xi_i; \xi_i \geq 0$$

C is regularization constant and ξ_i is slack variable. SMO is decomposition algorithm solving a sub-problem with two-point set size for each iteration step and converge depending upon the dataset.

Pseudo-code for Support Vector Machine Regression (SVMR)

1. **Input:** Read the training dataset.
 2. **Input:** Read the predictor (antecedent) variables and response (consequent) variable.
 3. Train the SVMR model using the corresponding function.
 4. Obtain the trained SVMR model and now check for model convergence.
 5. If the model does not converge, then retrain using standard data, else, stop the training.
 6. **Output:** For any test input data, the trained model should provide an output value.
 7. **End**
-

3.4.3 General Regression Neural Network (GRNN)

This technique [116-118] was incepted by D.F. Specht in 1991 as an alternative to radial basis function neural network (RBFNN) on kernel regression. The RBFNN units are dependent on various forms of probability density function which are required for the functionality of convergence with lesser number of training dataset. This method is an improvisation of non-parametric regression neural network which converge to an optimal solution in a faster way. GRNN is nowadays a more preferred prediction tool due to the following reasons:

- a. Forward propagation is needed for predicting the continuous variables, which eliminates the necessity of randomly assigning initial weight values as in case of backward propagation.
- b. Any arbitrary function can be predicted to map input and output variables from the training dataset. This is a faster learning technique having higher prediction accuracy and converges to optimal regression surface.
- c. This method can tackle input noise and requires lesser number of training dataset for function estimation. When the training dataset increases, although it becomes computationally complex but the prediction error tends towards zero.

The architecture of GRNN is indicated in Fig. 3.2.

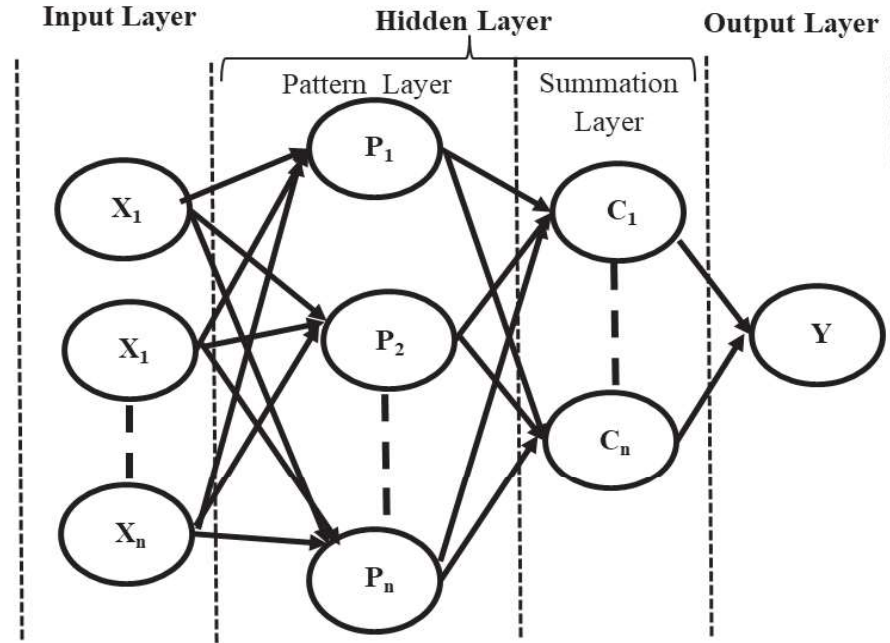


Fig. 3.2 GRNN architecture

Three layers persist in a GRNN, such as, input layer, hidden layer, and output layer. The hidden layer is divided into two sublayers, namely, pattern layer and summation layer. The input layer is joined with pattern layer; each neuron represents a particular training pattern. Pattern layer is attached with the summation layer which represents various summation types. Summation layer together with output layer formulates the normalized output. The neurons of each pattern layer are separately linked to the 'S' and 'D' summation layer neurons. The summation neuron 'S' calculates weighted sum of the pattern layer neuron output. Summation neuron 'D' computes unweighted output of the pattern neuron. The formula of GRNN is based on:

$$E[y | x] = \frac{\int_{-\infty}^{\infty} yf(x, y)dy}{\int_{-\infty}^{\infty} f(x, y)dy} \quad (3.8)$$

Where, $E[y|x]$ is expected output value, y is output of estimator, x is estimator input, $f(x, y)$ is joint probability density function (jpdf) of x and y ; $f(x, y)$ is calculated. Optimal function value y_j is estimated as shown below:

$$y_j = \frac{\sum_{i=1}^n h_i w_{ij}}{\sum_{i=1}^n h_i} \quad (3.9)$$

Where, Y is the output of hidden layer neuron; w_{ij} is target output with respect to input training vector x_i and the output j ; $Di^2 = (x - ui)^T (x - ui)$ is squared distance between input vector x_i and training vector u_i ; and σ is a constant which controls the degree of network generalization. If the smoothing factor σ is nearer to 1, then it will straighten the path of prediction line and enhance network generalization capability in terms of error prediction cost. Whereas, if σ tends to 0, it will create a dot-to-dot map which indicates deterioration of network generalization capability. That is why smoothing factor is to be chosen properly.

Pseudo-code for General Regression Neural Network (GRNN)

1. **Input:** Read the training dataset.
 2. **Input:** Read the predictor (antecedent) variables and response (consequent) variable.
 3. Train the GRNN model using the corresponding function.
 4. Obtain the trained GRNN model.
 5. **Output:** For any test input data, the trained model should provide an output value.
 6. **End**
-

3.4.4 Gaussian Process Regression (GPR)

This is also called the Bayesian state-of-the-art modeling technique [119-126] popularly used for various machine learning applications. It is a non-parametric tool conceived by Tony O'Hagan where the number of parameters increases with observed data. In SVMR, prior knowledge cannot be realized easily but GPR can infer the response even in presence of noise. This method is particularly applicable for multi-input and single-output process by finding out the concurrent correlation within tasks. A Gaussian process assumes unobserved latent function set and its likelihood is towards generation of posterior probabilistic observation. The combined multidimensional Gaussian contribution of training and testing dataset and predicted distribution is approximated by conditioning the training data properly. For a given dataset of input and output variables, $D = \{x, y\}, \{x_i, y_i\}_{i=1}^n$, is the regression model which can be expressed as, $y = f(x) + \epsilon$ (3.10)

Where, $x = [x_1, \dots, x_n]$ is an input vector of n-dimension; $f(\cdot)$ denotes the unknown function, and ϵ represents zero mean Gaussian noise having variance of σ_n^2 . The Gaussian process is depicted by mean function $m(x)$ and covariance function $C(x, x')$, which is represented by:

$$m(x) = E [f(x)] \quad (3.11)$$

$$C(x, x') = E[(f(x) - m(x))(f(x') - m(x')))] \quad (3.12)$$

The Gaussian Process is expressed as $f(x) \sim N(m(x), C(x, x'))$. If data can be properly scaled, then output response following a Gaussian process distribution can be represented by, $y \sim N(0, C(x, x'))$. For a given input x , joint distribution of training output y and test output y^* is

$$\begin{bmatrix} y \\ y_* \end{bmatrix} \sim N\left(0, \begin{bmatrix} C & k_* \\ k_*^T & C(x_*, x_*) \end{bmatrix}\right), k_* = [C(x_*, x_1), \dots, C(x_*, x_n)]^T$$

The prediction output y^* and variance σ^{*2} is represented by

$$y^* = k_*^T C^{-1} y \quad (3.13)$$

$$\sigma^{*2} = C(x_*, x_*) - k_*^T C^{-1} k_* \quad (3.14)$$

The covariance function $k(\cdot)$ have some parameters which are required to be tuned. These are called hyper-parameters which are determined by maximization of logarithmic like training data $\log p(y|x) = -0.5(y^T C^{-1} y) - 0.5(\log|C|) - 0.5n(\log|2\pi|)$ (3.15)

Hence, Gaussian Process Regression or Bayesian Regression is a tool for estimation of sensor data accurately for the problem considered in this study.

Pseudo-code for Gaussian Process Regression (GPR)

1. **Input:** Read the training dataset.
 2. **Input:** Read the predictor (antecedent) variables and response (consequent) variable.
 3. Train the GPR model using the corresponding function.
 4. Obtain the trained GPR model.
 5. **Output:** For any test input data, the trained model should provide an output value.
 6. **End**
-

3.4.5 Performance Criteria

Performance evaluation [127-130] of all the four types of regression methods are indicated as follow:

R^2 is considered as one of the most popular validation metric which can be represented by the following equation:

$$R^2 = 1 - \frac{\sum(Y_{obs} - Y_{pred})^2}{\sum(Y_{obs} - \bar{Y})^2} \quad (3.16)$$

Y_{obs} is the observed response, Y_{pred} is the predicted response, and \bar{Y} indicates test set mean value. The equation demonstrates prediction error model performance. If prediction

performance is degraded than mean then the model becomes unsuitable. If R^2 is equal or greater than 0.5 then the model becomes acceptable and moreover, if it is close to 1.0, the prediction performance confidence gets higher.

The other popular performance metrics used for model validation are mean absolute error (MAE), and root mean square error (RMSE). The equations for these methods are described as follow:

$$MAE = \frac{1}{n} \times \sum (Y_{obs} - Y_{pred}) \quad (3.17)$$

$$RMSE = \sqrt{\frac{1}{n} \times \sum (Y_{obs} - Y_{pred})^2} \quad (3.18)$$

These metrics, measure the prediction error with respect to total occurrence. MAE is a simple metric for predicting the errors. Both these metrics allot almost same weight to each error type. RMSE considers the squared term of prediction error, thus, if error is large even for single occurrence then more weight is assigned to it.

3.5 Experimental Set-Up for Estimation of Illuminance from Lux Sensor Data

Initially, prior to this study, the illumination sensor data was captured during the experiment at four corner locations. Also a standard lux meter was placed along the same position as that of the sensor. Now from both the illumination sensor data and standard lux meter data the multiplication factor was found out for each of the corner location. The mean multiplication factor was found out by calculating the average readings for each instance. But, the problem with this procedure was that only four corner locations were selected. Hence, the accuracy was limited only to the captured values instead of full scale reading of the sensor. Also, zero adjustment error for the sensor was not possible to find out using the aforesaid method. Moreover, due to environmental fluctuations, the multiplication factor is prone to vary, which can change the calculated readings accordingly. For the previously mentioned reasons, there came the requirement of finding out a method to obtain the predicted values of the sensor along the entire range with a desired level of accuracy such that its response mimics to that of a standard and calibrated illumination meter. Hence, sensor data is taken along the entire range in a dark room removing the bias signal from the readings and several regression techniques are undertaken to find out the best fit method. The sensor board is placed closer to the standard lux meter with minimal physical distance between their placements while the

experiment is conducted. The sensor output is displayed in a LCD screen by the help of a wireless microcontroller Node MCU ESP 8266 [131-135].

Next, offline analysis is done for each of the techniques: PR, SVMR, GRNN, and GPR; the theoretical background of each of them have already been described and R-squared error, mean absolute error (MAE) and root mean squared error (RMSE) are found out for each of the cases. The equations of the fitted polynomial are expressed individually [136-140]. Then, SVMR, GPR and GRNN techniques are also applied to find out the predicted lux value and similarly error analysis is done on them. A comparative performance analysis has been conducted to find out the most effective technique on the acquired dataset. The proposed system is comprised of the following sub-units:

- a. Client Module: The client unit is comprised of illumination sensor and 32-bit Node MCU ESP 8266 wifi enabled Tensilica L106 microcontroller based embedded system. The lux sensor used in our study is BH 1750 which is an ambient illumination sensor and it supports I2C mode of communication. This communication medium offers the advantage of integrating more sensors simultaneously with lesser number of pins to interface with a microcontroller. It offers the flexibility of measuring lux along a long range (1-65535 lx) at 1 lx resolution. It has inbuilt ADC and thus gives digital output directly using I2C (integrated circuit) interface. It eliminates infrared influence and gives spectral response which is close to human eye [141]. The illumination sensor is interfaced with the controller unit for acquiring the sensor data and transmitting them to the server unit through a wireless network. The lux sensor along with controller module together forms the client unit, which is powered by a competent power supply unit or by a rechargeable battery.
- b. Server Module: A wifi router is used as wireless access pointer which establishes client-server communication through an Ethernet port having specific IP address. The lux sensor values are stored at the server terminal and converted into illuminance data using the most appropriate regression technique. It can now be shared with the associated persons having dropbox cloud server application or web interface installed for remote monitoring. All of them can view the calculated values online using an IoT cloud server which is independent of computer configuration. Dropbox offers the potential to auto-update the computed parameters by legitimate users and also provides the flexibility to create a restore point. It uses 256-bit Advanced Encryption Standard (AES) for encrypting the dataset prior to its upload in remote cloud server and makes them available with the terminal users.

c. **Wireless Router:** A TP-Link made router acting as wireless access pointer is used in the experimental work. The wireless controller at the client module possess an IP address by which it captures the illumination values at indoor space and transmits them to any fixed port address of a wireless router. Then, it is redirected to server computer for conversion into lux values using the selected regression model followed by transmission via Dropbox based IoT cloud server application. The computed data is processed by an authorized user to check if it is below the threshold limit and thus a wireless client-server network is established.

Standard Lux Meter: Standard illumination meter (make-Metravi, model no: 1332) is available in the Illumination Engineering Laboratory of Jadavpur University. It is a light weighed, portable hand-held digital meter having range upto 2,00,000 lux with peak-hold and data-hold capability and it comes with an accuracy of $\pm 3\%$ which is within the satisfactory limit [142].

The lux data was captured in a dark room using a LED set-up. The sensing unit was turned on keeping a standard hand-held lux meter placed beside at the same elevation. Now the lux value can be changed by varying the intensity of the LED set-up using a potentiometer. At periodic intervals, the illumination data is acquired both from the standard lux meter and from the sensing unit. This experimental procedure is repeated and the observed data are plotted and the performance evaluation is done as shown in the next section.

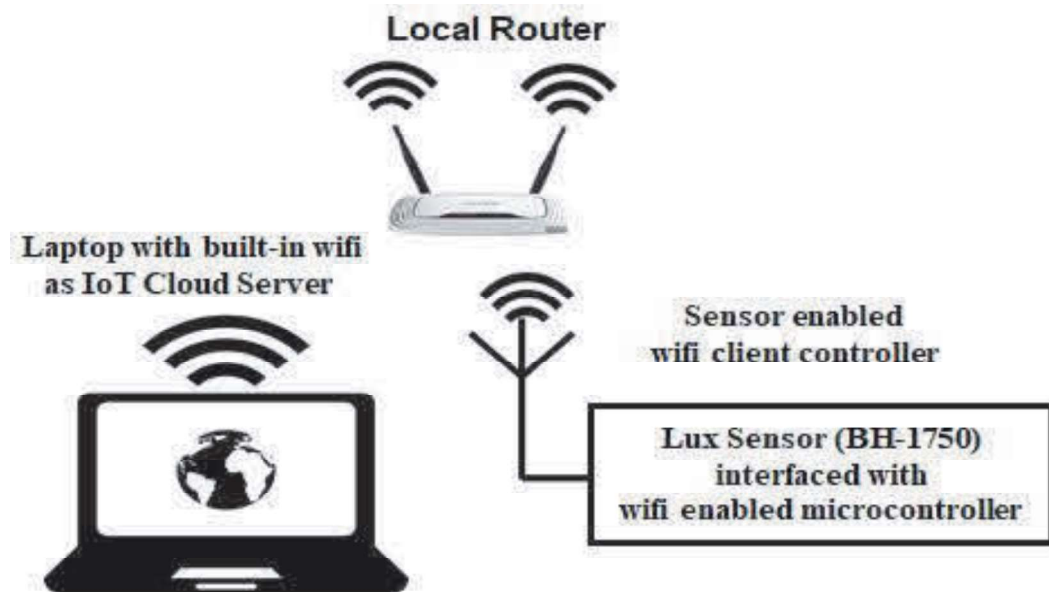


Fig. 3.3 Block diagram of proposed system using BH-1750

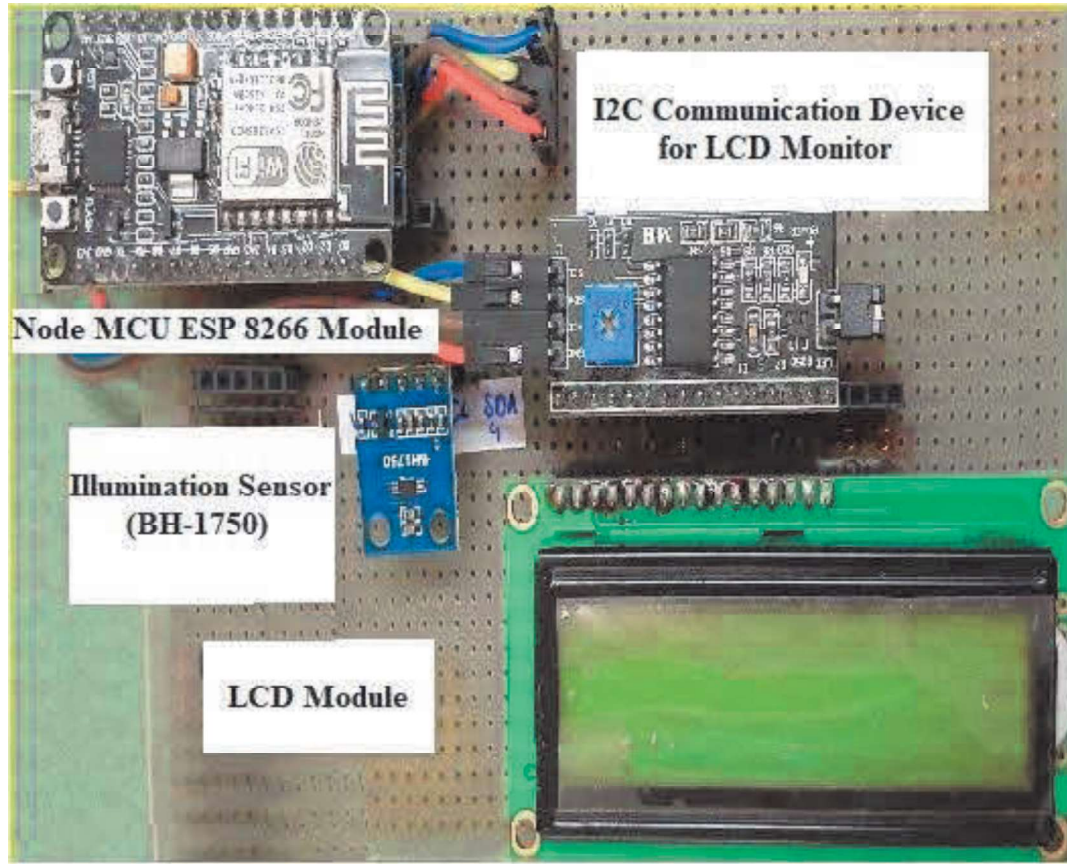


Fig. 3.4 Hardware set-up of experimentation unit using BH-1750

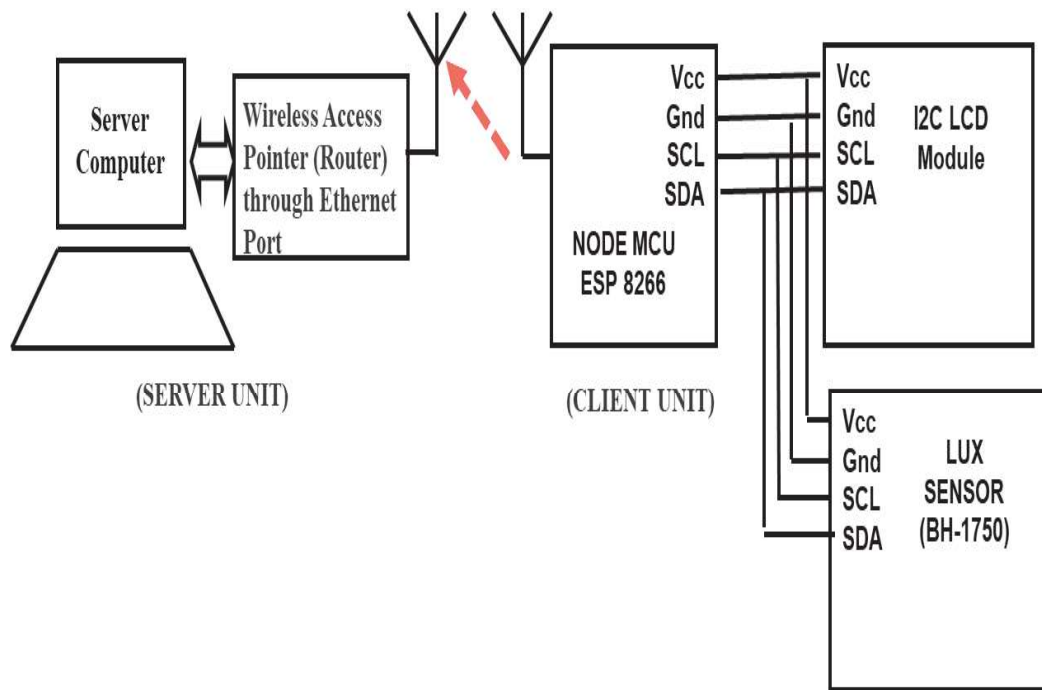


Fig. 3.5 Block diagram of experimentation unit using BH-1750

Fig. 3.3 and Fig. 3.4 represent the block diagram of proposed system and hardware set-up of the experimentation system respectively for performance analysis of the illumination sensor. Fig. 3.5 indicates the block diagram of the experimentation set-up. The client-server based network arrangement is done to eliminate the computational complexity at the client end and enable the server computer to perform the calculations therein. This helps in speeding up the measurement process and also the same network arrangement can be used as a mobile sensor node to conduct the illuminance monitoring of indoor space as elaborated in the next chapter of this thesis. The real-time picture of the standard lux meter is represented using Fig. 3.6. Initially, the proposed system is examined with a single illumination sensor. After successful implementation, it can be extended with more sensors within the same wireless network as the selected sensor is connected with I2C communication interface that permits the capability to integrate a larger number of sensors within the same network. For this reason, the selection of sensors as well as the controllers should be done carefully.

3.5.1 Results and Discussions

The training dataset for the illumination sensor and the calibrated lux meter is shown in Fig. 3.7, the testing dataset for the lux sensor and the reference illumination meter is illustrated in Fig. 3.8. The plot of illumination sensor dataset and the reference lux meter with added random noise is represented in Fig. 3.9.



Fig. 3.6 Real-time picture of standard lux meter

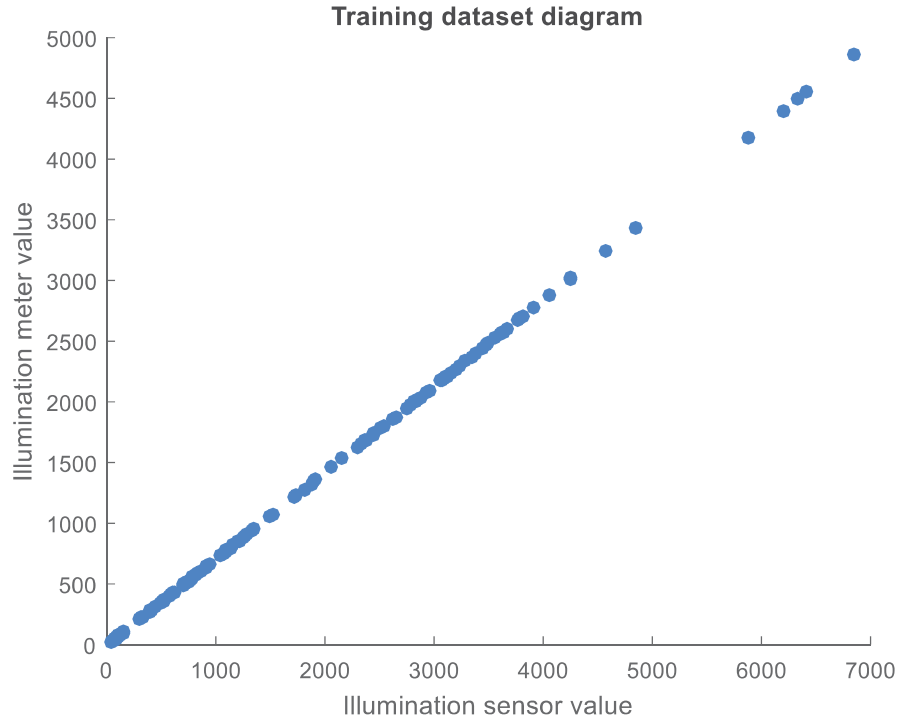


Fig. 3.7 Illumination training dataset for BH-1750

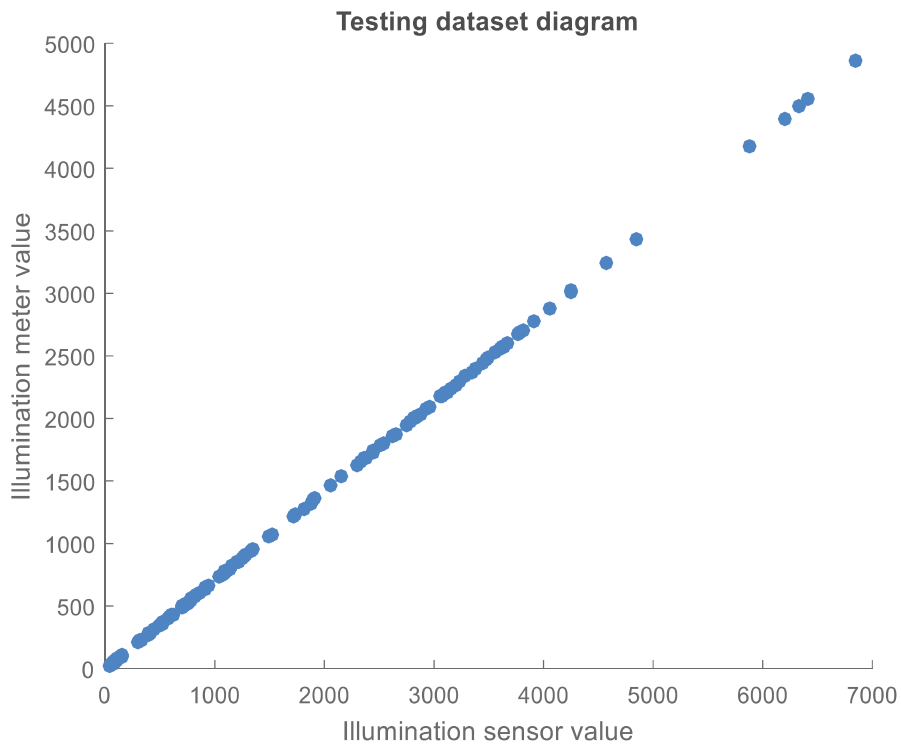


Fig. 3.8 Illumination testing dataset for BH-1750

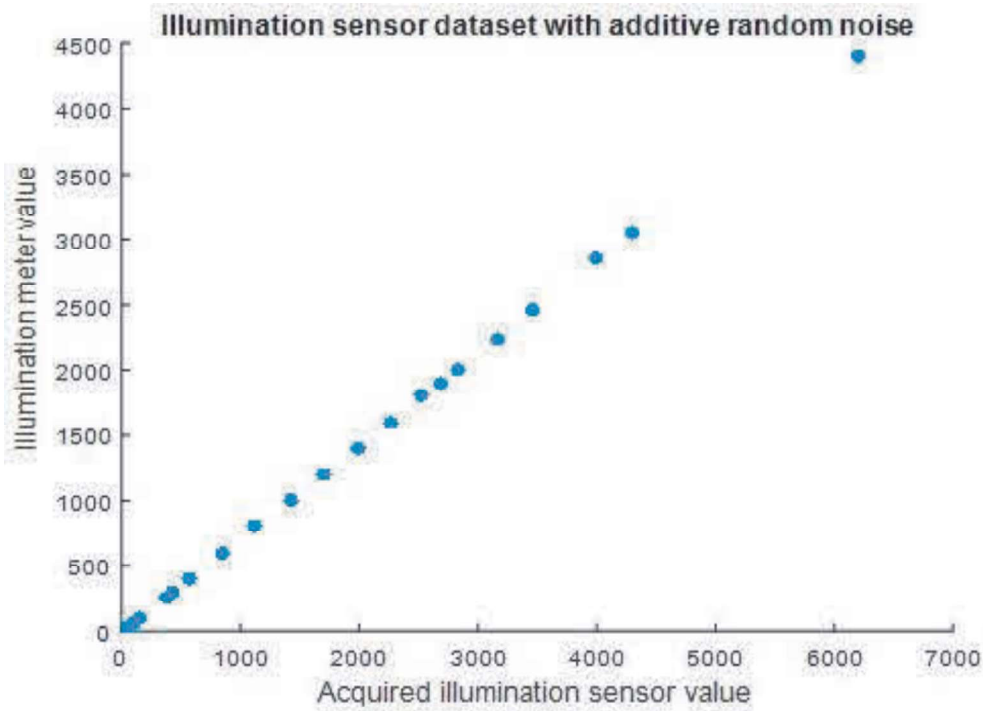


Fig. 3.9 Illumination dataset with added random noise for BH-1750

The acquired data from the illumination sensing board and standard lux meter is plotted and the experimental observations are noted. The Fig. 3.10 indicates the data plot using various scales e.g. 1st order polynomial scale, 2nd order polynomial scale, 3rd order polynomial scale, SVMR method, GPR method and finally GRNN method respectively. The unit of Standard Lux Meter data (along X-axis) and Sensor data (along Y-axis) is expressed in lux.

Equation for the predicted data with respect to standard lux meter data in 1st order polynomial regression scale:

$$\text{Predicted Sensor Data} = \beta_1 * x + \beta_0 \quad (3.19)$$

Whereas, $\beta_1=0.7114$, $\beta_0=-5.08$, $x=\text{Sensor Data}$

The data is first plotted in 1st order polynomial regression scale. The computed sensor data following equation (3.19) with respect to the standard lux meter is shown in Fig. 3.10 which depicts that the plot obtained after computation is better fitted.

Equation for the predicted data with respect to standard lux meter data in 2nd order polynomial regression scale:

$$\text{Predicted Sensor Data} = \beta_2 * x^2 + \beta_1 * x + \beta_0 \quad (3.20)$$

$\beta_2=0.000002$, $\beta_1=0.7017$, $\beta_0=2.983$, $x=\text{Sensor Data}$. After obtaining the 1st order polynomial regression plot, data is now plotted with respect to standard lux meter along the 2nd order polynomial regression scale as shown in Fig. 3.10 following equation (3.20). The

computed 2nd order polynomial regression plot of the sensor is slightly inferior to the 1st order polynomial regression plot.

Equation for the predicted data with respect to standard lux meter data in 3rd order polynomial regression scale:

$$\text{Predicted Sensor Data} = \beta_3 * x^3 + \beta_2 * x^2 + \beta_1 * x + \beta_0 \quad (3.21)$$

$$\beta_3=0.00000000087, \beta_2=0.0000087, \beta_1=0.6897, \beta_0=8.709, x=\text{Sensor Data.}$$

Next, the observed data is plotted in 3rd order polynomial regression scale with respect to the standard lux meter following equation (3.21), as shown in Fig. 3.10. It can be observed from the figure that this computed plot of the 3rd order polynomial scale is the most inferior to all the previous plots. Also, it is significant to mention that with increase in the degree of polynomial the system complexity increases but the performance is significantly degraded.

It can be observed from Fig. 3.10 that the GPR method is giving the best response than 1st order polynomial regression, 2nd order polynomial regression, 3rd order polynomial regression, SVMR, and GRNN techniques. The reason behind this may be due to the fact that a Gaussian model can capture the system uncertainty quite well although the computational complexity and computation time may remain on the higher side. Hence, for the acquired dataset GPR type regression technique is best fitted for mimicking the performance of a standard lux meter.

The percentage absolute error (PAE) plot for the computed sensor data along 1st order polynomial scale, 2nd order polynomial scale, 3rd order polynomial scale, SVMR scale, GPR scale, and GRNN scale with respect to the standard lux meter is shown in Fig. 3.11. The illumination values obtained from the sensor is in lux (along X-axis) and Percentage error values are presented in percent (along Y-axis). It was observed earlier that the deviation of sensor data from the true value in absence of proper regression technique is beyond the acceptable limit. Hence, it is justified to apply suitable regression algorithms and compute the data accordingly prior to its practical implementation in real-time application. It can be observed from Fig. 3.11 that the PAE for GPR method is considerably lower than the various grades of polynomial regression, SVMR and GRNN technique. The error is highest for the SVMR method, it reduces when 2nd order polynomial regression, 3rd order polynomial regression, and GRNN method is applied. It reaches almost close to the true value for all the test data in case of GPR method that gives the most suitable response.

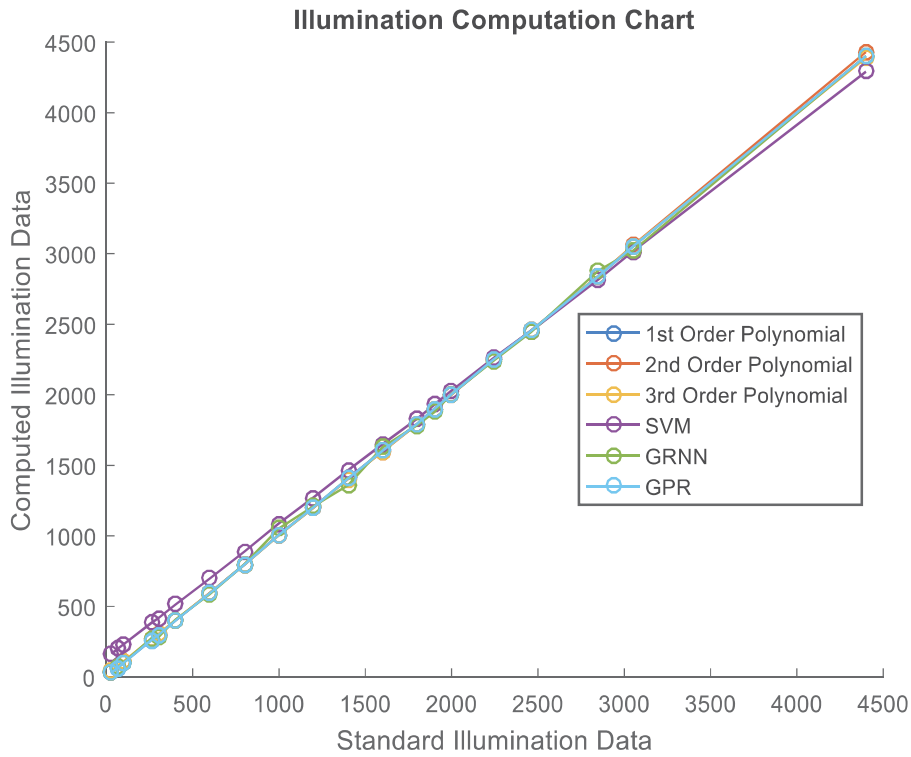


Fig. 3.10 Illuminance computation chart of different MLR techniques using BH-1750

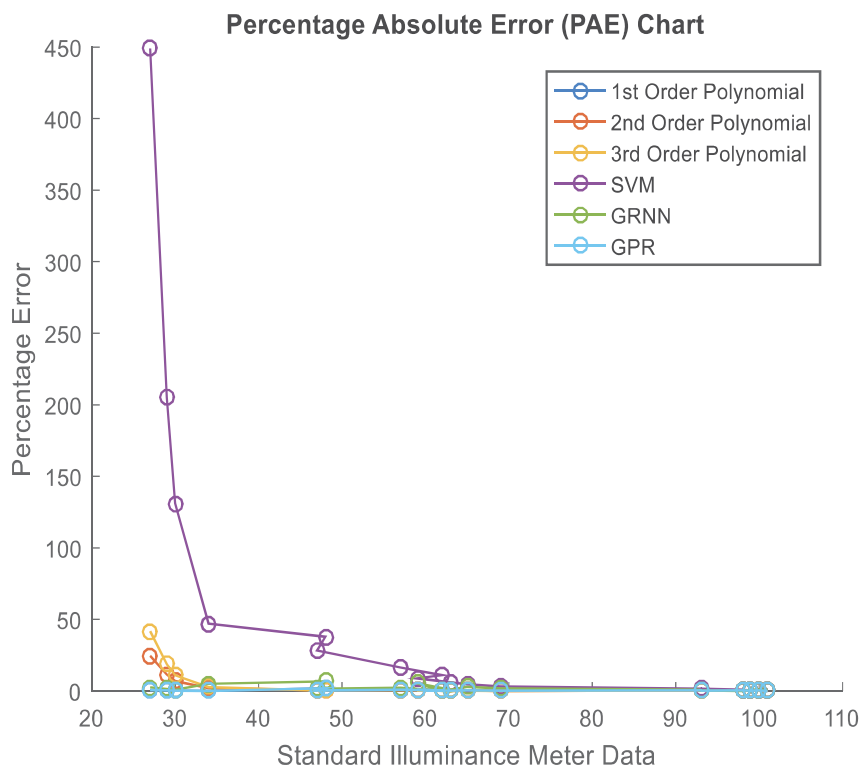


Fig. 3.11 PAE chart of different MLR techniques for lux estimation using BH-1750

Table 3.1: Evaluation of Performance Indices for Illuminance Estimation using BH-1750

Scale Type	R ²	MAE	RMSE	Avg. PAE	Avg. PAE (with random noise)
PR-Degree-I	0.99	3.86	4.95	0.44	0.49
PR-Degree-II	0.99	6.01	8.54	2.61	2.54
PR-Degree-III	0.99	5.75	6.90	4.14	3.97
SVMR	0.99	75.10	86.12	50.34	47.85
GRNN	0.99	15.47	21.20	1.90	1.94
GPR	0.99	3.72	4.93	0.43	0.49

Table 3.1 depicts the performance analysis of the sensor after application of PR, SVMR, GPR, and GRNN technique. For each case R-squared error, mean absolute error (MAE), root mean squared error (RMSE), average percentage absolute error (PAE) both in absence of noise and in presence of random noise is calculated. It can be observed from the table that the value of R² remains same for each method. The MAE, RMSE, and average PAE in absence of noise as well as in presence of random noise is most satisfactory for the GPR method, followed by 1st order polynomial regression technique, GRNN method, 2nd order polynomial regression, and 3rd order polynomial regression. However, SVMR method gives the worst response. It is of worth mentioning that there were 180 training data and 20 testing data available in the real-time acquired dataset. It is noteworthy to mention that the performance of the 1st order polynomial regression method is also satisfactory to some extent and in comparison with other peers but anyhow the regression response is inferior if compared with the GPR method.

Hence, GPR technique is considered to be the most suitable regression technique from our conducted analysis after taking into account the MAE value, RMSE data, and the average PAE values both in absence as well as in presence of random noise to predict the illumination sensor data with respect to a standard lux meter.

3.6 Experimental Set-Up for Estimation of Illuminance and Correlated Colour Temperature from RGB Sensor Data

The experimentation system help in measurement of illumination and Correlated Colour Temperature (CCT) values using a RGB sensor that is interfaced with wifi enabled microcontroller. The RGB sensors are installed at strategically important indoor space and serves as the client terminal. The sensors transmit RGB, illumination and CCT values to a computer that functions as a server unit in a wireless network. The problem with this notion is that it will be more time consuming to send all the acquired parameters collectively to the server terminal. However, considerable amount of time can be saved if fewer parameters are sent and the remaining parameters are calculated therein. The processing speed of the system will be maximized with minimal memory requirement and energy consumption at the client terminal. A better proposition will be to acquire the RGB data, transmit them through the client terminal and process them using regression techniques to find the sensor model to predict all required parameters at the server end. These data may also be shared in a cloud network with the permitted users to alert the maintenance section to take corrective actions if the measured values fall below a threshold level. Moreover, preventive actions may be taken if the CCT values approach towards the threshold level because of ageing effect or any other reasons. Hence, both corrective maintenance as well as preventive maintenance can be planned properly [143]. The block diagram of our proposed system is shown in Fig. 3.12 and the real-time picture of the developed setup is represented using Fig. 3.13. Fig. 3.14 indicates the block diagram of the experimentation system.

This experiment is initiated with a single RGB sensor in I2C communication mode and afterwards the wireless network can be extended with more sensors within the same network configuration. The proposed system is comprised of the following sub-units:

- a. Client Terminal: The client module consists of TCS34725 RGB sensor using I2C communication mode to integrate more sensors and 32-bit ESP 8266 wifi-enabled Tensilica L106 microcontroller based embedded system. The RGB sensor is interfaced with Node MCU ESP 8266 controller unit to capture the sensor data and transmit them to the server terminal using a wireless network. The RGB sensor along with the controller module together forms the client terminal, which is powered by a proficient power source or by a rechargeable battery.

b. Server Terminal: A wireless router establishes client-server communication through Ethernet port having particular IP address. The RGB sensor values are stored at the server terminal and converted to CCT values using the most appropriate regression technique.

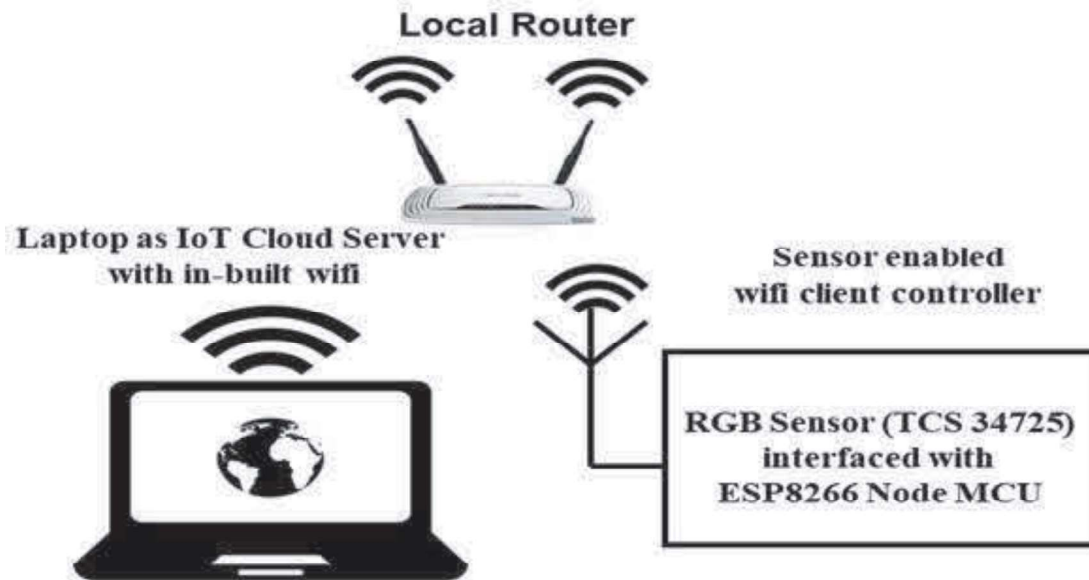


Fig. 3.12 Block diagram of proposed system using TCS 34725

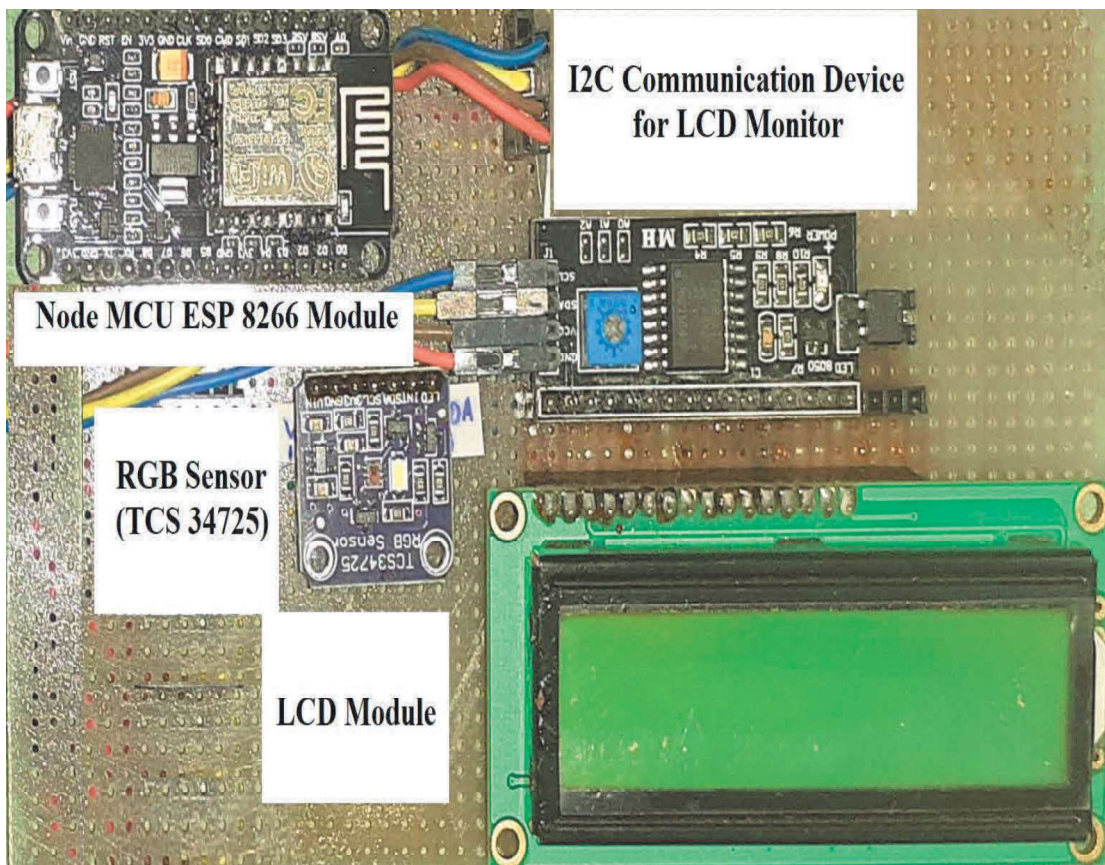


Fig. 3.13 Real-time picture of experimentation unit using TCS 34725

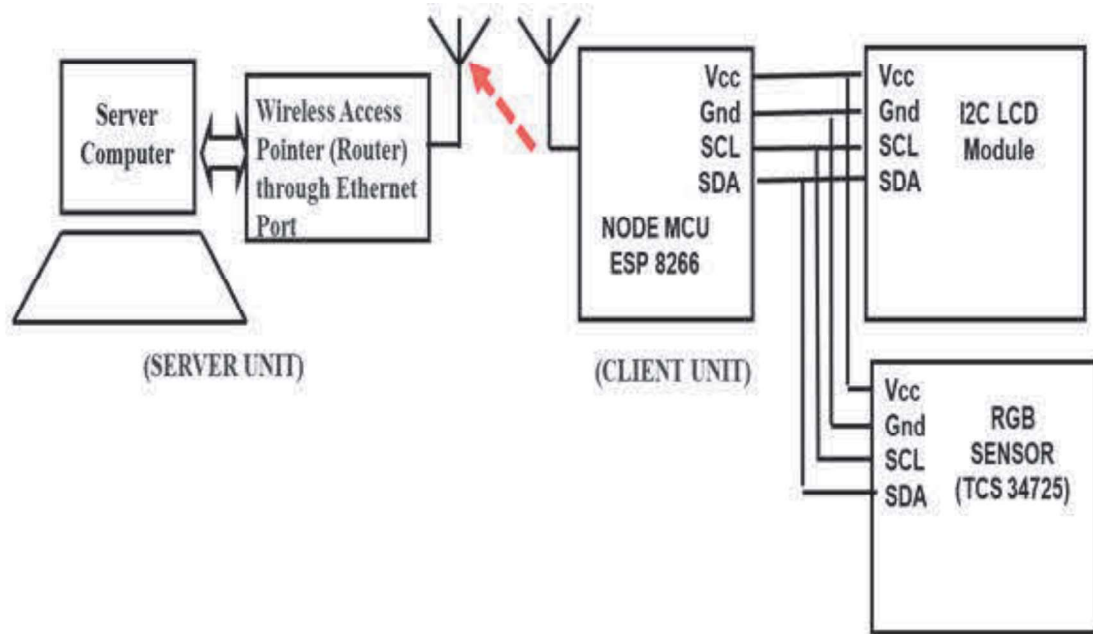


Fig. 3.14 Block diagram of experimentation unit using TCS 34725

c. **Wireless Router:** A TP-Link made wireless router is used in the experiment. The wireless controller at the client terminal consists of an IP address through which it acquires RGB values at the indoor location and transmits them to the fixed port address of wireless router. It is redirected to the server computer to convert into CCT values using different types of regression model. An authorized user can check whether the computed data are below the threshold limit and thus a wireless client-server network is established.

d. **Chroma Meter:** The CCT values for each RGB input is noted by the help of a chroma meter (Model No: CL-200A, S/L No: 30D10039), which is available in the Illumination Engineering Laboratory of the Jadavpur University. The total specification of the Konika made Chroma meter is available in [144]. The real-time picture of the standard chroma meter is represented using Fig. 3.15.

3.6.1 Results and Discussions

The illuminance parameter is computed using four different types of machine learning modelling techniques from the acquired RGB values. The input values are varied by changing the LED luminaries for different lighting conditions. The training dataset and validation dataset have been represented using Fig. 3.16 and Fig. 3.17 respectively. Fig. 3.18 and Fig. 3.19 show the sensor dataset diagram for illumination and CCT measurement respectively with added random noise.



Fig. 3.15 Real-time picture of standard chroma meter

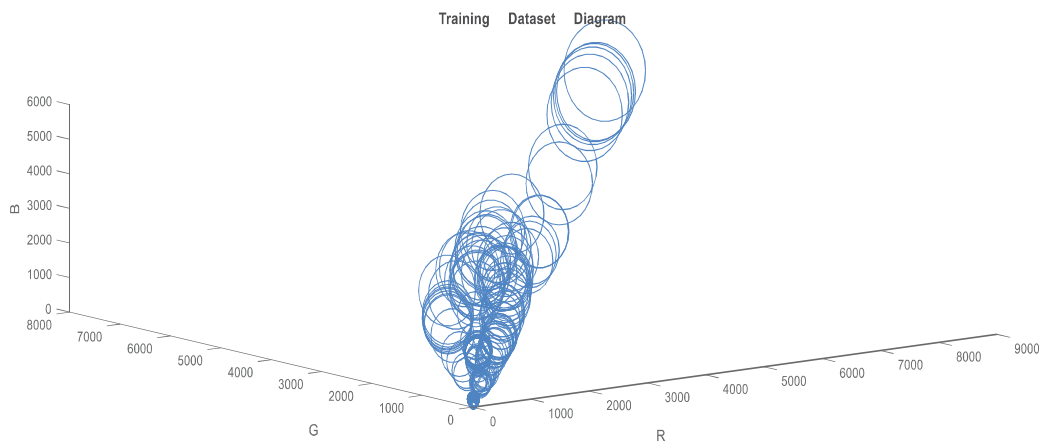


Fig. 3.16 Training Dataset Diagram for TCS 34725

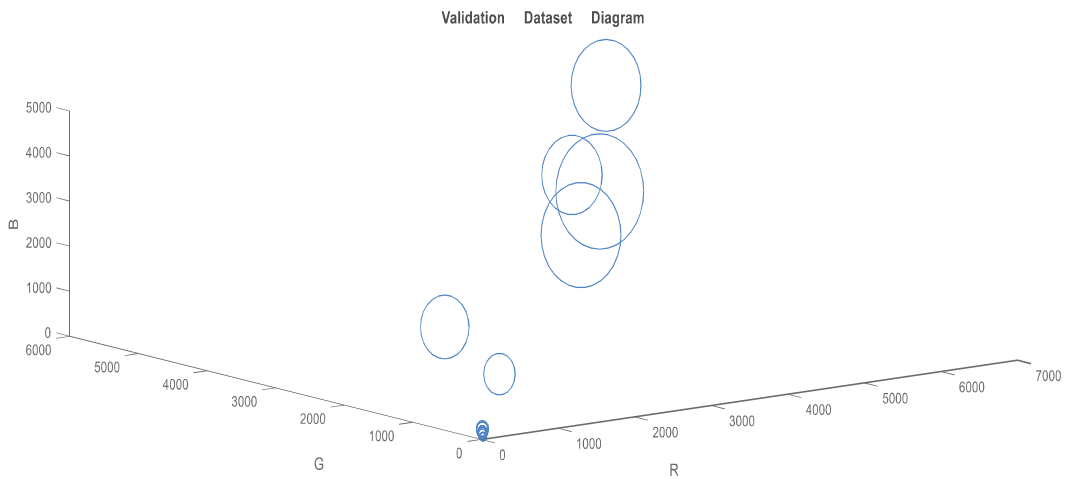


Fig. 3.17 Validation Dataset Diagram for TCS 34725

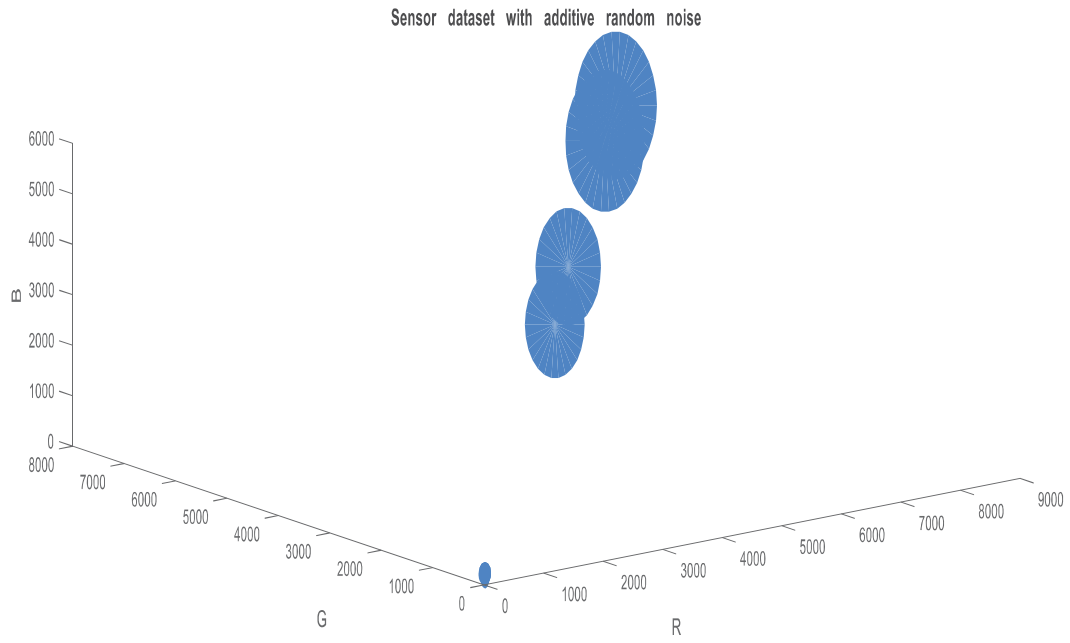


Fig. 3.18 Sensor Dataset for Illumination Measurement with added random noise for TCS 34725

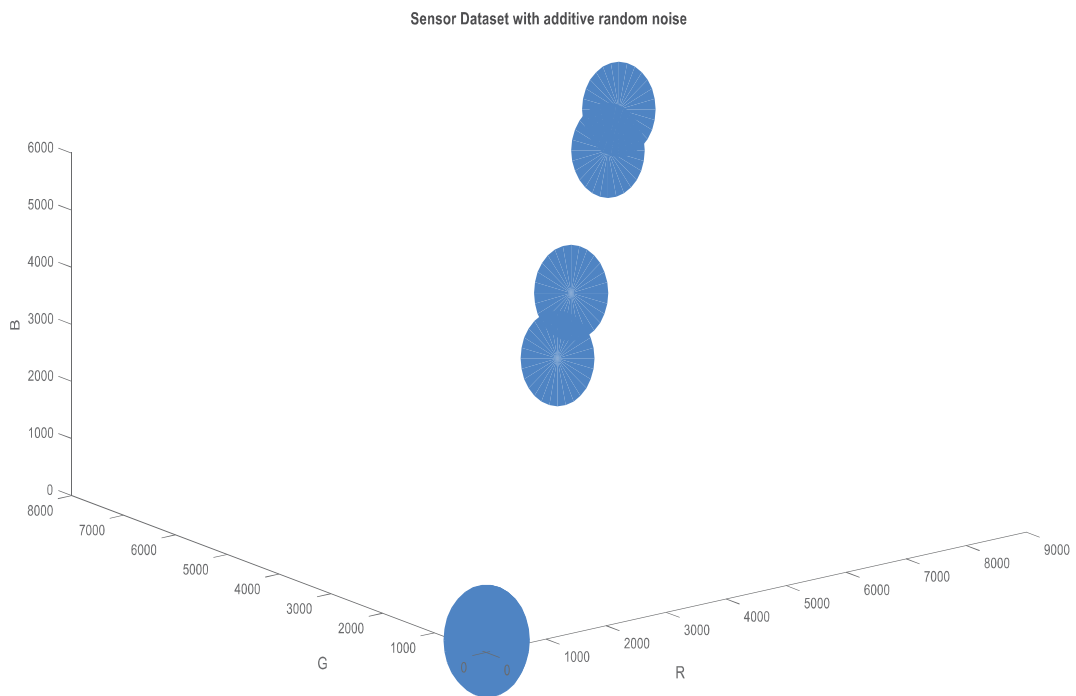


Fig. 3.19 Sensor Dataset for CCT Measurement with added random noise for TCS 34725

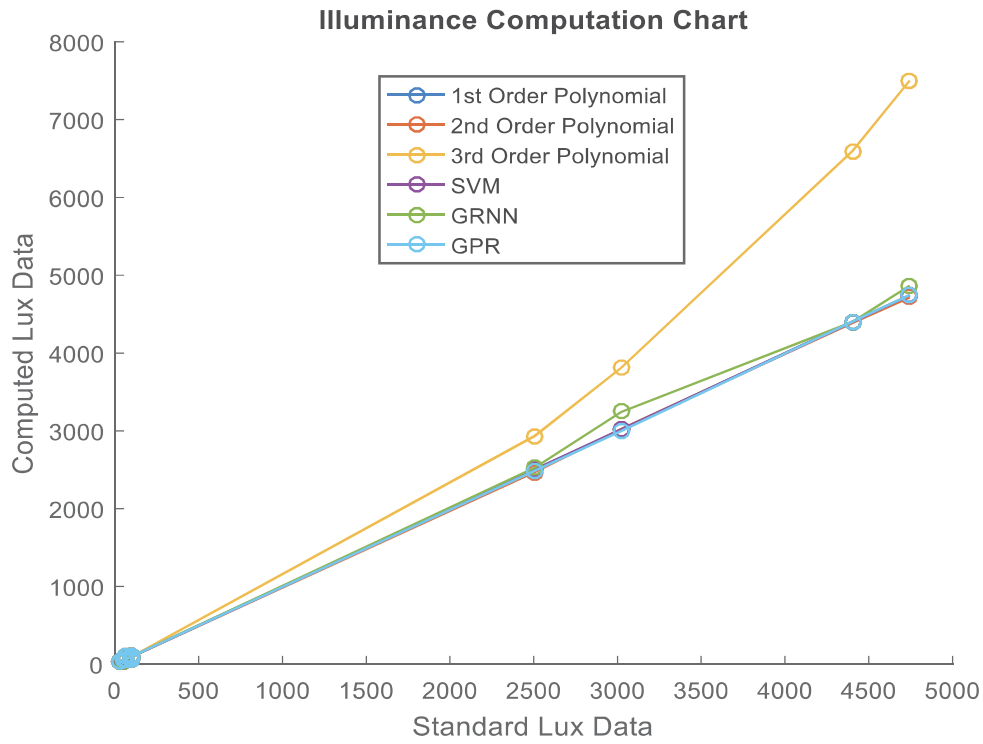


Fig. 3.20 Illuminance computation chart of different MLR techniques using TCS 34725

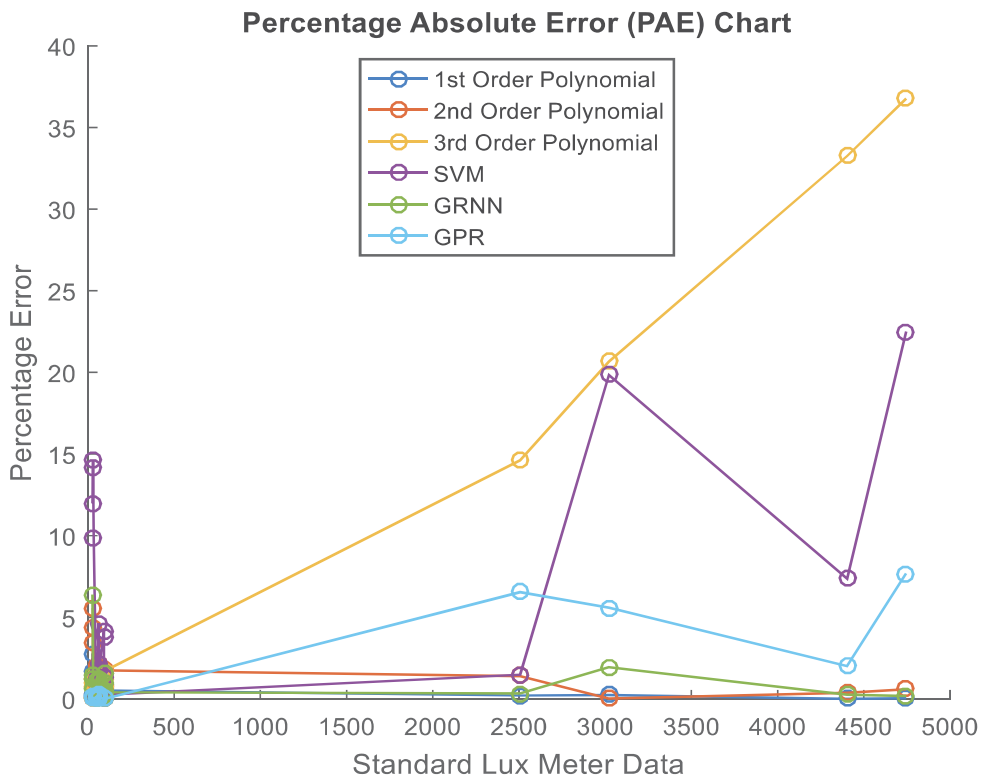


Fig. 3.21 PAE analysis chart of different MLR techniques for lux estimation using TCS 34725

Now, these parameters were considered for regression analysis to select the best model for predicting the lux parameters from RGB values in terms of performance evaluating indices. The feature engineering technique used here was outlier handling. Outliers in the dataset were removed using moving median filter as it provides a satisfactory estimation of the data under study. The research findings along with their performance curves for all the regression methods are listed below followed by the data analysis table. The obtained results are analyzed in detail to find the single best model amongst all the considered techniques that can be used for prediction of lux from any unknown RGB value.

The illuminance and CCT parameters are computed using four different types of machine learning modeling techniques from the acquired RGB values. The input values are varied by changing the LED luminaries for different lighting conditions. The number of real-time training data considered for this experimental study was around 180 and the number of validation data considered for this work was 20. Now, these parameters were considered for regression analysis to select the best model for predicting the lux and CCT parameters from the RGB values in terms of performance evaluating indices. The research findings along with their performance curves for all the regression methods are listed below followed by the data analysis table. The obtained results are analyzed in detail to find the single best model amongst all the considered regression techniques that can be used for prediction of the lux and CCT parameters from any unknown RGB value.

Computation chart of all the considered regression techniques for estimation of illuminance values is represented in Fig. 3.20, whereas, Fig. 3.21 represents the percentage absolute error analysis in predicting the lux values. Next, the formula obtained for prediction of illuminance from the RGB sensor values are to be found out.

The formula for prediction of lux using 1st order polynomial regression is as follows:

$$Lux1 = \alpha_0 + \alpha_1 * R + \alpha_2 * G + \alpha_3 * B \quad (3.22)$$

The coefficients are, $\alpha_0 = -0.66421$, $\alpha_1 = -0.39438$, $\alpha_2 = 1.718$, $\alpha_3 = -0.81213$

The formula for prediction of lux using 2nd order polynomial regression is as follows:

$$Lux2 = \alpha_0 + \alpha_1 * R^2 + \alpha_2 * G^2 + \alpha_3 * B^2 + \alpha_4 * R + \alpha_5 * G + \alpha_6 * B + \alpha_7 * R * G + \alpha_8 * G * B + \alpha_9 * R * B \quad (3.23)$$

The coefficients are, $\alpha_0 = 2.4599$, $\alpha_1 = -0.0060158$, $\alpha_2 = -0.0077577$, $\alpha_3 = 0.0064361$, $\alpha_4 = -1.0277$, $\alpha_5 = 3.1942$, $\alpha_6 = -1.826$, $\alpha_7 = 0.016477$, $\alpha_8 = -0.0054618$, $\alpha_9 = -0.0031938$

The formula for prediction of lux using 3rd order polynomial regression is as follows:

$$Lux3 = \alpha_0 + \alpha_1 * R^3 + \alpha_2 * G^3 + \alpha_3 * B^3 + \alpha_4 * R^2 + \alpha_5 * G^2 + \alpha_6 * B^2 + \alpha_7 * R + \alpha_8 * G + \alpha_9 * B + \alpha_{10} * R * B^2 + \alpha_{11} * G * B^2 + \alpha_{12} * G^2 * B + \alpha_{13} * R * G + \alpha_{14} * G * B + \alpha_{15} * R * B + \alpha_{16} * R * G^2 + \alpha_{17} * R^2 * B + \alpha_{18} * R^2 * G + \alpha_{19} * R * G * B \quad (3.24)$$

The coefficients are, $\alpha_0=-0.4263$, $\alpha_1=-0.00000543$, $\alpha_2=-0.000175$, $\alpha_3=0.000122$, $\alpha_4=0.00582$, $\alpha_5=-0.00923$, $\alpha_6=-0.02546$, $\alpha_7=-0.321$, $\alpha_8=1.4774$, $\alpha_9=-0.60053$, $\alpha_{10}=0.000114$, $\alpha_{11}=-0.000399$, $\alpha_{12}=0.000467$, $\alpha_{13}=-0.0106$, $\alpha_{14}=0.04197$, $\alpha_{15}=-0.00396$, $\alpha_{16}=0.0001488$, $\alpha_{17}=0.0000549$, $\alpha_{18}=-0.0000267$, $\alpha_{19}=-0.0002999$

Table 3.2 depicts the evaluation of performance indices for estimation of illuminance values. From the table it can be understood that 1st order Polynomial regression technique can be applied on the observed data as it can map the model almost accurately. Hence, the expression obtained can be applied for estimation of lux. Also, GPR technique provides satisfactory response with respect to most of the performance parameters except RMSE. Therefore, either of these methods may be chosen if it can map the other parameter i.e. CCT values accurately. The performance of 2nd order Polynomial regression method and the SVMR technique is degraded than 1st Order Polynomial regression and GPR techniques but it gives better performance than 3rd order Polynomial regression method and GRNN technique.

Table 3.2: Evaluation of Performance Indices for Lux Estimation using TCS 34725

Scale Type	R ²	MAE	RMSE	Avg. PAE	Avg. PAE (with random noise)
PR-Degree-I	0.99	0.912	1.917	1	2
PR-Degree-II	0.99	4.081	9.972	1	2
PR-Degree-III	0.99	268.469	758.225	5	10
SVMR	0.99	5.597	11.427	5	3
GRNN	0.99	20.304	53.898	1	2
GPR	0.99	1	13.055	1	1

Fig. 3.22 represents the computational chart of the machine learning based regression techniques for prediction of CCT values. On the other hand, percentage absolute error analysis in estimating the CCT values is expressed in Fig. 3.23. Now, the formula obtained for prediction of CCT data from the RGB sensor value are to be found out.

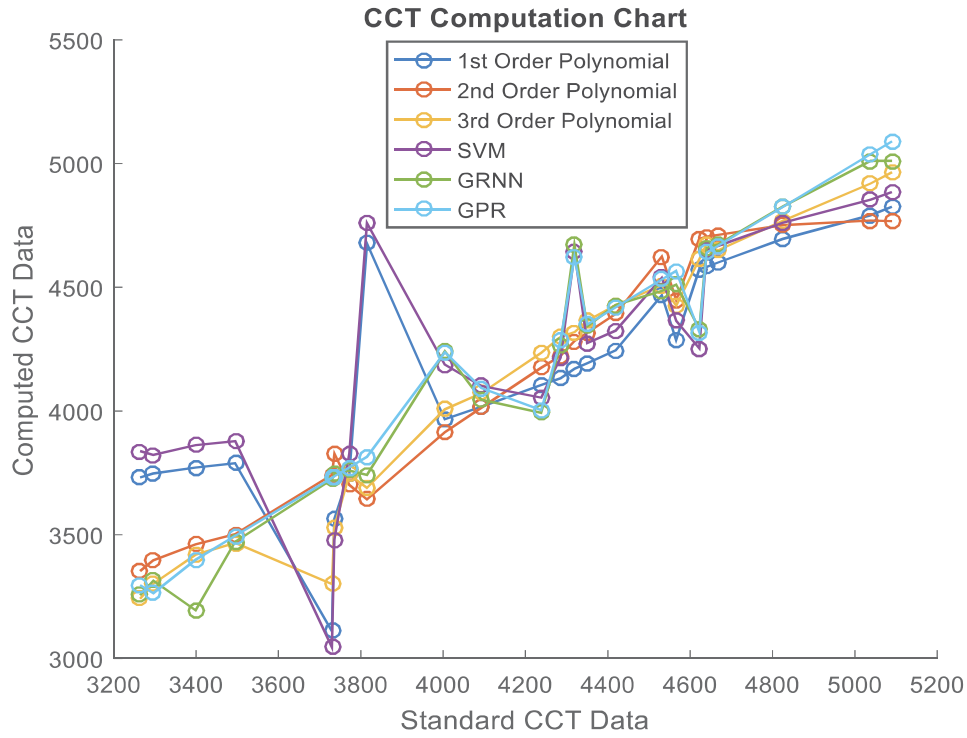


Fig. 3.22 CCT computation chart of different MLR techniques using TCS 34725

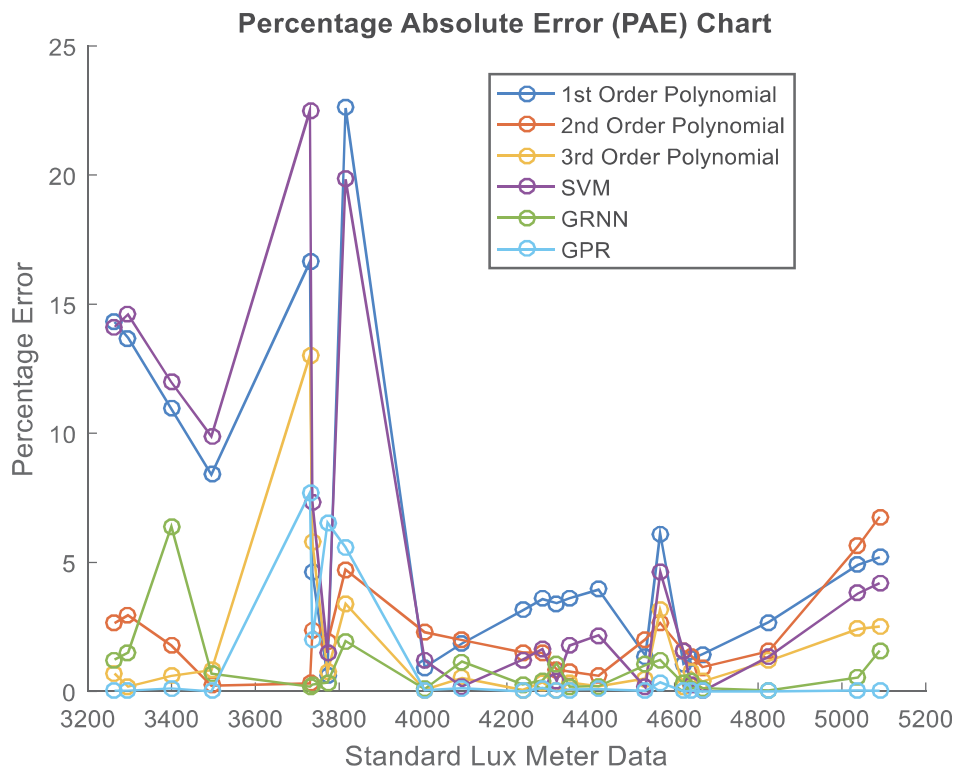


Fig. 3.23 PAE analysis chart of different MLR techniques for CCT estimation using TCS 34725

The formula for prediction of CCT value using 1st order polynomial regression is as follows:

$$CCT1 = a_0 + a_1 * R + a_2 * G + a_3 * B \quad (3.25)$$

The coefficients are, $a_0 = 3896.9588$, $a_1 = -19.723382$, $a_2 = 17.724858$, $a_3 = 7.3987894$

The formula for prediction of CCT value using 2nd order polynomial regression is as follows:

$$CCT2 = a_0 + a_1 * R^2 + a_2 * G^2 + a_3 * B^2 + a_4 * R + a_5 * G + a_6 * B + a_7 * R * G + a_8 * G * B + a_9 * R * B \quad (3.26)$$

The coefficients are, $a_0 = 3765.0872$, $a_1 = -0.47228144$, $a_2 = -0.4014306$, $a_3 = -0.074886073$, $a_4 = -43.437815$, $a_5 = 36.638271$, $a_6 = 19.402285$, $a_7 = 0.86364855$, $a_8 = -0.29820113$, $a_9 = 0.34547207$

The formula for prediction of CCT value using 3rd order polynomial regression is as follows:

$$CCT3 = a_0 + a_1 * R^3 + a_2 * G^3 + a_3 * B^3 + a_4 * R^2 + a_5 * G^2 + a_6 * B^2 + a_7 * R + a_8 * G + a_9 * B + a_{10} * R * B^2 + a_{11} * G * B^2 + a_{12} * G^2 * B + a_{13} * R * G + a_{14} * G * B + a_{15} * R * B + a_{16} * R * G^2 + a_{17} * R^2 * B + a_{18} * R^2 * G + a_{19} * R * G * B \quad (3.27)$$

The coefficients are, $a_0 = 3709.327$, $a_1 = -0.026882$, $a_2 = 0.030058$, $a_3 = 0.003391$, $a_4 = -1.448997$, $a_5 = -1.68641$, $a_6 = -0.27325$, $a_7 = -28.8987$, $a_8 = -6.229048$, $a_9 = 55.55895$, $a_{10} = 0.00531$, $a_{11} = -0.013587$, $a_{12} = 0.02657$, $a_{13} = 3.0297$, $a_{14} = -0.27045$, $a_{15} = 0.547907$, $a_{16} = -0.093398$, $a_{17} = 0.00867$, $a_{18} = 0.088377$, $a_{19} = -0.02828$

The performance evaluation parameters for estimation of CCT values are enumerated in Table 3.3. From the table, it can be described that GPR technique can be applied successfully as it can map the model almost accurately than all the other methods. Thus, the obtained model can be applied for estimation of CCT values. Furthermore, 3rd order polynomial regression technique provides satisfactory response closer to the GPR method in terms of some performance evaluating metrics. Therefore, either of them may be chosen for estimation of CCT data. The performance of 2nd order polynomial regression method and GRNN technique is degraded than the aforesaid two techniques but better than the 1st order polynomial regression process, and SVMR technique.

Table 3.3: Evaluation of Performance Indices for CCT Estimation using TCS 34725

Scale Type	R ²	MAE	RMSE	Avg. PAE	Avg. PAE (with random noise)
PR-Degree-I	0.665	230.389	307.190	6	6
PR-Degree-II	0.961	89.264	115.282	2	2
PR-Degree-III	0.966	63.272	114.221	2	2
SVMR	0.578	255.130	351.662	7	7
GRNN	0.944	78.261	130.134	2	2
GPR	0.955	49.478	113.286	1	1

The advantages of polynomial regression are that it provides best approximation relationship between the dependent and independent variables, simultaneously; it offers a wide range of curve-fitting functions. This regression technique is more flexible and an empirical model can be developed as the transformation from the input to the output can be interpreted easily. However, it suffers from the fact that it is very much sensitive to outliers; hence, with the increase in the number of outliers, its response gets severely affected. We can observe that some polynomial techniques can map the illuminance and CCT values satisfactorily but any single model cannot be applied to predict both of them as a whole. Moreover, with the increase in the order of polynomial, the prediction performance is minimally enhanced sometimes but at the cost of increase in the number of coefficients, which further escalates the system complexity. This is the reason for non-consideration of polynomial regression technique as a preferable solution. Further, we have used SVMR technique. This method works well for unstructured or semi-structured data, it scales high-dimensional data profoundly and it has generalization capability, hence the risk of model overfitting is less. However, selection of an ideal kernel is not easy and the training time increases with large number of data. In case of illuminance and CCT prediction we have used linear kernel and the observed response is non-satisfactory. Also we have used SMO type optimizer to reach the optimal solution in short duration but because of the selection of linear kernel, the performance seems unacceptable. Then, we have used GRNN technique which is a variant of radial basis function. It is a kind of single pass learning, so backward propagation is not required. It can handle noise in the captured data and requires lesser amount of data to give an accurate estimation but it suffers in handling a large dataset to become computationally complicated and it is comparatively insensitive to outliers. For prediction of lux, the performance of GRNN technique is inferior to 1st order polynomial regression, 2nd order polynomial regression, SVMR technique, and GPR technique but it is superior to 3rd order polynomial regression. However, for predicting the CCT value, it is superior to 1st order polynomial regression and SVMR technique but inferior to 2nd order polynomial regression and 3rd order polynomial regression technique. GRNN technique gives a faster solution at the expense of larger memory space. That is why it gave satisfactory response in comparison to some of the techniques although it did not appear to be the single best model. Finally, we will discuss the GPR technique which gives probability distribution function in Bayesian inference. The advantage of this powerful multivariate interpolation technique is that it can handle the model uncertainty very well using proper covariance function and gives a nice fit with equally good performance even in presence of noise. The main advantage lies in its

usability and flexibility in addressing non-linearity as it gives probability distribution over possible functions using Bayes' rule. Overall, if a single regression modelling technique is to be selected for prediction of both illuminance and CCT values from RGB sensor, it is the best to use GPR model considering its superior performance than its all other counterparts as a whole.

It is noteworthy to mention that a sensor may be exposed to various conditions which can never be considered as a whole in a simple regression procedure. Also, the sensor output accuracy may be different when it is facing extreme adversities. Moreover, ageing, frequency of use, atmospheric condition may also degrade the performance of an instrument. The different regression methods described in this thesis is easy to design, cost-effective and quite easily achieves high-accuracy with simple calculations. Amongst all the techniques considered here, GPR method is giving the most accurate response similar to that of a calibrated lux meter. However, some other versions of illuminance sensors and other types of regression techniques may also be tested to find out the most effective method. The experiment was conducted in a dark room which can also be done in presence of natural light and can become a part of our future investigation.

A sensor may be exposed to varying conditions and all of them should be considered in the training dataset prior to the selection of any appropriate regression model. The different methods discussed here are standard techniques yet cost-effective and also some of them yield high accuracy. Amongst the regression models considered for this study, GPR method gives the best possible response similar to that of a pre-calibrated reference meter. However, some more accurate sensors, if available in the market, may also be tested. To find out the efficacy of any regression method, an enhanced training and validation dataset can be used. The techniques that have been used here are popular for giving satisfactory response even in presence of noise. The experiment was conducted in a dark room which can also be done in presence of natural light and may be part of our future findings. Some other types of regression techniques can also be explored as a separate study to obtain better performance. The selected model may be used in some allied applications to understand the suitability of the regression method. These are all being investigated now and to be accomplished in near future.

Chapter Summary

This chapter depicts the different types of machine learning regression techniques for estimation of illuminance using sensor data prior to its use in any application. Two different types of sensors viz. illumination sensor and RGB sensor were used for estimating the lux values using four types of regression techniques in presence of a pre-calibrated reference meter and the experimental outcomes were overall satisfactory. If the reference meter is not available due to cost or some other reasons then the acquired sensor models may be used for finding out the true sensor value from the raw sensor data. Over and above, from the RGB sensor data apart from illuminance, CCT values may also be found out using the similar regression techniques that have been used for estimating the value of illuminance data and also forms a part of our experimental analysis. The next chapter depicts the method of automated illuminance monitoring in indoor space using both lux sensor and RGB sensor in a wireless network.

Chapter 4

Automated Indoor Illuminance Monitoring System

4.1 Introduction

The rising demand for improving the quality of life requires for increase in system complexity. Nowadays the physical objects are connected to a network which can be wired or wireless in nature and can be accessed through the internet, which is called the ‘Internet of Things’. The objects contain embedded technology by which it can interact with the external environment. The sensor values obtained from the connected objects can be displayed, recorded for future use as well as can be transmitted to a remote location for display, monitoring, control or any other purpose. It was estimated that by 2020 almost 50 billion objects were to be connected with internet and for every person on an average almost six devices were to be internet enabled.

Efficient lighting design is one of the challenging tasks in today’s life. Fraudulent design may lead to partial or improper fulfilment of the application for which it has been designed. With the development of advanced sensors, and wireless networking, the systems those are built today, are quite superior to its antecedents. Major areas of public as well as private entities still use inefficient technologies e.g. fluorescent tubes and halogen lamps. They are yet to be completely replaced by present day LEDs throughout the globe [145]. In modern time, with

the development of science and technology, indoor lighting control system refers to many aspects like acquisition environment site, sensors used, remote monitoring, and man-machine interface to name a few. In this research work, the lighting technology used is not to be studied nor does it envisage about various sensors that may be used for lux monitoring. It also does not take into account of methodologies for improving the power system efficiency [146-147]. The designed system uses an electronic sensor for measuring illuminance at various areas of indoor space and remotely transmits the data to a client computer connected through a wireless link. The collected data can be saved in a file for future processing. A remote car integrated with the sensor is used to collect data from various sites of the selected indoor area. It uses a four channel infrared remote car to move in four different directions as and when required-forward, backward, right and left. This low cost, energy efficient system may also be applied for various other allied applications.

4.2 Objective of this Study

The objective of this work is to develop an intelligent illuminance monitoring system for efficient lighting design in indoor space using mobile sensor module. The sensor module comprises of lux sensor for capturing the illuminance values and also an IR transceiver module for detecting its location in indoor space. The sensor system is connected to the client unit and is mounted over a remote operated car whose movement is controlled by RF operated remote key pad. The car traverse through different locations at any selected indoor space and captures the lux values. The client unit communicates to the server unit via wi-fi router. The server unit stores the lux data of different position of indoor space in a file for further processing. The generated lux map can be compared with the reference lux map designed by an expert at different coordinate locations and based on the error in lux values preventive measures can be taken for modification of lighting design. Thus an efficient lighting system can be developed.

4.3 Related Literatures

An urban street light monitoring and remote control system was reported in [148] that comprised of sensor node installed at each lamp pole using multi-hop routing transmission protocol of Wireless Sensor Network (WSN) for detection and on/off control of lamp. The control system is developed using ATmega 128 MCU; it can minimize energy consumption

as well as maintenance cost, and improve the standard of public satisfaction. An intelligent LED based low cost, highly secured lighting system was proposed in [149] using raspberry pi processor with X-bee wireless communication between two modules which can be accessed from any place with internet connectivity. An embedded system called Hitchhiker was conceived in [150] that were installed over the roof of fixed route vehicles and the collected illumination readings were stored in Google server to identify faulty street lights. Another similar type of designed system was invented in [151] to mitigate the shortfalls of traditional lighting management systems and staff shortage. A robust real-time web based monitoring and controls of electrical appliances installed in a building were implemented in [152-153]. Security features of a ZigBee protocol to perpetrate various types of cyber threats were evaluated in [154].

In short, the gradual advancements since 2007 from street light monitoring through remote control system to the check of cyber threats have been developed step-wise to this date, is vividly discussed to look at the on-side modernization of the technique vis-à-vis unmanned smart rescue operation to server client based communication using low powered wifi module instead of a ZigBee module with limited operating range. Last but not the least; the data production rate is growing rapidly with the miniaturization of devices. This huge amount of data, also known as big data cannot be utilized unless proper analytics of the captured data set is done. Also, data compression, energy conservation and data security is still a large issue and these challenges are to be resolved shortly for better usage of the captured data in any application [155-156].

Here, we started with the block diagram of the experimental setup and description of various system modules. Then, we proceeded with the experimentation set up followed by observations obtained from the conducted experiment. Finally, the study ends with a conclusion.

4.4 Indoor Illuminance Monitoring System using Lux Sensor

The setup of integrated instrumentation platform is shown in Fig. 4.1. Fig. 4.2 represents the block diagram of the online illumination monitoring system using BH-1750. The developed system comprises of the following building blocks.

a. Client Unit: The client unit comprises of sensor and controller module. The sensor module consists of an illumination sensor (BH 1750) for monitoring illuminance of the area from where the car is traversing through and an IR transceiver, to locate various positions of a

moving car. The sensing system is interfaced with the NodeMCU controller module having on-chip wifi (ESP 8266) embedded with it in inter-integrated-circuit (I²C) mode of communication to develop the remote sensing system.

The controller module comprises of 32-bit Tensilica L106 microcontroller and ESP8266 based wifi unit to connect with secured wireless network; powered by rechargeable battery. A four-channel car integrated with client unit is used to drive the mobile car across various locations of the indoor space via RF keypad and the acquired sensor values are stored in a file at the server end.

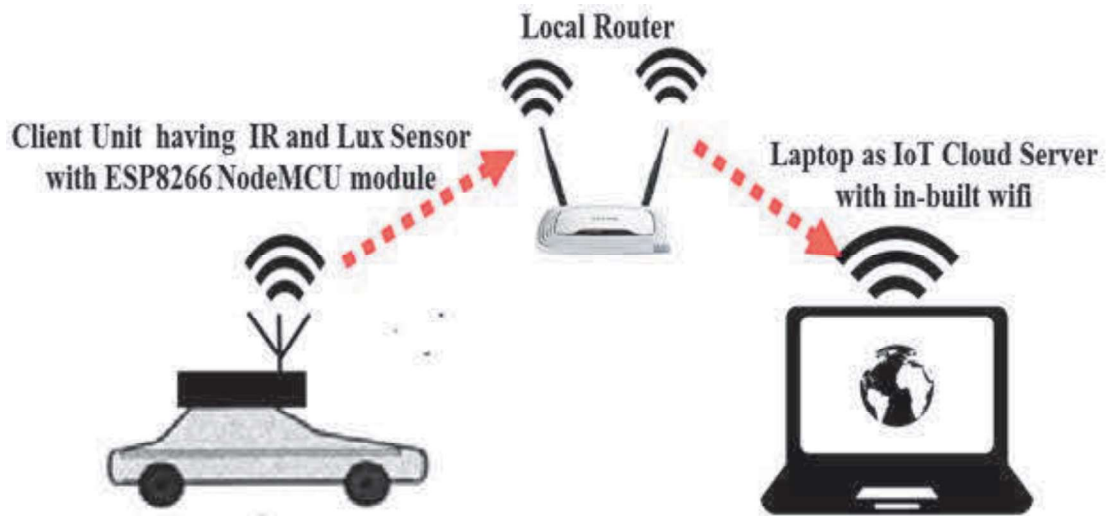


Fig. 4.1 Online illuminance monitoring system using BH-1750

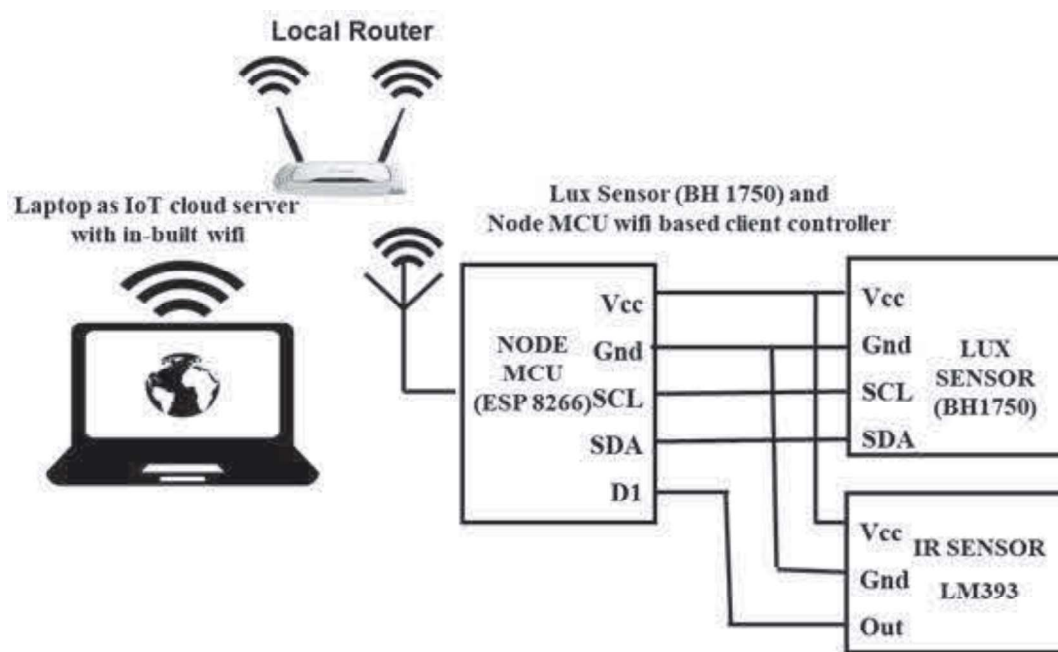


Fig. 4.2 Block diagram of online illuminance monitoring system using BH-1750

- b. Server Unit: A laptop with Intel Core i3 (fifth generation/newer) with MS-Windows 8.1/10 x32/x64 bit Operating System, 4 Gb RAM, Display: 14" LCD, Network Adapter: 802.11ac 2.4/5 GHz wireless functions as the server unit. The laptop should be connected to a secured local router via network cable.
- c. Router Unit: A local wifi router having one/two antennas, 12-20 Mbps speed, wireless standard IEEE 802.11X and security WEP/WPA/WPA2 may be used which acts as wireless access pointer to setup communication link between client and server node. This is connected to Ethernet port with IP address. Alternatively, without using wifi router, a GSM based system can also upload the sensor values directly to cloud server network.
- d. Cloud Server: Dropbox is a cloud storage service with free storage upto 2GB. It is required by the integrated system to upload positional lux data to its cloud network, even for future use. Dropbox must be configured properly after registration otherwise it will not automatically access files under any other running environment on the server computer [157]. Here, the NodeMCU controller with on-chip ESP8266 wifi module is interfaced with lux sensor in station mode and is established by an Access Point (WiFi Router Network). In Station (STA) mode, ESP8266 gets IP address from wireless router through which it can establish web server configuration and deliver webpages for all connected devices under existing wifi network. The primary task of client unit is acquisition of lux data from sensor and thereby transmitting to server computer (laptop) via wifi link under supervision of local wifi router according to path direction of Fig. 4.3. The lux data is stored as .txt/MS-Excel file in Dropbox cloud server post configuration and activation from where it can be shared with the collaborators having Dropbox cloud server application/web-interface installed for remote tracking by the users having accessibility of the sensor data.

4.4.1 Experimental Framework

The experiment is started by capturing illumination data at indoor coordinate locations by RF car interfaced with the lux sensor and IR transceiver with wireless microcontroller unit. Before the actual measurement is taken, the calibration of illumination sensor is done by reference light meter (Make-Metravi, Model-1332). The illuminance data is recorded both by the sensor and by the reference meter at floor corner locations marked as START or SOUTH-LEFT, then NORTH-LEFT, followed by NORTH-RIGHT and FINISH or SOUTH-RIGHT (Fig. 4.3). The experiment for sensor calibration is repeated and the average readings are noted from both the sensor as well as the standard meter positioned at same elevation level. From their mean values across each corner, the multiplication factor (MF) is calculated using

formula: $MF=Lx/Ls$, where Lx and Ls are illumination readings measured by reference meter and sensor respectively. The mean MF is calculated by considering illumination readings across floor corner positions. Alternatively, the illuminance sensor may be calibrated using machine learning based regression techniques and on receiving both the sensor readings and the pre-calibrated reference lux meter values, the obtained model can be used to find out the true value of the lux sensor data.

RF keypad is used to drive the car in forward, backward, right, as well as left directions to capture data through the entire indoor space. When the car traverses along a directed track, the client unit captures X-Y coordinate location values from IR transceivers connected with the wheels of remote car and illumination data from the lux sensor at the client end. The captured sensor values are then transferred to server computer and saved as text/MS-Excel file via wireless router from the measurement system developed at the client end.

The data file once saved can be shared using dropbox IoT cloud server to the authorized users for remote monitoring. Also, filtering of certain data may be done by the allowed users. From the captured dataset, data processing may be done to determine the shortfall of illuminance values below a certain threshold design limit. If any indoor space is found to have lesser than the required lux level, attention of the maintenance section may be drawn to take adequate steps for installation or modification of the luminaries and maintaining the illuminance values to the designed level.

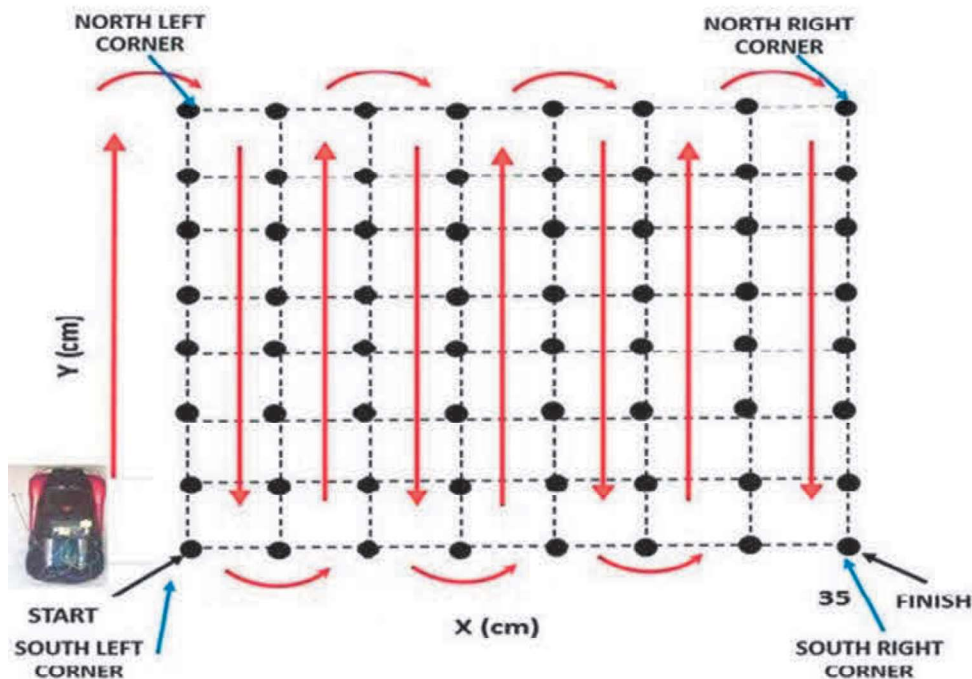


Fig. 4.3 Directional movement of car to measure lux

4.4.2 Results and Discussions

The experiment is started when the car (Fig. 4.4) is ready to move from the initial position which is captured using IR transceiver system as X-Y coordinate location once the wheel of the car starts rotating. The lux values from the illumination sensor are captured too. The car is moved now at 20 cm/sec. speed using forward remote key. After the car is moved forward by 50 cm, IR transceiver system captures X-Y position reading and considers them as present values. The present X-Y value is calculated by deducting the starting value from the present value and it is repeated at 50 cm intervals until the final position is reached. Now, right remote key button is pressed to move the car in 50 cm right direction and by pressing backward remote key button, car is rotated in backward direction. Following the sequence depicted in Fig. 4.3, the measurement is taken till the car reaches at stop or FINISH location. Before the actual readings are taken, the calibration of illumination sensor is done as indicated earlier to find out the mean MF and correct the raw lux sensor readings. Another approach can be followed as indicated in the previous chapter is to apply machine learning based regression techniques to calibrate the illumination sensor using the reference pre-calibrated lux meter. Once, the true model for the illumination sensor is obtained, the generated model can be used to find out the accurate lux values of the developed system. Now, the experiment is conducted and the acquired lux data is stored in a tabulated file. After that, the data is logged, saved and the file is shared with the permitted users using Dropbox IoT cloud server network. The allowed users have the flexibility of further data processing, if so desired by them. After application of data filtering, the updated file is saved and re-uploaded for the legitimate users. Thus, an intelligent illumination monitoring system is developed.

As the location and the illumination values are stored in the server, the file may be reutilized for finding out the contrast in lux for a selected indoor floor area. The 3-D surface plot of illuminance data is shown in Fig. 4.5. The reference illuminance level as provided by the lighting designer inside the indoor space is considered to be 200 lux. The difference lux map is formed by subtracting the benchmark lux values from the captured values. The colour variation in the lux surface map of Fig. 4.6 shows dissimilar illuminance level in the considered indoor space. Fig. 4.7 represents the ratio map between the measured lux to the reference lux.

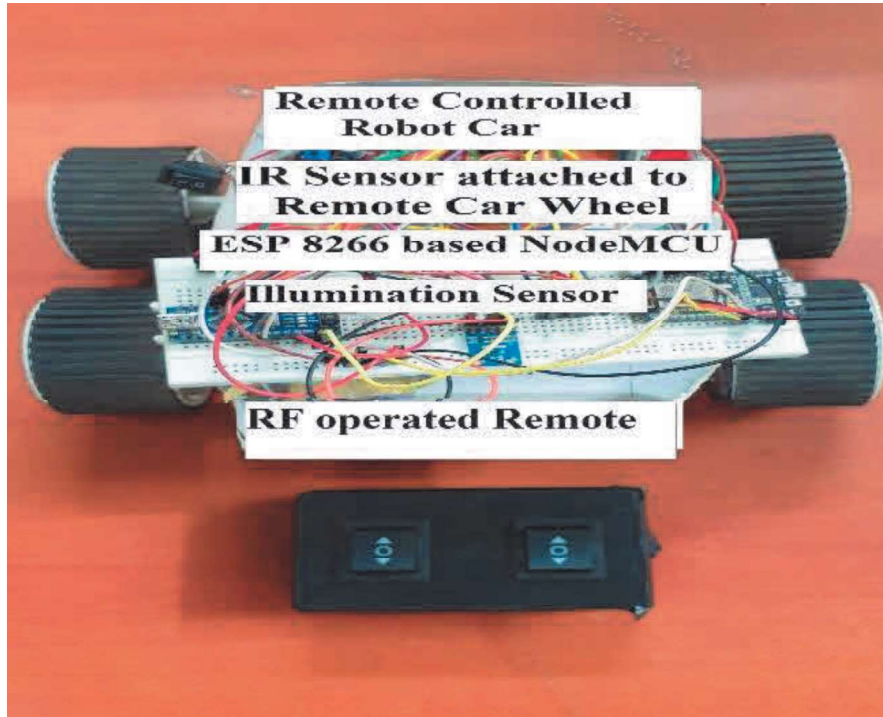


Fig. 4.4 Remote with circuit connected car using BH-1750

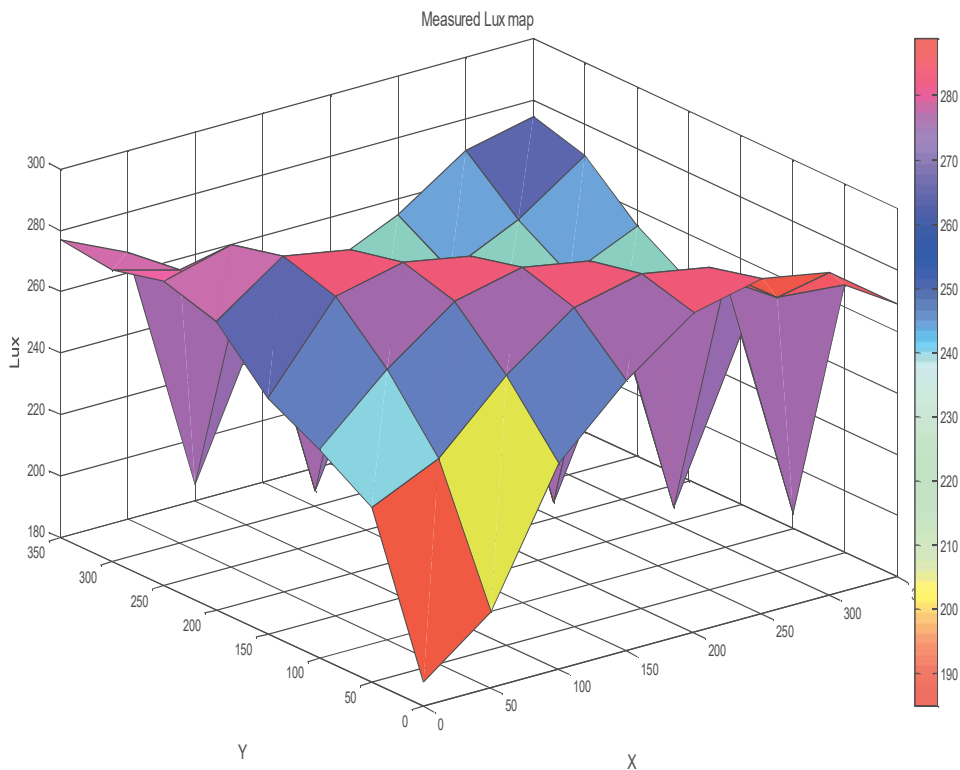


Fig. 4.5 3-D illuminance map for BH-1750

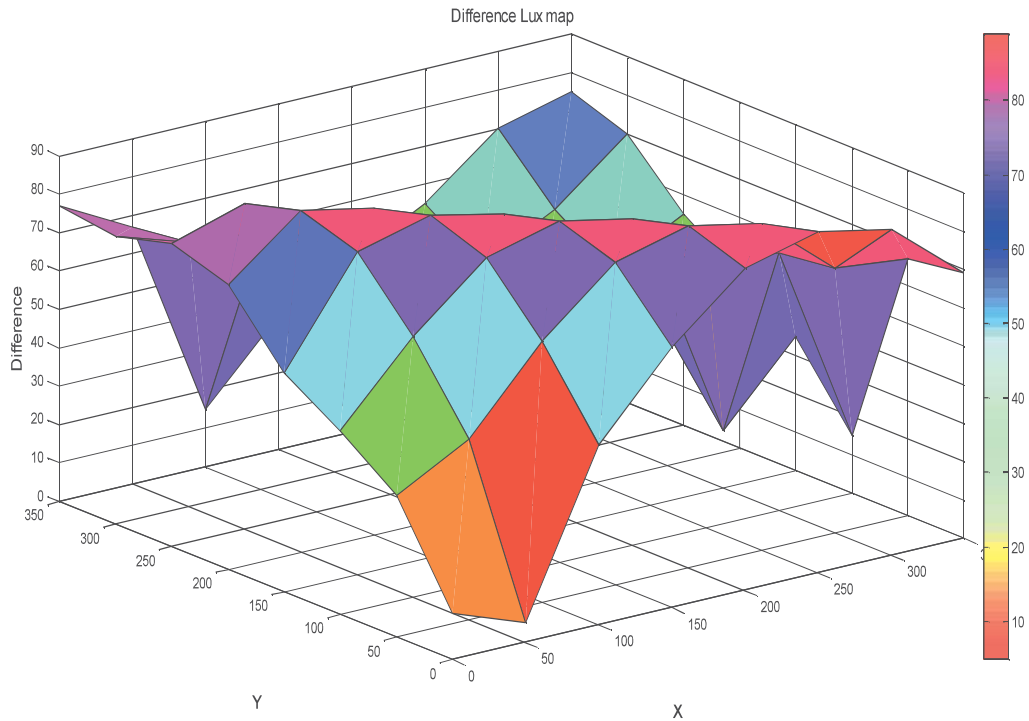


Fig. 4.6 Difference illuminance map with respect to standard illuminance map for BH-1750

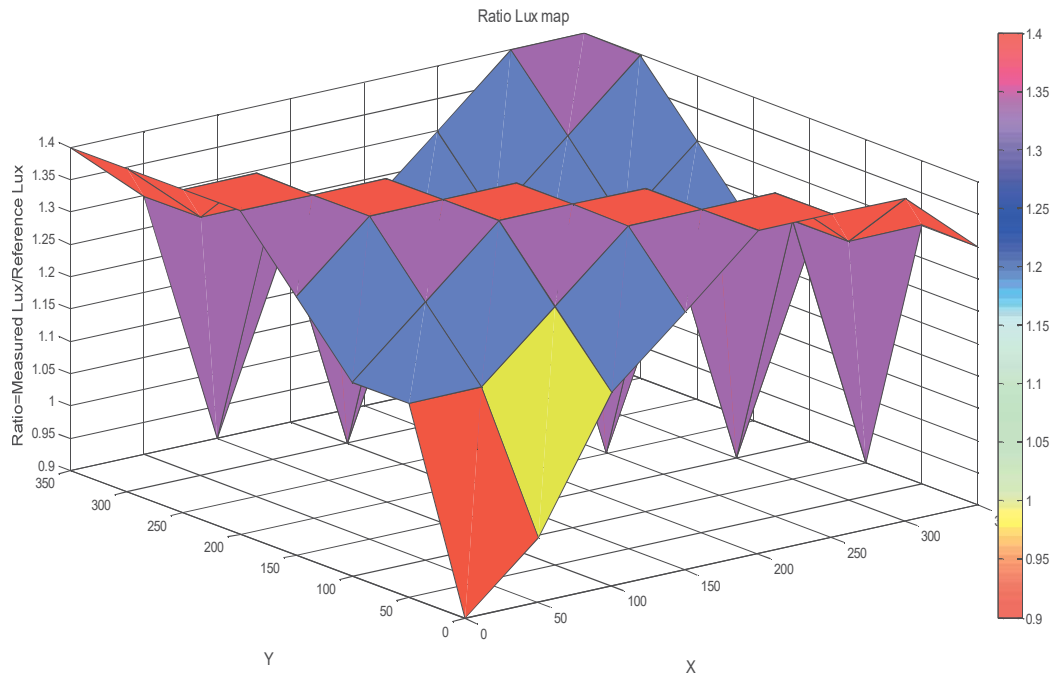


Fig. 4.7 Ratio map between measured lux to reference lux for BH-1750

The illuminance readings which are beyond the threshold limit (200 lux) indicate locations in the indoor space where curative action is not required to be taken. Whereas, the acquired illuminance values which are lesser than benchmark level (200 lux) specifies indoor floor

locations where remedial action is to be taken to bring back the lux values within the designed limit.

4.5 Obstacle Detection using Computer Vision Methods

Unmanned surface vehicles (USV) have been gaining applications since the last decade. These vehicles are utilized to perform various household tasks and they are also used in industrial applications. Some of them are interfaced with different type of high-end sensors to perform repetitive tasks and the captured values may be converted to image for feature extraction. Sometimes, the RGB-camera modules are used when the colour information is required, while other camera modules can only detect black and white colour for recognition of the shape of an object. Our aim was not to use any type of vision sensor, rather, use of a cost effective, easily available illumination sensor integrated with the robotic system to acquire the lux information throughout the indoor space. Then suitable edge detection methods have been applied to find out an object by detecting the regions from a picture having sharp colour contrast. The edges detected can differentiate the object boundaries with a clear idea about its orientation. An infrared sensor array was utilized for frontal plane obstacle detection [158] from a short distance. Kinect based solutions were reported in [159-161] for outdoor obstacle identification. Edge detection methods were applied for extraction of important image information [162]. All these techniques were studied for indoor obstacle detection from the reconstructed image acquired from a real-time lux sensor. Edge detection algorithms using computer vision methods have been applied for identification of the possible location and stationary obstacle characteristic of the selected indoor space. Edges are detected between the region boundaries and it provides information about a possible object shape from the image under study [162-164]. The edge detection methods are applicable provided the intensity data of two regions are available. The light intensity values are converted into grayscale image and then only edge detection techniques can be applied for obstacle identification. Without having these image segmentation tools, the illumination sensor connected with the client unit cannot single-handedly detect the presence of an object from the data itself.

4.5.1 Proposed Methodology

While the literature survey was conducted, no similar applications were found to be in existence in illumination engineering domain. Some applications required usage of costly

RGB cameras, whereas, some other studies required complex image processing algorithms. Instead, here low level image processing techniques have been used to find out the edges if an obstacle is envisaged along the path of a remote control car. From the captured data itself, the possible shape and probable position of the obstacles can be easily found out.

During conduction of our earlier experiments in the selected indoor space, it was observed that the light intensity values declined suddenly instead of a steady change. Primarily, it was presumed to be a concern with the installed lighting system. Therefore, the case was forwarded to the concerned superintendent engineer. Post inspection, no issue was reported neither with the installation procedure nor with the lighting system. Then, after detailed analysis of the issue, it was believed that the shadow of an object may be the reason behind it. Various techniques were available to address the given issue. Some offered costly solutions, while others were complex enough. Finally, computer vision methods were studied and some popular edge detection techniques were utilized to find a solution to the persisting problem. Furthermore, qualitative and quantitative analysis of all selected edge detection methods were conducted in this real-time experimental analysis to find out the most preferred solution.

The illumination values are acquired using a server-client setup as indicated in Fig. 4.1. The light intensity data along a selected indoor plane are acquired and is transformed to an image. Prior to the conversion, Gaussian noise filtering method is applied for linear type noise removal and median type filter is applied for impulse type nonlinear noise removal and achieve a superior type image. Now, low-level image processing techniques are applied to find out a sudden decline in the acquired light intensity level. Edge detection algorithms can be helpful in detection of an obstacle if an abrupt drop in the lux level is noticed. Here, we have selected four different edge detection methods as explained below:

a. Canny Edge Detection Technique: John Canny conceived this method, where Gaussian filter having proper sigma value is used for noise removal. Now, the top ridges of gradient image magnitude are selected by the edge-point and zero values are assigned to other pixels followed by hysteresis type of thresholding and lastly edge-linkage procedure is accomplished. The pair of 3x3 convolution kernels for Canny type edge detection technique is shown in Fig. 4.8(a) and direction of gradient is decided by particular angle pixel-scan [165].

+1	+2	+1	-1	0	+1
0	0	0	-2	0	+2
-1	-2	-1	-1	0	+1

Fig. 4.8(a) Canny type edge detection kernels

Pseudo-code for edge detection using Canny Method

1. **Input:** Read x, y (8X8) co-ordinate location data along the entire floor space.
 2. **Input:** Read the respective illuminance values (64 nos.).
 3. Read the corresponding illuminance values for each x, y floor co-ordinate positions.


```

A=ones (8, 8)
for i=1:8
  for j=1:8
    for c=1:64
      if (x(c)==i && y(c)==j)
        A(i, j)=l(c)
      end
    end
  end
end
end
A=uint8 (A)

```
 4. Enter the Gaussian Filter co-efficients and find the convolution of image by the respective Gaussian Filter co-efficients.
 5. Enter the Filter for horizontal and vertical direction:

$$KG_x = [1, 0, -1; 2, 0, -2; 1, 0, -1]$$

$$KG_y = [-1, -2, -1; 0, 0, 0; 1, 2, 1]$$
 6. Find the revised convolution of image by application of horizontal and vertical filter.
 7. Calculate the orientations and convert each negative direction into positive orientation to the nearest of 0, 45, 90, or 135 degree.
 8. Evaluate the magnitude of the image and apply Non-Maximum Suppression.
 9. Apply Hysteresis Thresholding using eight inter-connected components.
 10. **Output:** Canny edge detection result.
 11. **End**
-

b. Prewitt Edge Detection Technique: Prewitt discovered the magnitude-measurement and edge-orientation based tool. Its operator consists of two 3x3 kernels indicated in Fig. 4.8(b). This is unaffected by noise as it differentiates and averages in both the directions simultaneously [166].

-1	0	+1	-1	-1	-1
-1	0	+1	0	0	0
-1	0	+1	+1	+1	+1

Fig. 4.8(b) Prewitt type edge detection kernels

Pseudo-code for edge detection using Prewitt Method

1. **Input:** Read x, y (8X8) co-ordinate location data along the entire floor space.
2. **Input:** Read the respective illuminance values (64 nos.).
3. Read the corresponding illuminance values for each x, y floor co-ordinate positions.

A=ones (8, 8)

for i=1:8

 for j=1:8

 for c=1:64

 if (x(c)==i && y(c)==j)

 A(i, j)=l(c)

 end

 end

 end

end

A=uint8 (A)

4. Enter the Filter for horizontal and vertical direction:

$KG_x = [-1, 0, -1; 0, 0, 0; 1, 0, 1]$

$KG_y = [-1, 0, 1; -1, 0, 1; -1, 0, 1]$

6. Find the convolution of image along x-axis and y-axis by application of horizontal and vertical filter.
 7. Combine the edges detected along the X and Y axes.
 10. **Output:** Prewitt edge detection result.
 11. **End**
-

c. Sobel Edge Detection Technique: Sobel introduced the gradient-based edge identification tool. It has two 3x3 convolution kernels at 90° apart as shown in Fig. 4.8(c). Sobel kernel relies on central difference and it is superior to Prewitt kernel in terms of noise suppression.

+1	0	-1	+1	+2	+1
+2	0	-2	0	0	0
+1	0	-1	-1	-2	-1

Fig. 4.8(c) Sobel type edge detection kernels

Pseudo-code for edge detection using Sobel Method

1. **Input:** Read x, y (8X8) co-ordinate location data along the entire floor space.
2. **Input:** Read the respective illuminance values (64 nos.).
3. Read the corresponding illuminance values for each x, y floor co-ordinate positions.

A=ones (8, 8)

for i=1:8

 for j=1:8

 for c=1:64

 if (x(c)==i && y(c)==j)

 A(i, j)=l(c)

 end

 end

 end

end

A=uint8 (A)

4. Enter the Filter for horizontal and vertical direction:

$KG_x = [1, 2, 1; 0, 0, 0; -1, -2, -1]$

$KG_y = [1, 0, -1; 2, 0, -2; 1, 0, -1]$

6. Find the convolution of image along x-axis and y-axis by application of horizontal and vertical filter.
 7. Combine the edges detected along the X and Y axes.
 10. **Output:** Sobel edge detection result.
 11. **End**
-

d. Laplacian of Gaussian (LOG) Edge Detection Technique: David Marr and Ellen C. Hildreth introduced this fast approximation by Gaussian difference method for edge detection depending upon the sudden change in image intensity and the kernels are shown in Fig. 4.8(d). Although, it detect false edges and produces localization error at curved edges [167].

+1	-2	+1	-1	-1	-1
-2	+4	-2	-1	+8	-1
+1	-2	+1	-1	-1	-1

Fig. 4.8(d) LOG type edge detection kernels

Pseudo-code for edge detection using Laplacian Of Gaussian (LOG) Method

1. **Input:** Read x, y (8X8) co-ordinate location data along the entire floor space.
2. **Input:** Read the respective illuminance values (64 nos.).
3. Read the corresponding illuminance values for each x, y floor co-ordinate positions.

A=ones (8, 8)

for i=1:8

 for j=1:8

 for c=1:64

 if (x(c)==i && y(c)==j)

 A(i, j)=l(c)

 end

 end

 end

end

A=uint8 (A)

4. Enter the Filter for horizontal and vertical direction:

$KG_x = [1, -2, 1; -2, 4, -2; 1, -2, 1]$

$KG_y = [-1, -1, -1; -1, +8, -1; -1, -1, -1]$

6. Find the convolution of image along x-axis and y-axis and reduce noise by the application of Gaussian smoothing Filter.
7. Application of Laplacian Filter to remove any further noise before computation of the second order derivative.
10. **Output:** Combine both the Gaussian and Laplacian Filter to find the LOG edge detection result.

11. **End**

4.5.2 Results and Discussions

This data capture continues as per the direction indicated in Fig. 4.3 and ends when the car reaches the FINISH position. Locational lux data are sent from the client unit to the server computer under the influence of a wireless router and is stored there for further processing.

The acquired positional light intensity values are converted to a lux map image. Prior to further processing, the formed image is filtered to eliminate the presence of any noise. The edge detection algorithms of Canny technique, Prewitt technique, Sobel technique, and LOG technique are now applied for object identification along the selected floor space. Also, the possible location and shape of the object can be assumed if the techniques can be applied properly. A cost effective lux sensor with the help of edge detection algorithms can eradicate usage of high cost RGB-camera or Kinect and is capable enough to predict the location as well as obstacle shape properly. Captured sensor data are saved in a laptop, which functions as the server unit. Noise-filtering techniques are now applied on the acquired dataset. Then, Canny type, Prewitt type, Sobel type, and LOG type technique is applied to find out any obstacle inside an indoor space as indicated in Fig. 4.9(a)-4.9(d). Edge detection methods are utilized to observe the response and find out if any static object is present inside the indoor space. Fig. 4.9(a) shows the outcome of Canny edge detection technique for finding out the position and the closest shape of an obstacle. Prewitt edge detection technique of Fig. 4.9(b) is simpler, can give an idea about the position of obstacle although can be affected by perturbation and cannot give an estimation of its probable shape. Sobel edge detection technique of Fig. 4.9(c) is also simple and gives proper position of obstacle but unable to predict its true shape. LOG edge detection technique shown in Fig. 4.9(d) can identify the position but cannot predict the shape properly. Table 4.1 represents quantitative response of the edge detection techniques considered here [168-169].

$$\text{Recall (R)} = (n_1/n_2) \quad (4.1)$$

$$\text{Precision (P)} = (n_1/n_3) \quad (4.2)$$

$$\text{F1 value (f)} = ((2 * P * R) / (P + R)) \quad (4.3)$$

Here, n_1 represents a true positive set, n_2 is the set of actual value, and n_3 is an estimated set value. Recall gives the ratio between true object detection to actual object detection. Precision is the ratio between true object detection to a set of estimated object detection. F1 value informs on precision and sensitivity of the edge detection techniques.



Fig. 4.9(a) Response for Canny type edge detection technique



Fig. 4.9(b) Response for Prewitt type edge detection technique



Fig. 4.9(c) Response for Sobel type edge detection technique



Fig. 4.9(d) Response for LOG type edge detection technique.

Table 4.1: Quantitative Performance Analysis of different Edge Detection Techniques

Sl. no.	Edge detection technique	Recall	Precision	F1 value
1	Canny	0.97	0.97	0.97
2	Prewitt	0.81	0.83	0.82
3	Sobel	0.80	0.71	0.75
4	LOG	0.81	0.71	0.76

Table 4.1 clearly indicates that the performance parameters are best for Canny edge detection method, followed by Prewitt algorithm, then LOG technique and worst for Sobel algorithm. Canny type edge detection method has emerged to be the finest technique in the real-time investigation as the quantitative parameters give the closest approximation to the position and shape of the actual object. In addition, the designed method and some other methods can also be applied for similar applications in a large space as and when required [170].

4.6 Indoor Illuminance and Correlated Colour Temperature Monitoring System using RGB Sensor

The experimentation system helps in measurement of illumination and Correlated Colour Temperature (CCT) values at the indoor space using RGB sensors interfaced with wifi enabled microcontroller and is installed over the roof of a radio-frequency (RF) remote operated robot car that serves as the client terminal. The positional movement is captured by the help of infrared (IR) transceivers installed beside the wheels of the remote car. The sensors transmit positional RGB, lux and CCT values to a computer that functions as the server unit in a wireless network. The formulas for calculation of illumination as well as CCT values from RGB sensor data are embedded in the program itself as obtained using machine learning based regression model described in the last chapter. These acquired positional lux and CCT data may also be shared in a cloud network with the permitted users to alert the maintenance section and take corrective actions if the measured values fall below a threshold level. Moreover, preventive actions may be taken if the illumination and/or CCT values approach towards the threshold level because of ageing or any other reasons. Hence, both corrective maintenance as well as preventive maintenance can be planned properly. In this experimentation system, the illumination values have been considered for alert generation purpose, whereas, CCT values have been considered for monitoring purpose only. Fig. 4.10 represents the set-up of online illuminance and CCT monitoring system. The block diagram of our proposed system is shown in Fig. 4.11.

a. Client Terminal: The client module consists of TCS34725 RGB sensor using I2C communication mode to integrate more sensors as and when required and 32-bit ESP8266 wifi-enabled TensilicaL106 microcontroller based embedded system. The RGB sensor is interfaced with NodeMCU ESP8266 controller unit to capture the sensor data and transmit to the server terminal using a wireless network. The RGB sensor along with the controller module together forms the client terminal, which is powered by a rechargeable battery. The illumination and CCT values are computed from the RGB sensor data prior to transmission to the server unit.

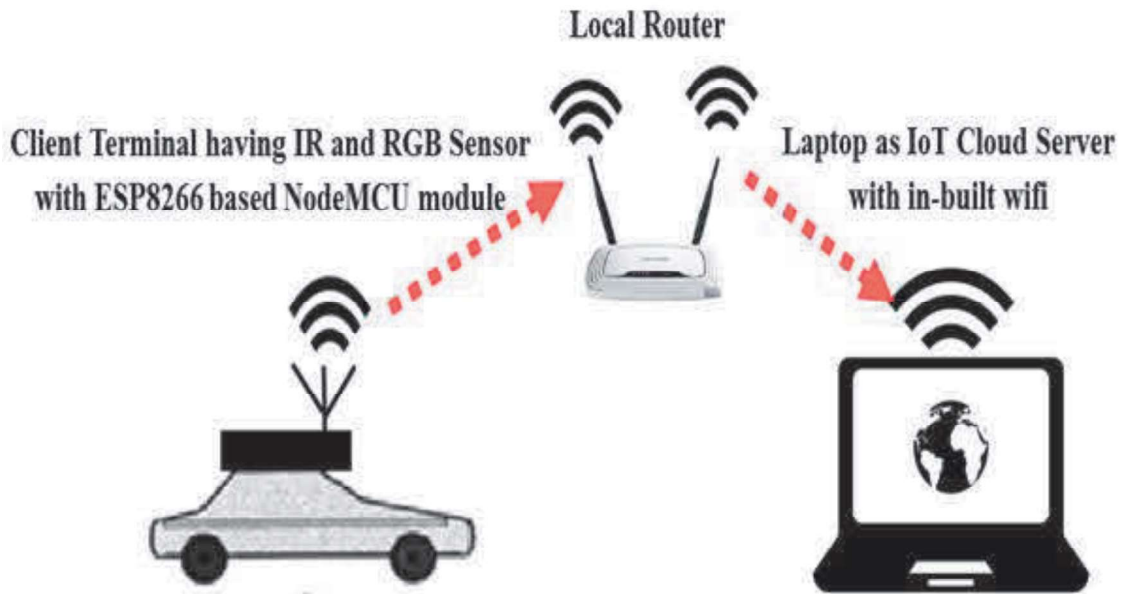


Fig. 4.10 Online illuminance and CCT monitoring system using TCS 34725

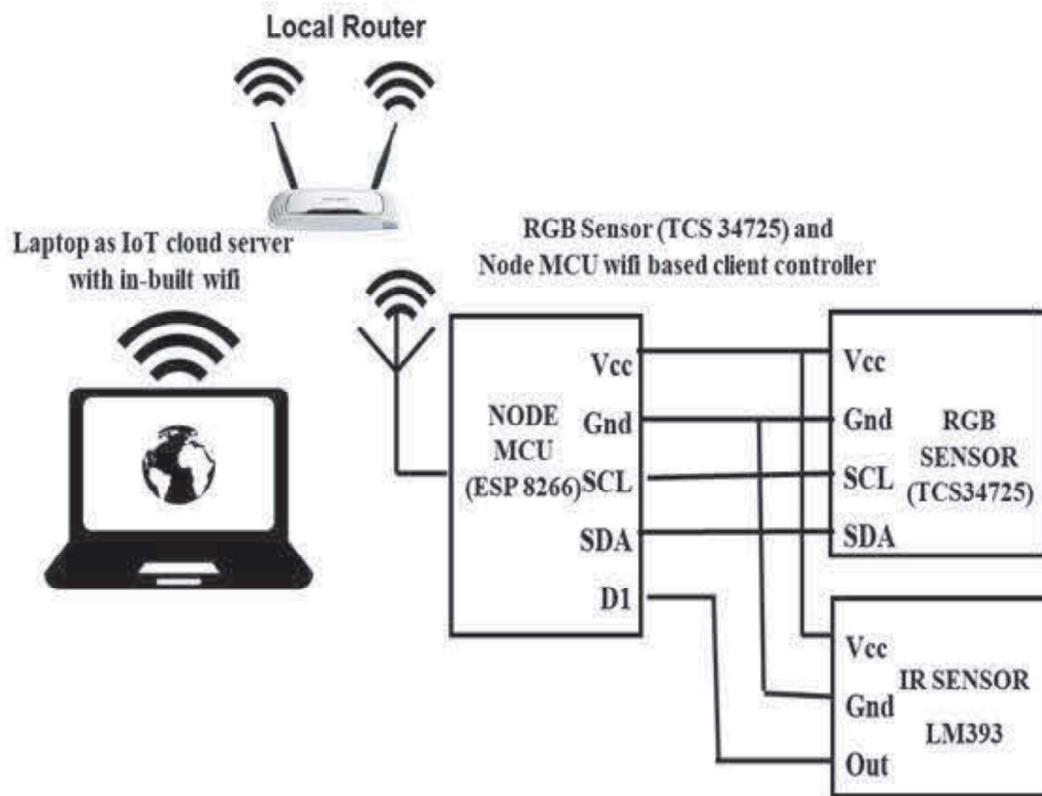


Fig. 4.11 Block diagram of online illuminance and CCT monitoring system using TCS 34725

b. Server Terminal: A wireless router establishes client-server communication through Ethernet port having a particular IP address. The positional RGB sensor values along with

illumination and CCT data are stored at the laptop which serves as the server unit and can be shared in a cloud network with the permitted users.

c. Wireless Router: A TP-Link made wireless router is used in the experiment. The wireless controller at the client terminal possesses a static IP address through which it acquires locational RGB values at the indoor space, computes the illumination and CCT values for each RGB data therein and transmits them to the fixed port address of wireless router. It is redirected to the server computer thereafter. An authorized user checks if the computed data are below the threshold limit to decide upon the control action, if it is required to be taken and thus a wireless client-server network is established.

d. Chroma Meter: The illumination and CCT values for each RGB input is noted by the help of a Chroma meter (Model No: CL-200A, S/L No: 30D10039), which is available in the Illumination Engineering Laboratory of the Jadavpur University. The total specification of the Konika made Chroma meter is referred in the last chapter. This meter is used to calibrate the TCS34725 RGB sensor in-terms of the illumination and correlated colour temperature values using the machine learning based regression models that are already discussed in the preceding chapter as mentioned earlier.

d. Cloud Server: The cloud server that has been used in this experimental work is Dropbox, which offers a free service up to 2GB of cloud storage. This cloud storage service has been used by the experimentation model to upload positional RGB as well as computed illumination and CCT data to the virtual storage network, even if it is a future requirement. After registration, it is required to configure the Dropbox appropriately, else automatic accessibility of the files in any processing atmosphere on server computer will be impossible. Here, ESP8266 based NodeMCU wireless controller is interfaced with the IR sensor as well as with the RGB sensor in station (STA) type communication mode and is well-established by the help of an Access Point that is the wireless router network. In this mode of communication, NodeMCU ESP8266 receives the IP address through the wireless router by which it establishes the web server arrangement and delivers the webpages on behalf of all coupled appliances in the same wifi network configuration. The prime assignment of the client unit is acquirement of positional RGB values from the sensor and converting them to the illumination and correlated colour temperature data and conveying them to the server laptop (or computer) through the wireless link under the control of a native wifi router rendering to the path direction as indicated in Fig. 4.3. The illumination and CCT values are deposited as either text or as MS-Excel file in the Dropbox based cloud server after proper configuration and post activation, then only it is shareable with the permitted persons having

Dropbox type cloud server application or web-interface established for remote monitoring. The legitimate users will have the accessibility of RGB sensor data as well as computed illuminance and correlated colour temperature values for each location.

4.6.1 Experimental Framework

The experiment is started by capturing RGB sensor data at indoor coordinate locations by RF car interfaced with the RGB sensor and IR transceiver with wireless microcontroller unit. Before the actual measurement is taken, the calibration of RGB sensor is done by a reference Chroma meter (Make- Konica Minolta, Model No: CL-200A, S/L No: 30D10039) using machine learning based regression techniques and on receiving both the RGB sensor readings and the reference Chroma meter values, the obtained model can be used to find the true value of the lux sensor. For ease of implementation, polynomial regression model (Degree-I) was embedded in the sensing system to calculate the illumination value for each positional RGB data. Similarly, polynomial regression model (Degree-III) was embedded in the sensing system to calculate the CCT values for each positional RGB data.

Similar to the experimentation study using lux sensor, here also, radio frequency key is utilized to move the car in the required directions as indicated in Fig. 4.3 to acquire positional RGB data in the selected indoor location. While the remote car moves through the selected space, the client terminal gathers X-Y positional locations through IR transceivers attached to the robot car wheels and RGB data from the interfaced sensor with the wireless microcontroller at the client terminal. Moreover, the illumination values and the correlated colour temperature values are computed from the RGB sensor values as indicated earlier. The captured RGB sensor data as well as the calculated lux and CCT values are now transmitted from the measurement unit at the client terminal to the server laptop/computer and saved therein as text/MS-Excel file under the influence of a TP-link made wireless router.

After the data file is saved, it can be shared with the permitted persons using Dropbox based IoT cloud server. The values can also be filtered by the legitimate users. The acquired dataset may prove to be useful in determination of the illuminance values if it comes below the set point limit given by the lighting designer or as set by the corresponding Indian standard. If the lux level is below the lower threshold limit, then the maintenance section may be given alert accordingly to take necessary actions and bring back the lux values towards designed levels. Sometimes, luminaries may also be required for modification, if the situation such demands.

4.6.2 Results and Discussions

The experimentation is commenced when the remote operated car (Fig. 4.12) is prepared to travel from the primary location that is acquired by the help of an IR transceiver arrangement as X-Y coordinate position as soon as wheel of the remote car begins revolving. The RGB, illumination and CCT values are captured by the RGB sensor. The remote car transports at a slow speed that is around the same as earlier by using the forward moving key. The remote operated car is now moved in the forward direction by 50 cm, IR transceiver mechanism gathers X-Y location values and treat them to be present position values. The current X-Y coordinate value is determined by subtracting the initial value from the existing value and this process is repetitive in nature at every 50 cm interval till the car reaches at the concluding place. By pressing the right key of RF remote, the car is now moved to 50 cm in the right path and by the press of back remote key, the car can be switched to the backward track. Fig. 4.3 depicts the sequence of movement of the remote car and data acquisition process is continued until the car arrives at penultimate or FINISH point. Prior to data capturing process, the RGB sensor is calibrated by the help of a Chroma meter for the entire range of the sensor. Several machine learning based regression techniques are applied to calibrate the RGB sensor using the reference pre-calibrated Chroma meter in finding the illuminance and CCT values for every single combination of RGB values. If an actual model for RGB sensor can be obtained, the formulated model may be utilized to compute the precise illuminance and CCT values of the established scheme. Subsequently, the investigation is carried out and the assimilated RGB values along with the computed illuminance and CCT data are preserved in a tabularized file. After logging the acquired positional RGB values and computed illuminance and CCT data, the file is saved and can be shared with the legitimate operators by the help of Dropbox based IoT cloud server network. The permitted handlers possess the flaccidity of additional data filtering, if anticipated by them. Once the data is processed, the file is updated, saved and uploaded further for the appropriate users. In this way, a smart illuminance and CCT assessment arrangement is established.



Fig. 4.12 Remote with circuit connected car

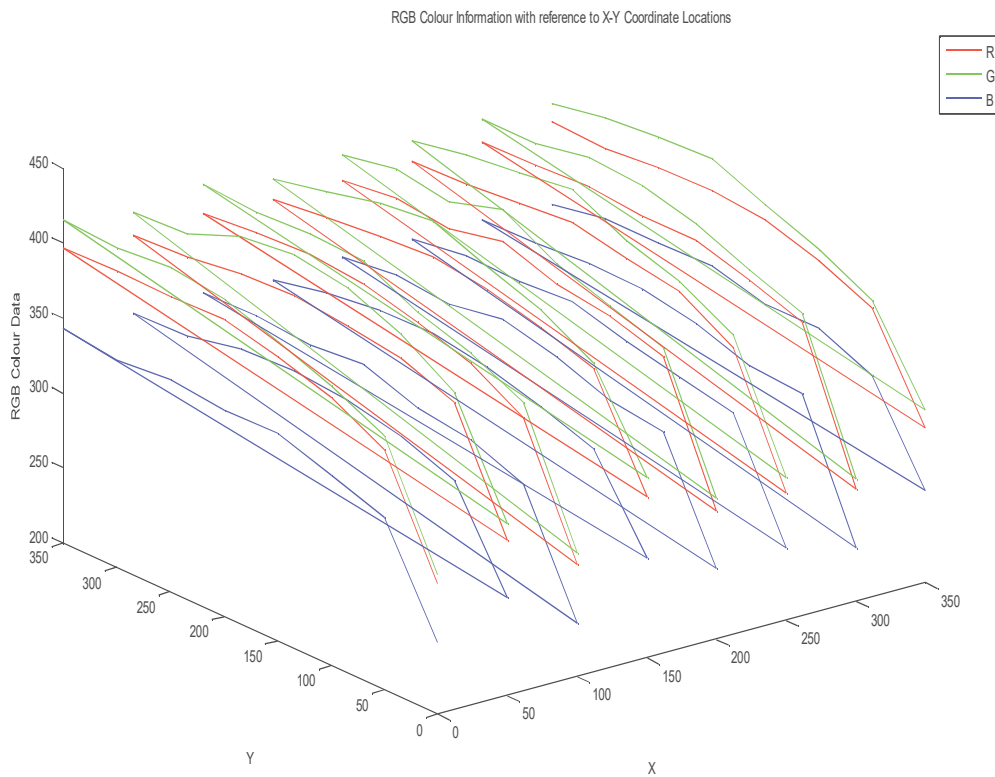


Fig. 4.13 RGB Colour Data with reference to X-Y Coordinate Location

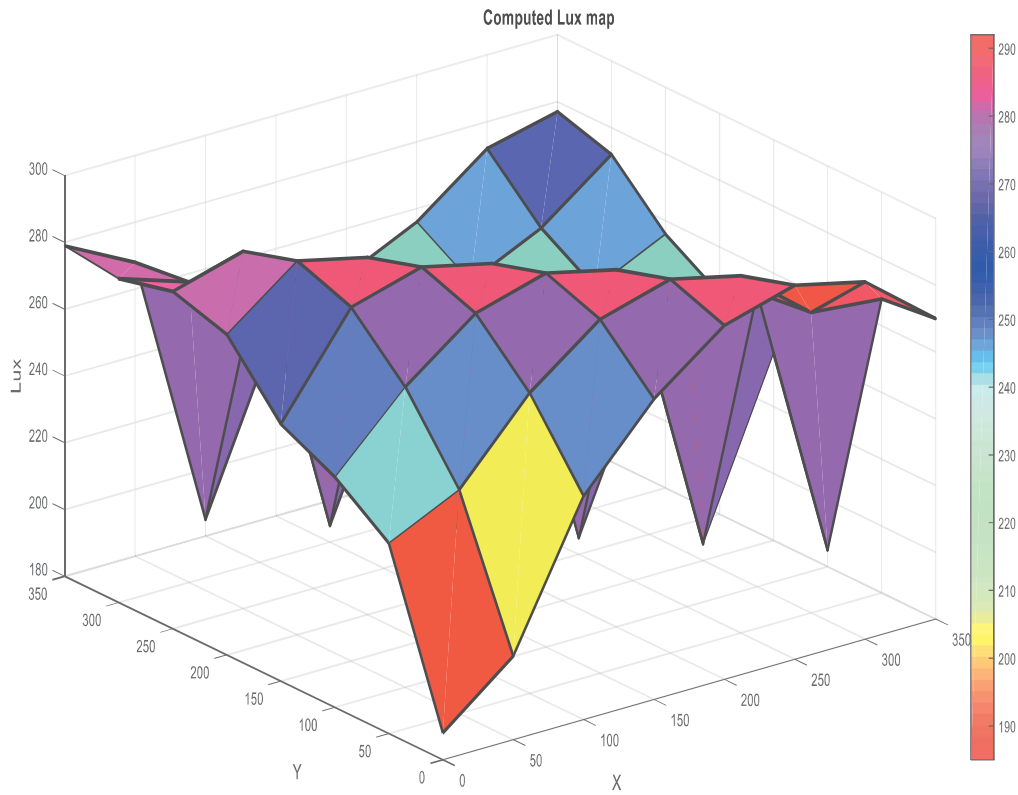


Fig. 4.14 3-D illuminance map for TCS 34725

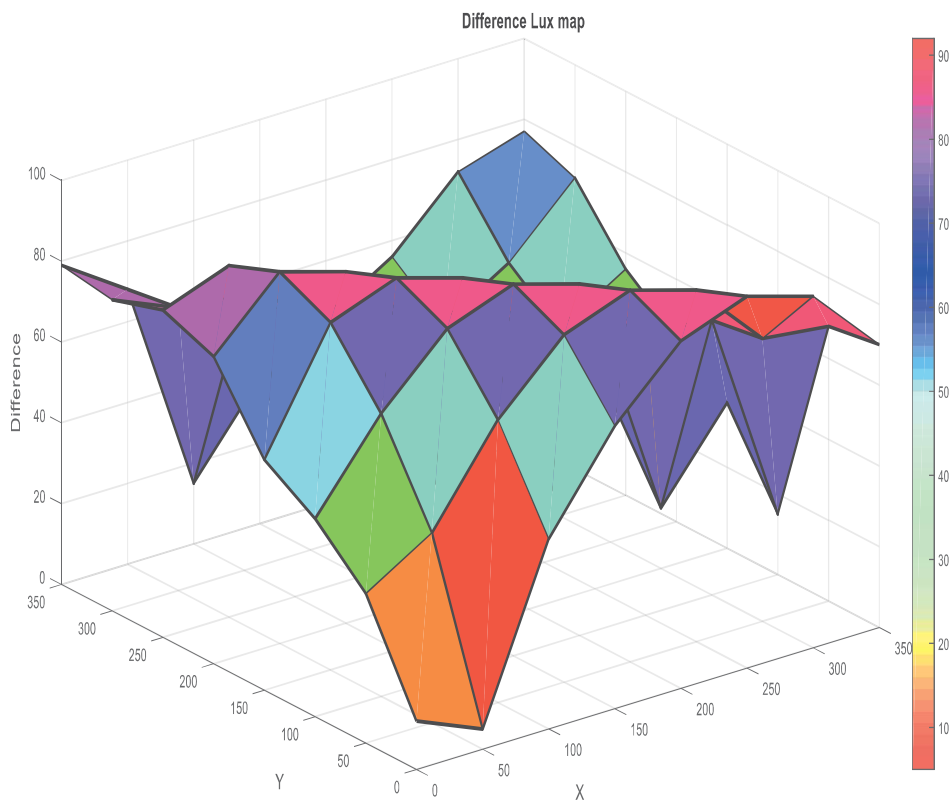


Fig. 4.15 Difference illuminance map with respect to standard illuminance map for TCS 34725

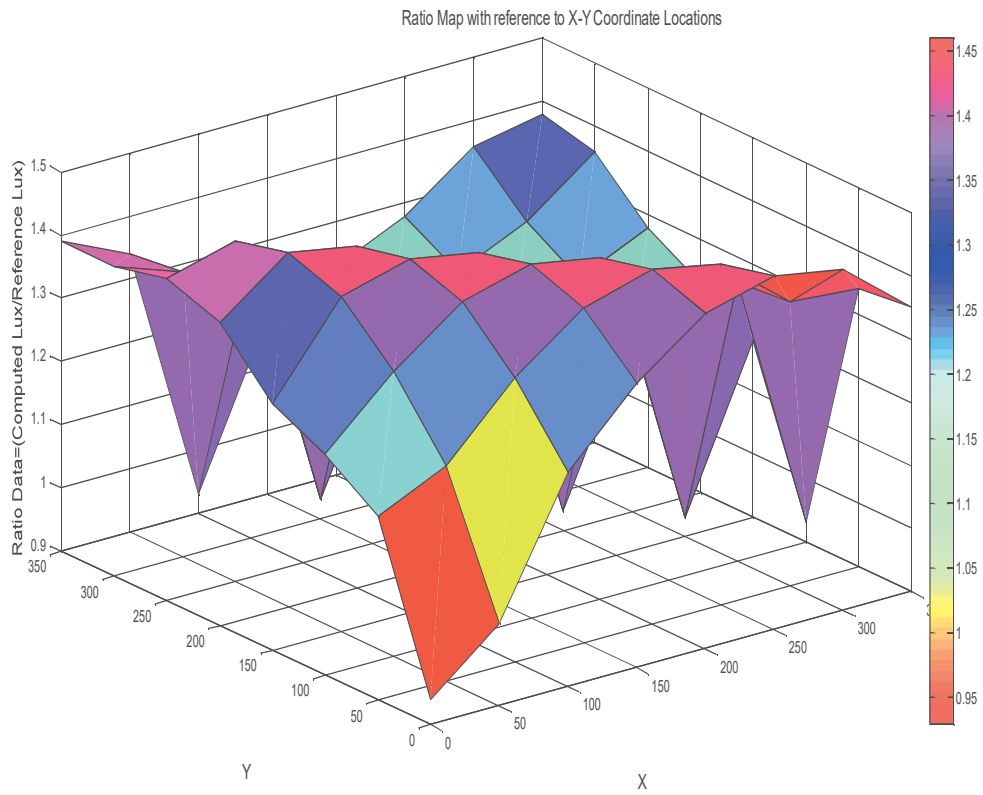


Fig. 4.16 Ratio map between measured lux to reference lux for TCS 34725

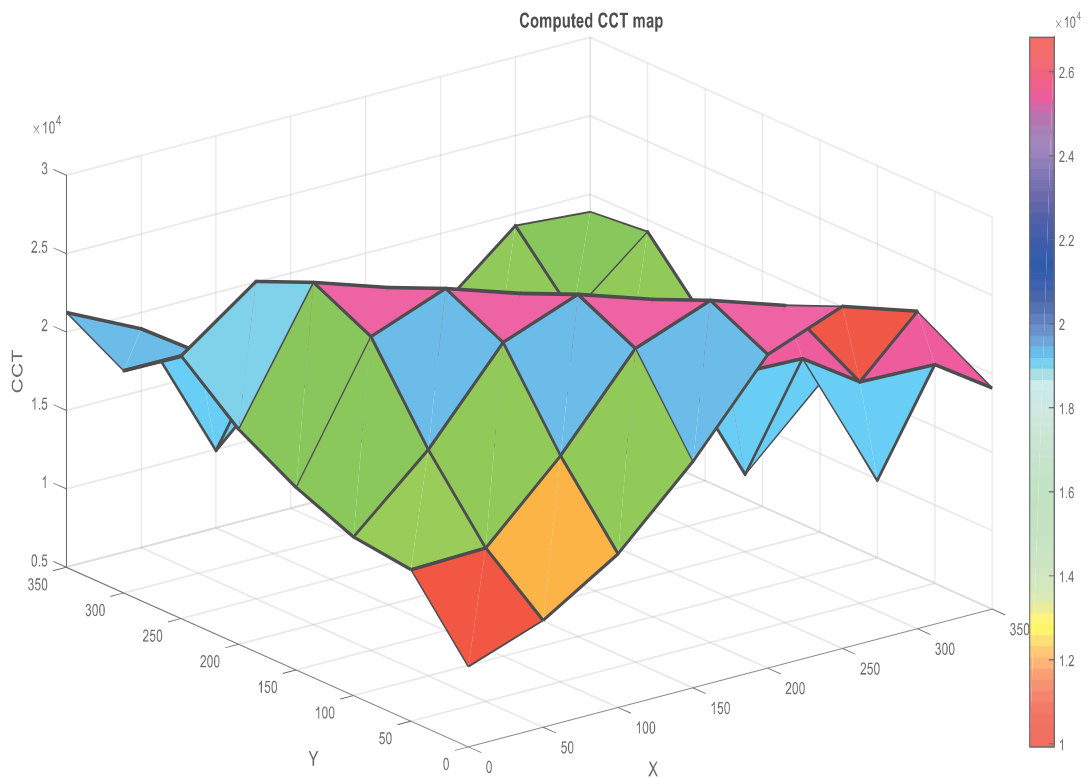


Fig. 4.17 3-D CCT map for TCS 34725

As the positional RGB, illuminance and CCT data are deposited in a server computer, the tabular file can be reused for ascertaining the contrast for illuminance and CCT for a designated indoor space. However, this study is limited to finding out the dissimilarity regarding lux values only with reference to a set point value. Fig. 4.13 represents the three-dimensional RGB colour map with respect to X-Y coordinate locations. Three-dimensional plot of illuminance values are shown in Fig. 4.14. The colour distinction in illuminance surface map is shown in Fig. 4.15 that depicts the difference map between the computed illuminance data and the reference lux data with reference to X-Y coordinate locations. Fig. 4.16 characterizes the ratio map between measured lux to reference lux with reference to X-Y positions. Fig. 4.17 indicates the three-dimensional plot of CCT values with respect to X-Y coordinate locations. The reference illuminance level is set by an illumination designer within the selected indoor space and is set at 200 lux for the entire location. The contrast illuminance map is formulated by the difference of standard illuminance data from the computed lux values.

The illuminance values that are afar from the set point level (200 lux) signifies the indoor space positions where remedial measures are not compulsory. On the other hand, the computed illuminance data that are inferior to the standard limit (200 lux) stipulates the indoor base sites where counteractive measures are required to evoke the illumination values within a premeditated level.

Similar to that any reference CCT level can be set and difference CCT map of the measured CCT level and reference CCT level may be found out. Also, ratio CCT map can be found out, if required. From those plots, the measurement sites where CCT correction may be required can be decided upon and corrective measures can be taken accordingly.

At the outset, the designed prototype using wireless transceiver based client-server network configuration yields satisfactory experimental observation in a selected indoor space. The car along with the sensors integrated with controller moves through various locations and in the process it tracks the location and illuminance values continuously and store in a file to maintain the light levels within benchmark limit. Further, filtering of the acquired lux data is done by any authorized person using Dropbox based IoT cloud server communication medium and the updated file is re-shared for perusal of others. Initially, calibration of lux sensor with the standard lux meter is done prior to data capturing to eradicate the impact of indoor wall reflectance in the acquired data. For any indoor space, provision should be available for free movement of the remote car for homogeneous data capturing. Furthermore intelligence can be incorporated by generating an alarm as and when the illumination values

fall below the threshold limit and accordingly inform the maintenance section to take corrective measures and regain the benchmark level. Moreover, usage of the developed system in some other possible applications is presently under investigation.

The performance analysis of different edge detection techniques for obstacle identification inside an indoor space is presented here. Amongst them, Canny edge detection technique gave the best approximation for the shape and possible position of the object. The proposed method is capable of detecting both frontal and hanging stationary obstacles using offline image processing. Non-stationary, online obstacle identification techniques are being studied which can be a part of our future exploration.

Chapter Summary

This chapter describes the technique for automated illuminance monitoring in indoor space using client-server wireless network. The sensing unit is mounted over the roof of a RF-remote operated robot car and is comprised of an illuminance sensor or a RGB sensor depending upon the configuration. IR based transceiver is there to capture the positional information. The sensing unit is interfaced with a wireless microcontroller and it is considered as the client unit. The client unit transmits the positional sensor data to a server computer/laptop. The sensors are calibrated prior to its real-time application. If a RGB sensor is used instead of an illumination sensor, then it can compute lux as well as CCT values, provided the conversion formula is embedded in the execution program. The developed model can be applied in the indoor space to capture the positional illuminance information of the selected indoor space. The next chapter depicts the procedure for classification of illuminance images using suitable image processing techniques. The positional lux information is acquired from an illumination sensor while the RF remote car moves through the selected indoor space. It is then converted into an image from the captured illumination data. Afterwards, PCA-Eigenface based image processing method and image histogram technique are applied to classify any test illuminance image. Depending upon the similarity factor based performance metric, a comparative performance evaluation of the aforesaid techniques have also been conducted in the next chapter of this thesis.

Classification of Illuminance Images

5.1 Introduction

Processing of an image is regarded as a sub-domain of signal processing. Two important categories of image processing techniques are analog image processing that considers time-dependent two dimensional signal processing and digital image processing that inspects and controls digital signal's character and intensity disposition. Digital image processing is accomplished by the application of various algorithms using a compatible instrument. A computer is used to improve image quality or extraction of valuable cognizance [171]. Generation of illumination images [172] from lux sensor data and processing them for finding out the quality of the formed images can prove to be quite beneficial for certain applications particularly where camera cannot be used. This technique provides a detailed overview of the homogeneity as well as non-homogeneity of the formed image in comparison to a reference image. The inferred information is very much essential in terms of quality and various performance indices in different process engineering applications, when analysis is impossible without formation of an image. Similar studies for finding out the thermal characteristics and temperature dissemination within a predefined space is an ill-posed issue [173]. The system images, thus formed, can be processed later using various image processing algorithms for segmentation of image, extraction of image features, classification of image for further assessment and decision making process as and when required.

Incidentally, we have computed the performance of Eigenface technique for classification of the illumination quality of a selected indoor space. We are already aware that the Eigenface technique is conventionally used for effective recognition and characterization of human face. The said Eigenface procedure is dependent on Principal Component Analysis (PCA) technique that is basically a dimensionality reduction and orthogonality maintenance method. PCA is a well-admired pattern recognition technique for replacement and formation of a basis of dataset used from large correlated vectors to small uncorrelated vectors. The superiority of PCA is more effectiveness; low noise sensitivity and lesser necessity of memory for handling calculation details to form the base of Eigenface method [174-175], extensively applied in problems related to face recognition.

Furthermore, image histogram similarity analysis has also been carried out and a comparative performance analysis has been conducted to find out the similarity level of an unknown illuminance image with the images stored in the training lux dataset. Histograms are considered to be spatial frequency distribution of pixel intensity values. During the training stage, image histograms of each training image are created and deposited in the database. In the testing stage, histogram of an unknown image is compared with each stored training histograms using histogram similarity analysis technique that computes the overlapping region between them. If the overlapping region between them are similar then the two image histograms are considered to be of the highest probable values. The possibility of detecting the similarity level of the unknown or test images can be determined by their similarity factors either in-terms of overlapping regions between the trained image histogram and test image histogram or by the help of Euclidean distance between them. The illuminance level of an unknown or test phase is now evaluated depending upon the similarity level of each training data possessing the maximum histogram intersection similarity value for the most similar sample and minimum Euclidean distance between them.

5.2 Objective of this Study

The objective of this study is to classify an unknown or test lux image using image processing algorithms. The positional illuminance data is captured and converted into an image. This unknown or test lux image is then compared with a dataset of previously formed trained lux images using PCA-eigenface method, histogram based intersection technique, and histogram based euclidean distance method to identify the similarity classification. A

comparative performance analysis of the selected techniques have also been executed to determine their classification accuracy.

5.3 Related Works

In non-destructive testing procedure, the sensors that are attached generally never interfere with the flow path of the process. This type of technique is highly useful and overall successfully applied in homogeneous process. The prediction of the thermal characteristics by measurement of the induced boundary temperature from the connected sensors is a primitive boundary value issue [173]. Various engineering problems are available where the features and their value are exaggerated by higher temperature levels; therefore a pre-fixation of the temperature dissemination within the procedure is indispensable.

Numerical simulations are crucial tool for present engineering situation. Using numerous software simulation models constructed on probable depiction of physical occurrences and procedures, it is likely to pre-scrutinize the matters under test such that their vital characteristics can be well-defined and precisely optimized simultaneously.

Bestowing to Digital Signal Processing conception, the Digital Image Processing, its subgroup, also operate on images via some algorithms processing on a computer to obtain a transformed or superior form of the images or to assimilate some significant insights from them [171]. This is dependent on some practical methodologies like categorization, pattern identification, multi-scale exploration, feature mining, to name a few. The Principal Component Analysis (PCA) is a procedure for forecasting to a sub-space and is widely applied in pattern-approximation. The fundamental intentions of PCA method are the substitution of meticulously correlated large-sized vectors with entirely uncorrelated lesser-sized vectors and to find a criterion for the utilized database [176]. Lesser computational memory requirements, greater efficacy and minimal noise sensitivity and turbulences are the foremost benefits of PCA method, simultaneously; it is the keystone of the Eigenface method [174-176]. The essence of PCA and Eigenface can be utilized to exemplify human face images delicately. A set of actual face images of human beings was taken and then an optimal vector structure was formed to compress images and also categorized the said human faces [177]. In [178], the face-recognition system using Eigenface technique was similarly executed. The arrangement essentially is governed by the impression that for each and every individual there is an explicit facial architecture. By the use of those facial likelihood data acquired by the help of Eigenface technique, face-matching can be done using computerized

algorithms [175]. Euclidean distance was used for PCA based similarity detection in climatological data exploration [179]. An inimitable Image Euclidean Distance (IMED) perception was anticipated in [180] that had taken under consideration the spatial relation amongst pixels of an image. The concept of similarity index between the principal constituents of two dissimilar databases can be utilized for amid-class association [181]. Eigenface method is an equally decent calculation scheme for checking the resemblance of an image with pre-existing class [182]. An innovative similarity metric based on Extended Frobenius Norm (Eros) was suggested that is constructed on PCA for multivariate time-series database [183].

As on date, face identification perception has been executed in a number of applications, although it has been investigated that its efficiency depreciates when it is functional in some unrestrained situations, e.g. modification in brightness limit, transformation of manifestation, face location etc. To alleviate these type of problems, in [184], the researchers have intended to use the Histogram Oriented Gradient (HOG) method as a feature extraction process. The investigational outcomes indicate that HOG method collectively with various distance classifiers yields superior result than what is accomplished with our well-known Eigenface technique. Furthermore, in [185], it was demonstrated that Facial appearance abnormalities may be identified using an acceptable value of HOG factors. The scientists have coped with the notion of face recognition by mixture-of-Eigenface process that shows to be highly accurate for demonstrating facial images having high dissimilarities. They recommended this scheme that uses additional set of Eigenface approaching from the expectancy maximization learning process in the PCA mixed architecture. This system also outclasses conventional Eigenface scheme for variation in facial orientation and brightness level [186]. An amalgamation of second-order-Eigenface technique and mixture-of-Eigenface process can address furthermore, the snag of ordinary-Eigenface scheme for the assumed disparities [187].

As specified already, image histogram is plotting of tonal image distributed digitally. It is applied in equalization of an image, thresholding of an image, brightness and contrast adjustments of images under study, detection of image transformation, etc. Upper dimensional feature space stances an issue for the conventional image categorization executions. In [188], the researchers quantified that Support Vector Machines (SVM) abridge properly on analytical image categorization issues where upper dimensional histograms are the solitary feature. They developed heavy-tailed RBF kernel, which accomplishes way superior than customary polynomial or Gaussian RBF kernels. Histogram based image

segmentation is a popular method for object categorization and image grouping. Moreover, it was suggested in [189], to practice the Learning Vector Quantization (LVQ) algorithm for even higher effectual histogram design by the precise-tuning of codebook vectors. The precision of Interest Point Local Descriptors (IPLD) feature for image segmentation was enhanced by the projected technique. A unique image exemplification scheme was proposed by the mining of eloquent blends of visual characteristics. The recommended method is hinged on numerous arbitrary prognostications of input space, henceforth local thresholding of proposed histograms and demonstrating the images in the form of Histograms of Pattern Sets (HoPS) [190]. A histogram based illustration was instigated along with a time series investigation technique, Dynamic Time Warping (DWT), to categorize retinal images to recognize age-related macular deterioration [191]. Another method was conceived for iris identification of mobile devices using the Self Organizing Map (SOM) tool of unsupervised learning algorithms. Their suggested technique has prospered in segmenting at pixel grade iris features. The kurtosis and skewness type statistical descriptors can be extracted from the image histograms and are extensively applied in conjunction with the RGB iris information to establish the discriminative feature orientation structure [192].

Hence, it is noteworthy to mention that PCA-Eigenface method and image histogram technique can be applied for classification of generated illuminance images.

5.4 Proposed Methodology

The methodology adopted in this study has been mentioned in the following sub-section:

5.4.1 Principal Component Analysis (PCA)

The multivariate analyzable datasets are either large or may not be interpreted easily. The large dataset dimensionality is largely minimized in PCA, specifically where the number of feature variables is more in comparison with the sample dimensionality. No major information loss happens in PCA, orthogonality is maintained, new un-correlated variables are defined and variance is thus enhanced. The aim is to extrapolate the authentic vectored data, $X = [x_1 \ x_2 \ x_3 \ x_4 \dots x_p]^T$, encompassing explicit attributes to a newer vectored data $Z = [z_1 \ z_2 \ z_3 \ z_4 \dots z_m]^T$, where $m < p$. The actual vectored data X is constituted using linear amalgamation of equilateral vectored set v_i , where coefficient z_i , is composed of the following equations:

$$X = \sum_{i=1}^m z_i v_i \quad (5.1)$$

$$z_i = v_i^T X \quad (5.2)$$

PCA can be constructed using Eigen-value decaying technique, which is similar to coordinate tuning approach from a real dataset X to a newer coordinate dataset Z . For minimization of dimensions of the dataset, subset ($m < p$) of v_i vectors are formed and they are named as principal components – that persist intact as eigenvectors of a covariant matrix dataset. The reduction of dimensions from p to m generates estimation fallacy. This error may be reduced provided the Eigenvectors are determined from the covariance matrix having largest Eigenvalues comprising of more than 90% of the real information.

The superiority of PCA over SVM or similar types of classification techniques is that in PCA the dimensionality of the feature space is reduced to a large extent. Moreover, PCA method generates an orthogonal feature, which helps in gaining further insights to the classification capacity of the data.

Pseudo-code for computation of PCA using Covariance Matrix

1. **Input:** Original data set : $X = [x_1, x_2, x_3, \dots, x_D]$

2. **Output:** PCA transformed dataset: \tilde{X}

Given original dataset of D dimensions and N sample size:

$$X = \begin{bmatrix} x_{11} & x_{12} & \dots & x_{1D} \\ x_{21} & x_{22} & \dots & x_{2D} \\ x_{31} & x_{32} & \dots & x_{3D} \\ \dots & \dots & \dots & \dots \\ x_{N1} & x_{N2} & \dots & x_{ND} \end{bmatrix}, \text{ where } x_{i,j} \text{ represents the } i\text{-th sample of } j\text{-th dimension.}$$

3. Compute the mean of all dimension (D) according to: $\mu_i = \frac{1}{N} \sum_{i=1}^N x_{i,j}$

4. Subtract the mean from all samples:

$$5. D = \begin{bmatrix} D_{11} & D_{12} & \dots & D_{1D} \\ D_{21} & D_{22} & \dots & D_{2D} \\ D_{31} & D_{32} & \dots & D_{3D} \\ \dots & \dots & \dots & \dots \\ D_{N1} & D_{N2} & \dots & D_{ND} \end{bmatrix}, \text{ where } D_{i,j} = \frac{1}{N} \sum_{i=1}^N x_{i,j} - \mu_i$$

6. Compute the covariance matrix according to: $cov = \frac{1}{N} \sum_{p=1}^N (x_p - \mu)(x_p - \mu)^T$

7. Compute the eigenvectors V and eigenvalues λ of the covariance matrix Σ .

8. Select k no. eigenvectors that have largest eigenvalues $W = \{v_1 v_2 \dots v_k\}$. The selected eigenvectors (W) represent the projection space of PCA.
9. All data samples in original data set are projected on the lower dimension space (k dimension, $k < D$) as follows: $\tilde{X} = W^T D$

10. **End**

5.4.2 Eigenface Method

PCA is the foundation of Eigenface method. The following procedure is to be maintained in this technique that includes extraction of unique image attributes and representing them as linear amalgamation of Eigenfaces extracted using component derivation method.

The principal constituent for the lux training database are primarily acquired. The recognition method is followed next, i.e. projecting them towards a space originated by Eigenfaces. A comparative performance analysis based on the Euclidian distance amongst the eigenvectors are determined that requires extraction of Eigenface between an unknown image and each training image. Now, if the composite distance is minimal to the empirical tolerance, the unknown lux image is recognized, otherwise, the image is not classified. The detailed method is explained using Fig. 5.1.

Euclidean distance of the unknown or the test image weight vector (w_M) from training image dataset weight vectors (w_T) is perceived from equation (5.3):

$$d(w_T, w_M) = (\sum_{i=1}^n (w_{Ti} - w_{Mi})^2)^{\frac{1}{2}} = \|w_T - w_M\| \quad (5.3)$$

Here, n is the quantity of selected Eigenface. For an unknown image, the Euclidian distance is smaller than a predetermined set-point and possesses a least value in the Eigenface lux training dataset. The unknown image is uncategorized if its Euclidean distance is more than the set-point. This technique is quite simpler to formulate as no hardware circuitry is required, yet the authentication accuracy of the image is on the higher side. Only lag is its computational time requirement that is very high to retrieve an image if the training image dataset is quite large.

5.4.2.1 Eigenface Calculation Procedure

The salient steps required to implement the calculation of Eigenface [193-196] are as follow:

- a) A database S consisting of training images ($\Gamma_1, \Gamma_2, \dots, \Gamma_n$) is created.
- b) The average (Ψ) value is calculated.

- c) The difference (Φ) between a training image (Γ_i) and the middle value (Ψ) is found out.
- d) The value of co-variance matrix (C_M) is computed.
- e) The Eigenvalue (λ) and the Eigenvector (E_V) of the co-variance matrix (CM) is determined.
- f) Finally, the Eigenfaces for each training image and the unknown images are evaluated. The similarity factor is computed based on the optimal composite difference using the Euclidean distance technique, which is mentioned in equation (5.4). Each and every sample is collated with the respective unknown or test matrix. If the obtained feature value is minimum at the completion time, then it is treated as the closest homogeneous sample.

$$D_{j,k} = \sqrt{\sum_{i=1}^N (E_{j,i} - E_{p,i})^2}, j=1\dots n \text{ and } p=1\dots k \quad (5.4)$$

Pseudo-code for determination of Euclidean distance between eigenfaces of Training image dataset and eigenface of each Test image

1. **Input:** Read M no. of images from the image database that comprises of three different classes of reference images. Resize each of them to 50X50 dimension. Create Training image dataset as Im_O of size 2500XM
2. **Input:** Read the corresponding test image, resize it to 50X50 dimension and store it as Im_T
3. $AV_{Im} \leq$ calculated mean image of Im_O
4. Calculate normalised face vector as $A = Im_O - AV_{Im}$
5. $A_{test} = Im_T - AV_{Im}$
6. Calculate covariance matrix of reduced dimension as $C = A^T * A$ (C has dimension of MXM)
7. Calculate eigenvectors or eigenfaces of C as $[V, E] = \text{eig}(C)$
8. Calculate eigenface of original dimension as $V_L = A * V$
9. Sort eigenvectors V_L according to the eigenvalues in descending order
10. Select $k=3$ eigenfaces that will represent >90% of information and store it as V_L'
11. Store $V_T \leq \text{transpose}(V_L')$
12. Calculate weight vector of training dataset as $W = V_T * A$
13. Calculate weight vector of test image as $W_m = V_T * A_{test}$
14. Calculate Euclidean distance, $d = \| W - W_m \|$

15. **Output:** Test image is classified as the image that is showing minimum Euclidean Distance d . The corresponding image is considered to belong from that particular training image class.

16. **End**

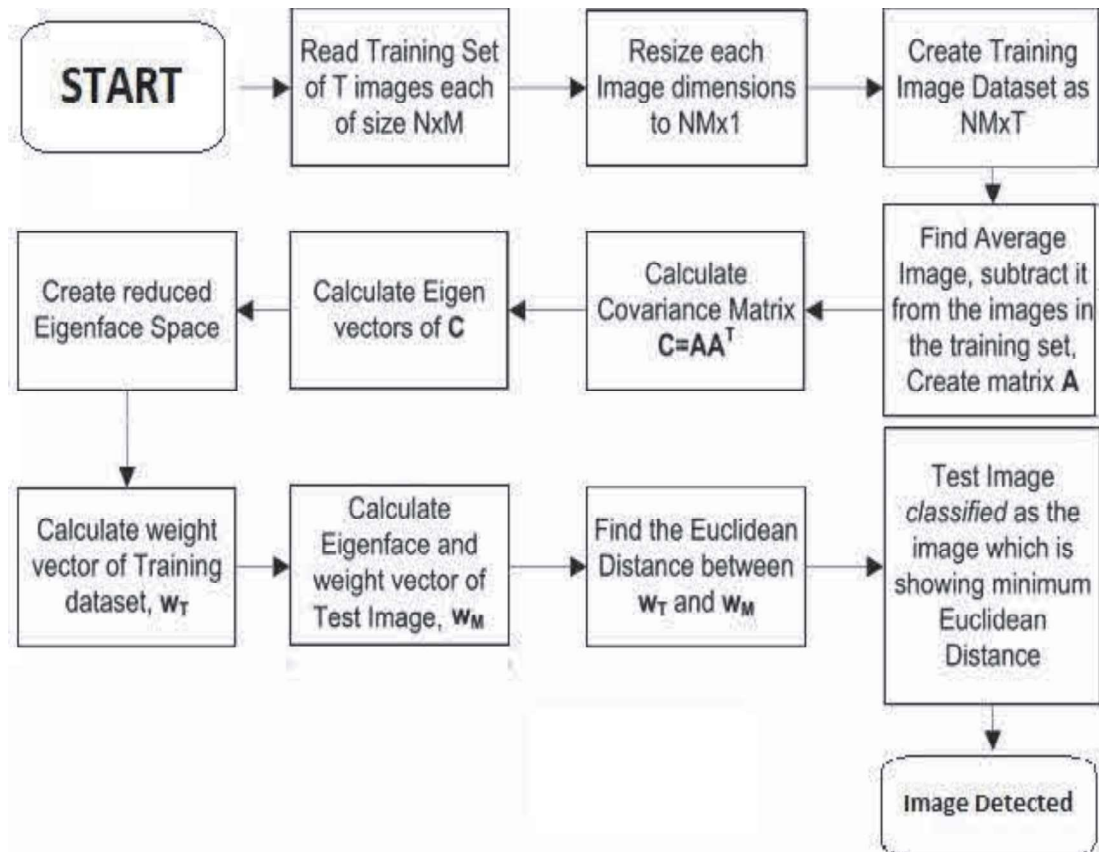


Fig. 5.1: Eigenface image recognition technique flowchart

5.4.3 Histogram Method

The pixel intensity data distribution is designated as histogram of the image in perspective of digital image processing. There are two methods as discussed henceforth.

5.4.3.1 Histogram Intersection Method

Histogram is truly value dispersal of digital image into a graphical procedure. This value scattering helps in determination of an image or object. This modest image classification is centered on the similarity of two separate histograms, i.e. for each training image and an unknown/test image. Now, if the intersectional area or overlapping zone of both the histograms can be found out then the similarity between the distinct set of images can be

estimated. Moreover, if the intersectional area becomes high, the two histograms will be similar in nature, or in other words, the similarity factor between the two set of images will be high. The simple least height scheme can be utilized for finding out the intersectional area. In this thesis, both test and reference image histograms are found out and the similarity factor for each image is determined. Afterwards, the net histogram similarity factor between a test image and the reference images is achieved by assigning an equal weightage level to each individual plane histogram similarity values. The obtained value can then be used for finding out the image similarity.

Pseudo-code for computation of Image Similarity using Histogram Intersection Method

1. **Input:** Image A and Image B as two image files that are to be compared
2. **Output:** d as area made by intersection of two images Image A and Image B
3. Size of input images are found out using the following functions:
 $[m1\ n1]=\text{size}(\text{Image A})$ and $[m2\ n2]=\text{size}(\text{Image B})$
4. The histogram counts and bin-locations for both the images are determined
5. The histogram of Image A is determined by using the following functions:
 $\text{Hist}_A = \text{zeros}(256, 1)$
for $i = 1:m1$
 for $j = 1:n1$
 $km = \text{Image A}(i, j) + 1$ (One is added to avoid indexing by zero)
 $\text{Hist}_A(km, 1) = \text{Hist}_A(km, 1) + 1$
 end
end
end
6. The normalized histogram is found next by the relation:
 $\text{Hist}_A_pdf = (1/(m1 * n1)) * \text{Hist}_A$
7. Similarly the histogram of Image B is found out by the following functions:
 $\text{Hist}_B = \text{zeros}(256, 1)$
for $i = 1:m2$
 for $j = 1:n2$
 $km = \text{Image A}(i, j) + 1$ (One is added to avoid indexing by zero)
 $\text{Hist}_B(km, 1) = \text{Hist}_B(km, 1) + 1$
 end
end
end
8. The normalized histogram of Image B is also found out by the relation:

$\text{Hist}_B_{\text{pdf}} = (1/(m2*n2)) * \text{Hist}_B$

9. The intersection between Image A & Image B computed next.

Inter_Value = 0;

for i=1:256

 km1=HistA_PDF(i,1);

 km2=HistB_PDF(i,1);

 km12= [km1; km2];

 Inter_Value= Inter_Value + min (km12);

end

10. Intersectional area value between two images is determined to be the similarity factor between two images and is given by the relation: $d = \text{Inter_Value}$

11. **End.**

5.4.3.2 Histogram Distance Method

This method is basically pairwise computation of the Euclidean distance between a normalized test image histogram and a normalized training image histogram. The Euclidean distance can be calculated using the following formula:

$$D = (\sum(\text{Hist}_{\text{test}} - \text{Hist}_{\text{trng}}))^2 \quad (5.5)$$

Where, $\text{Hist}_{\text{test}}$ is the normalized test image histogram and $\text{Hist}_{\text{trng}}$ is the normalized training image histogram. If this distance value is small, then, the two compared images are of higher proximity to each other, whereas, if the Euclidean distance is large, then, the compared images are of least vicinity.

Pseudo-code for Image Similarity computation using Histogram Distance Method

1. **Input:** Image A and Image B as two image files that are to be compared
2. **Output:** d as Euclidean distance of two images Image A and Image B
3. Read the test image A and find out its normalized histogram ($\text{Hist}_{\text{test}}$).
4. Read the training image B and find out its normalized histogram ($\text{Hist}_{\text{trng}}$).
5. Now, calculate the Euclidean distance (D) using the formula: $D = (\sum(\text{Hist}_{\text{test}} - \text{Hist}_{\text{trng}}))^2$
6. If D is small, then, test and training illuminance images are similar to each other and vice-versa.
7. **End.**

5.5 Experimental Set-Up

An experimental unit was originated to capture the lux data, after which it was transformed into a lux image. The illumination values (in lux) serve as the variable of interest in this study. Illuminance is defined as the luminous flux received at each unit area by any point on the surface that is subjected to incident light. PCA-Eigenface based classification technique, Histogram Intersection method, and Histogram Euclidean Distance technique were applied to categorize an unknown lux image. The comparative performance analysis was also executed for detecting the accuracy of the aforesaid techniques when compared with a test lux image of a concerned class and each training image of respective classes present in the real-time image repository.

5.5.1 Client-Server System

The lux values are acquired using a client-server network set-up as outlined in Fig. 5.2, whereas, the experimental data acquisition unit is represented in Fig. 5.3.

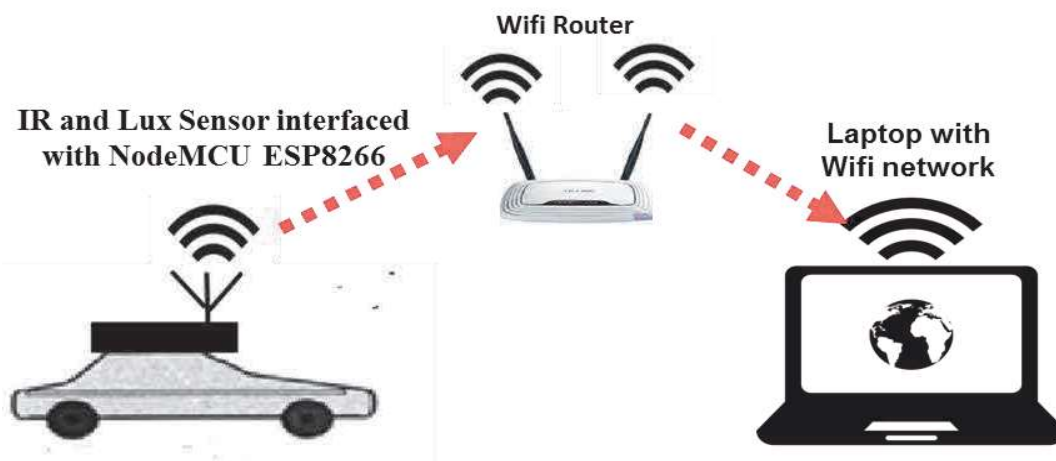


Fig. 5.2: Sensor data acquisition terminal



Fig. 5.3: Experimental unit for data acquisition

- a. Client Terminal: The client terminal consists of lux data acquisition unit and IR transceiver unit for capturing positional information. These sensors are interfaced with Node MCU ESP 8266 terminal having integrated Tensilica make microcontroller. ESP 8266 based wifi module works in I2C communication interface, runs on a rechargeable battery and is positioned at the roof of RF remote operated car. The client terminal moves along the selected indoor space position and in the process gathers lux information about the prefixed indoor position. Then, it sends them to the server terminal by the help of wireless router terminal for further processing.
- b. Server Terminal: The server terminal comprises of a computer with specification as laid down in last chapter with network adapter by the help of which it connects to a wireless router using a network cable of decent quality.
- c. Wireless Router Terminal: A double-antenna wireless router is used with the specifications remaining same as earlier. The lux data corresponding to every indoor space position is stored in the server terminal as MS-Excel file for future processing as and when required.

5.5.2 Transformation to Image Domain

The position based captured lux values in the X-Y floor coordinate locations are converted into an image at the server terminal. The captured data may be filtered to eliminate the presence of any noise during data acquisition. Gaussian type filtering technique removes any linear noisy data, whereas, median filter provides the ability to filter out the nonlinear impulse noise. Several types of lux ambience were formed and lux images were constructed and they are treated as training image. Three types of lux grades were formulated to generate lux training database for this study.

5.6 Results and Discussions

The training database that was utilized here consists of three numbers of lux images persisting in each of the three different image grades - Grade-I: Non-uniform illuminance (100-199 lux), Grade-II: Uniform illuminance (greater than or equal to 200 lux) and Grade-III: Highly non-uniform illuminance (lesser than 100 lux). Training images for Grade-I image class are represented in Fig. 5.4(a) – Fig. 5.4(c), Fig. 5.4(d) – Fig. 5.4(f) denote the Grade-II training image class, and Fig. 5.4(g) – Fig. 5.4(i) indicate the Grade-III training image class respectively. However, the threshold values of illuminance may be set as per IS 3646, part-I, 1992, which is the national standard for interior illuminance or can be decided by the

designer depending upon the application area. Every image has a dimension of 3600×2400 pixel. Now, these images are resized to 1600×1500 pixel, after which they are converted from RGB colour palette to grayscale palette. To minimize the calculation fatigue and increase the processing speed, the trained images are then resized to a dimension of 160×150 pixel. After application of normalization process, the PCA-Eigenface based similarity detection technique is followed, and those Eigenfaces having largest eigenvalues are now derived from the training database. Each training image is contemplated as a linear amalgamation of obtained Eigenfaces and can be regenerated therefrom. The Eigenfaces that possess maximum eigenvalues denote significant contrast in lux-training dataset. For testing purpose, Fig. 5.5(a) – Fig. 5.5(c) represents Grade-I test image class, Fig. 5.5(d) – Fig. 5.5(f) indicate the Grade-II test image class, and Fig. 5.5(g) – Fig. 5.5(i) denote the Grade-III test image class respectively. The composite distance between the training images and each testing image is used to find out the similarity factor. Any test illuminance image is said to symbolize a specific lux image class if the similarity factor is minimum for a particular image class amongst all the three specified illuminance image classes and vice-versa.



Fig. 5.4(a) Grade-I Training Image No.-I

Fig. 5.4(b) Grade-I Training Image No.-II

Fig. 5.4(c) Grade-I Training Image No.-III



Fig. 5.4(d) Grade-II Training Image No.-I

Fig. 5.4(e) Grade-II Training Image No.-II

Fig. 5.4(f) Grade-II Training Image No.-III

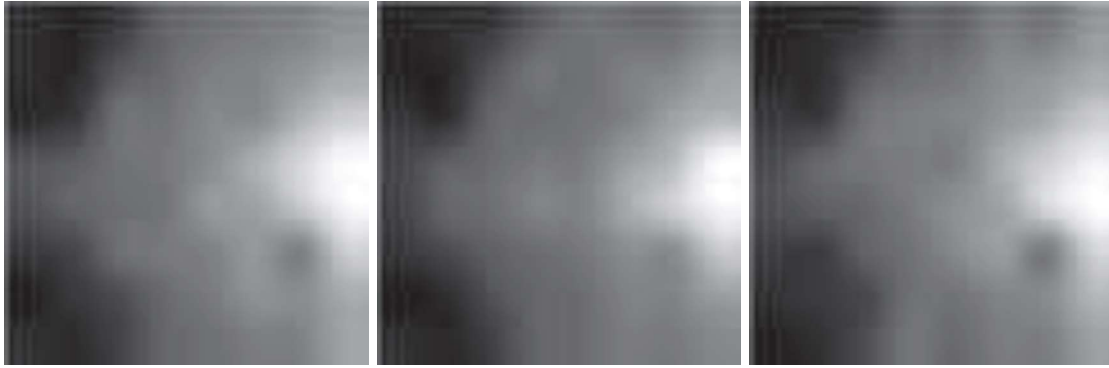


Fig. 5.4(g) Grade-III
Training Image No.-I

Fig. 5.4(h) Grade-III
Training Image No.-II

Fig. 5.4(i) Grade-III
Training Image No.-III

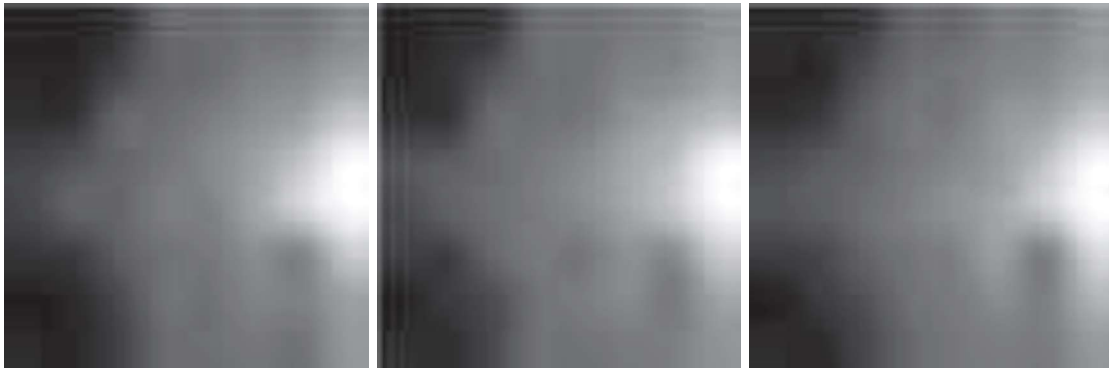


Fig. 5.5(a) Grade-I Testing
Image No.-I

Fig. 5.5(b) Grade-I Testing
Image No.-II

Fig. 5.5(c) Grade-I Testing
Image No.-III



Fig. 5.5(d) Grade-II Testing
Image No.-I

Fig. 5.5(e) Grade-II Testing
Image No.-II

Fig. 5.5(f) Grade-II Testing
Image No.-III



Fig. 5.5(g) Grade-III Testing
Image No.-I

Fig. 5.5(h) Grade-III
Testing Image No.-II

Fig. 5.5(i) Grade-III Testing
Image No.-III

Table 5.1: Performance Evaluation using PCA-Eigenface Method

Unknown image belonging to		Known Image Grades			Percentage Accuracy
		Grade-I	Grade-II	Grade-III	
Grade-I	Test Image-1	0.3207	0.3264	0.9502	89%
	Test Image-2	0.5817	0.6752	0.7609	
	Test Image-3	0.5733	0.7516	0.6459	
Grade-II	Test Image-1	0.4418	0.3647	0.9784	
	Test Image-2	0.6758	0.5394	0.7050	
	Test Image-3	0.5529	0.4995	0.8092	
Grade-III	Test Image-1	0.8755	0.6932	0.5139	
	Test Image-2	0.9062	0.7140	0.4901	
	Test Image-3	0.4216	0.4980	0.9222	

It can be observed from Table-5.1 that the similarity factor of Grade-I Test Image-1, Grade-I Test Image-2, and Grade-I Test Image-3 is minimum when compared with Grade-I training image than with Grade-II and Grade-III training image. Likewise, the similarity factor of Grade-II Test Image-1, Grade-II Test Image-2, and Grade-II Test Image-3 is minimum when compared with Grade-II training image than with Grade-I and Grade-III training image. Moreover, the similarity factor of Grade-III Test Image-1, and Grade-III Test Image-2 is minimum when compared with Grade-III training image than with Grade-I and Grade-II training image. Last but not the least, the similarity factor of Grade-III Test Image-3 is minimum with Grade-I training image than with the trained image of other grades. Finally, it can be inferred that PCA-Eigenface method can successfully classify eight test images out of the total nine test images. Only for a single instance it misclassifies the test image. The percentage accuracy is almost 89% for PCA-Eigenface method and hence, it can be applied for corrective and preventive measures in classification related applications.

This method can find its applications in related experiments for determining the uniformity when measurements using sensors are strenuous to obtain. An image consists of valuable intelligence on a particular event or it can be formulated as an experimental outcome. The similarity between two images cannot always be separable by a human eye. In this research analysis, it has been observed, that if the measured lux boundary values are known, the lux distribution within a contour can be approximated accurately.

Fig. 5.6(a) – Fig. 5.6(i) represent the histograms of Grade-I test images and respective training images pertaining to the same grade.

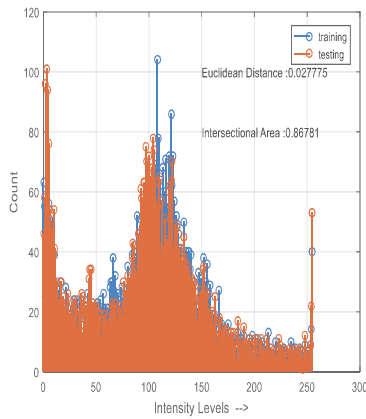


Fig. 5.6(a) Histogram of Grade-I Test Image-I and Training Image-I

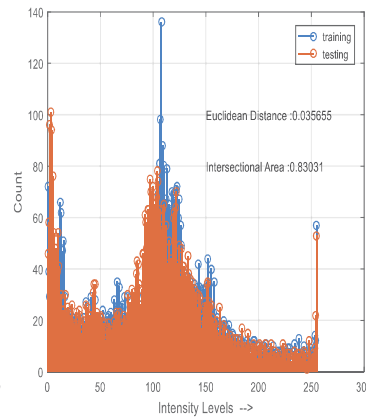


Fig. 5.6(b) Histogram of Grade-I Test Image-I and Training Image-II

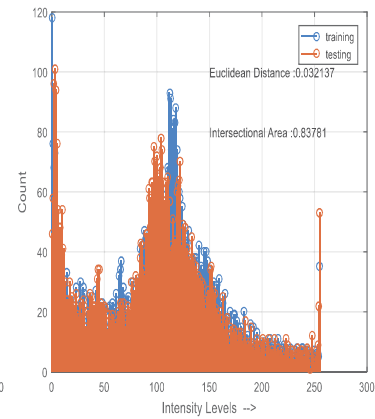


Fig. 5.6(c) Histogram of Grade-I Test Image-I and Training Image-III

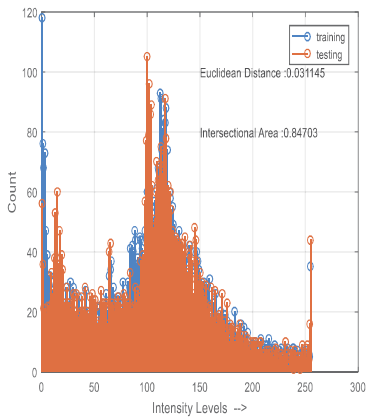


Fig. 5.6(d) Histogram of Grade-I Test Image-II and Training Image-I

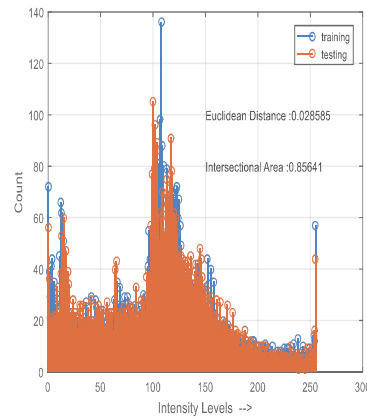


Fig. 5.6(e) Histogram of Grade-I Test Image-II and Training Image-II

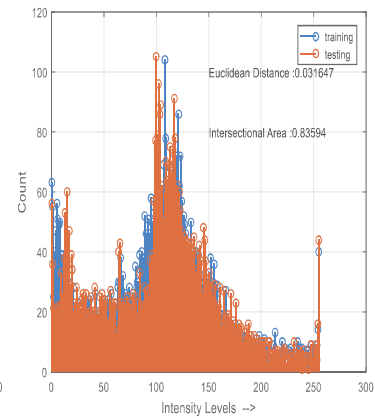


Fig. 5.6(f) Histogram of Grade-I Test Image-II and Training Image-III

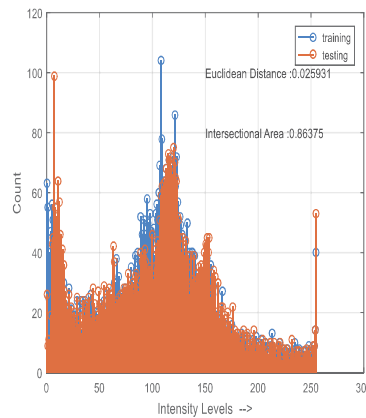


Fig. 5.6(g) Histogram of Grade-I Test Image-III and Training Image-I

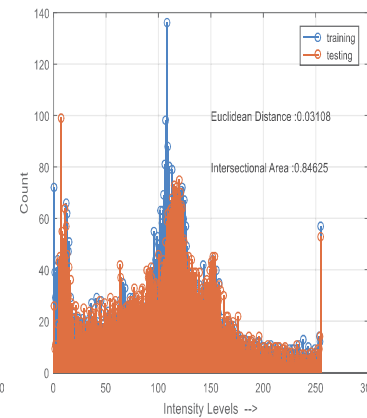


Fig. 5.6(h) Histogram of Grade-I Test Image-III and Training Image-II

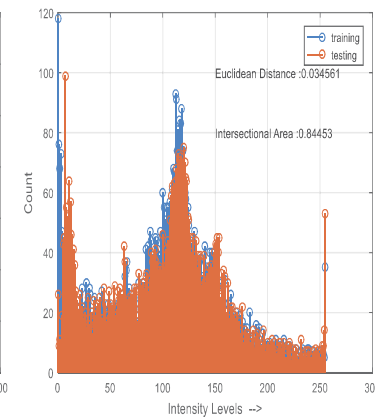


Fig. 5.6(i) Histogram of Grade-I Test Image-III and Training Image-III

Fig. 5.7(a) – Fig. 5.7(i) represent the histograms of Grade-II test images and respective training images of the same grade.

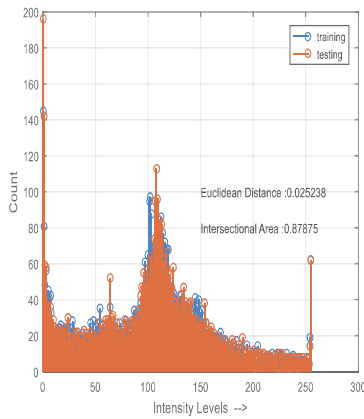


Fig. 5.7(a) Histogram of Grade-II Test Image-I and Training Image-I

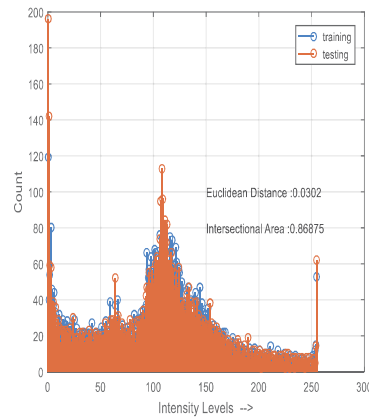


Fig. 5.7(b) Histogram of Grade-II Test Image-I and Training Image-II

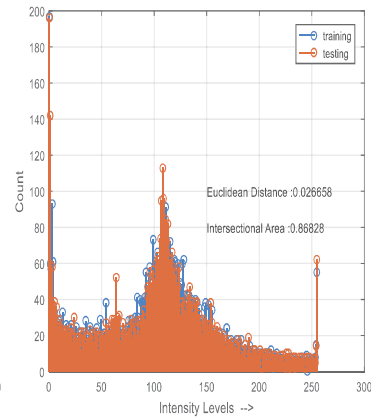


Fig. 5.7(c) Histogram of Grade-II Test Image-I and Training Image-III

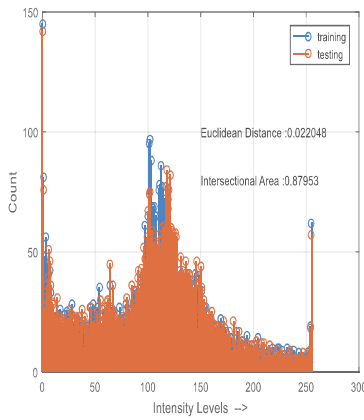


Fig. 5.7(d) Histogram of Grade-II Test Image-II and Training Image-I

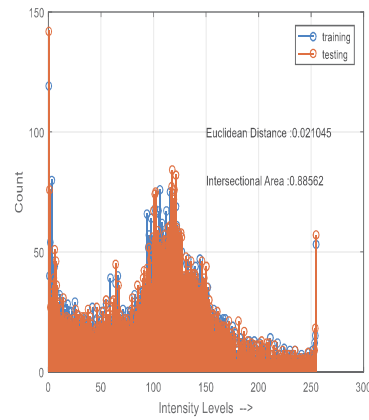


Fig. 5.7(e) Histogram of Grade-II Test Image-II and Training Image-II

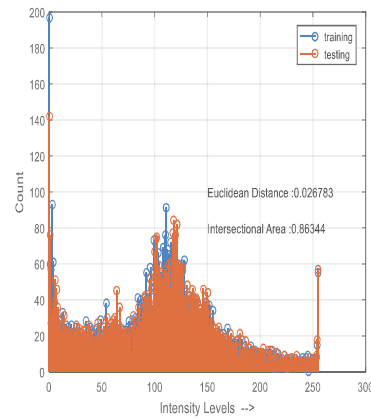


Fig. 5.7(f) Histogram of Grade-II Test Image-II and Training Image-III

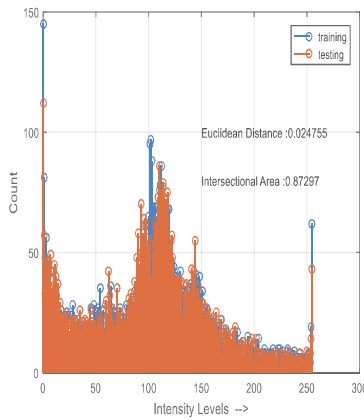


Fig. 5.7(g) Histogram of Grade-II Test Image-III and Training Image-I

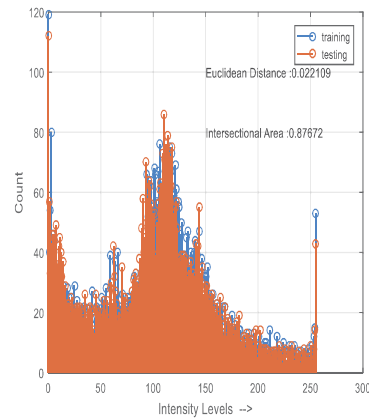


Fig. 5.7(h) Histogram of Grade-II Test Image-III and Training Image-II

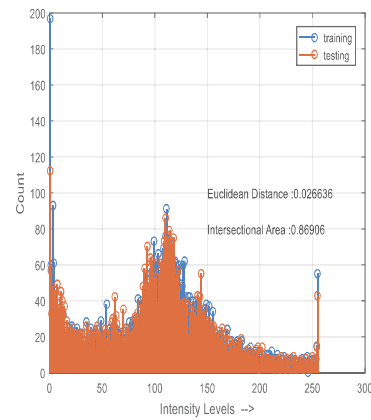


Fig. 5.7(i) Histogram of Grade-II Test Image-III and Training Image-III

Fig. 5.8(a) – Fig. 5.8(i) represent the histograms of Grade-III test images and respective training images belonging to the same grade.

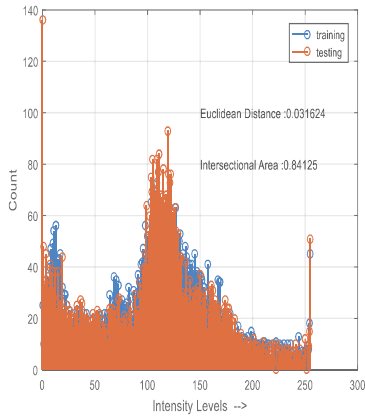


Fig. 5.8(a) Histogram of Grade-III Test Image-I and Training Image-I

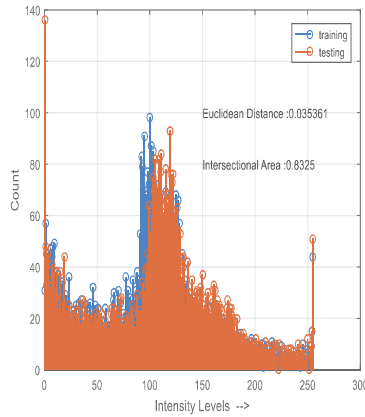


Fig. 5.8(b) Histogram of Grade-III Test Image-I and Training Image-II

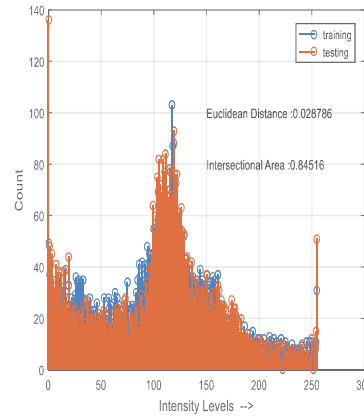


Fig. 5.8(c) Histogram of Grade-III Test Image-I and Training Image-III

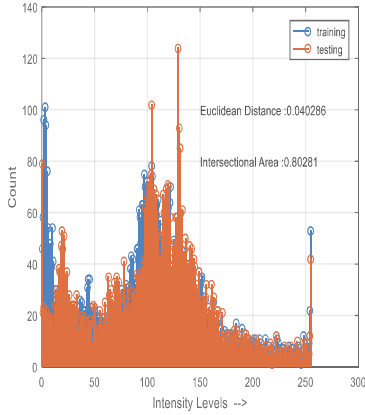


Fig. 5.8(d) Histogram of Grade-III Test Image-II and Training Image-I

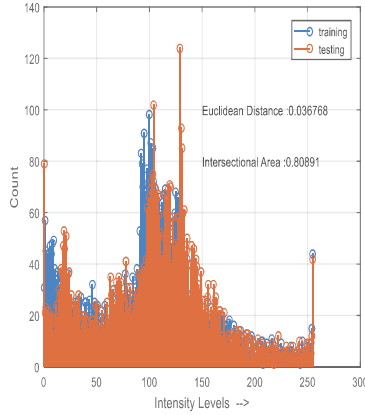


Fig. 5.8(e) Histogram of Grade-III Test Image-II and Training Image-II

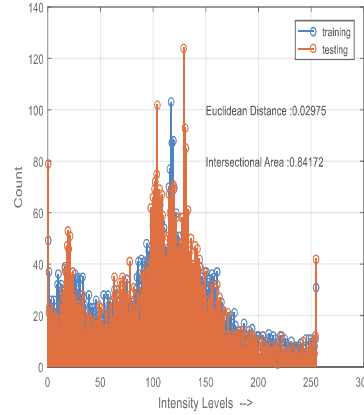


Fig. 5.8(f) Histogram of Grade-III Test Image-II and Training Image-III

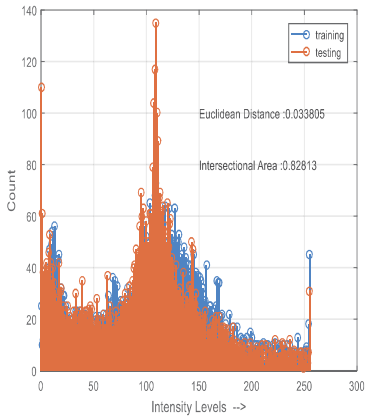


Fig. 5.8(g) Histogram of Grade-III Test Image-III and Training Image-I

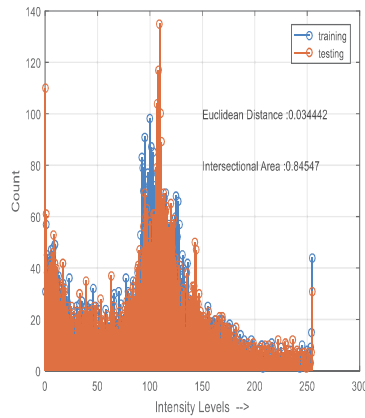


Fig. 5.8(h) Histogram of Grade-III Test Image-III and Training Image-II

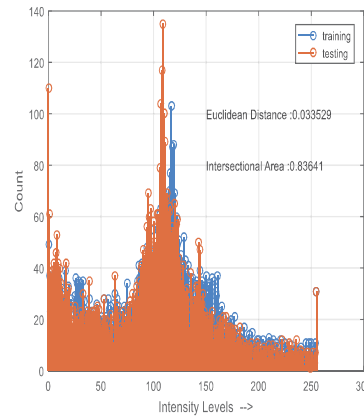


Fig. 5.8(i) Histogram of Grade-III Test Image-III and Training Image-III

Table 5.2: Performance Evaluation using Histogram Intersection Method

Unknown image belonging to		Known Image Grades			Percentage Accuracy
		Grade-I	Grade-II	Grade-III	
Grade-I	Test Image-1	0.8678	0.8303	0.8378	67%
	Test Image-2	0.8470	0.8564	0.8359	
	Test Image-3	0.8637	0.8462	0.8445	
Grade-II	Test Image-1	0.8787	0.8687	0.8682	
	Test Image-2	0.8795	0.8856	0.8634	
	Test Image-3	0.8729	0.8767	0.8690	
Grade-III	Test Image-1	0.8412	0.8325	0.8451	
	Test Image-2	0.8028	0.8089	0.8417	
	Test Image-3	0.8281	0.8454	0.8364	

Table 5.2 represents the comparative performance analysis of the test illuminance images of respective grades when compared with the training images of known image grades. If the intersectional or overlapping area is highest for a test image in comparison with a training image of concerned class, then the particular test image is considered to be most similar with that specific training image. Here, it can be observed that the intersectional area values of Grade-I Test Image-1, and Grade-I Test Image-3 are maximum when compared with Grade-I training image than with Grade-II and Grade-III training image. The overlapping area value of Grade-I Test Image-2 becomes highest for Grade-II training image than with Grade-I and Grade-III training image. Hence, the classification is proper for two images and it misclassify for a single case. Likewise, the overlapping area values of Grade-II Test Image-2, and Grade-II Test Image-3 are maximum when compared with Grade-II training image than with Grade-I and Grade-III training image. Whereas, the intersectional area value of Grade-II Test Image-1 is highest for Grade-I training image than with Grade-II and Grade-III training image. Therefore, the classification is accurate for two images and it is improper for a test image. Lastly, the intersectional area values of Grade-III Test Image-1, and Grade-III Test Image-2 are maximum when compared with Grade-III training image than with Grade-I and Grade-II training image. The overlapping area value of Grade-III Test Image-3 becomes highest for Grade-II training image than with Grade-I and Grade-III training image. Hence, the classification is appropriate for two images and it is unsuitable for a test image. Finally, it can be inferred that the Histogram Intersection method can successfully classify six test

images out of the total nine test images. For three instances, it misclassifies the test image. The percentage accuracy is almost 67% for this method and hence, it can be considered as quite unsuitable for corrective and preventive measures in classification related applications. A possible reason behind this response may be due to the fact that Histogram Intersection method considers global minima, in this process introduces false minima and possess less generalization capability.

Table 5.3: Performance Evaluation using Histogram Distance Method

Unknown image belonging to		Known Image Grades			Percentage Accuracy
		Grade-I	Grade-II	Grade-III	
Grade-I	Test Image-1	0.0277	0.0356	0.0321	78%
	Test Image-2	0.0311	0.0285	0.0316	
	Test Image-3	0.0259	0.03108	0.0345	
Grade-II	Test Image-1	0.0252	0.0302	0.0266	
	Test Image-2	0.0220	0.0210	0.0267	
	Test Image-3	0.0247	0.0221	0.0266	
Grade-III	Test Image-1	0.0316	0.0353	0.0287	
	Test Image-2	0.0402	0.0367	0.0297	
	Test Image-3	0.0338	0.0344	0.0335	

Table 5.3 characterizes the performance comparison of the test illuminance images of respective grades when compared with the training images of known image grades. If the Euclidean Distance of the histogram is minimum for a test image in comparison with a training image of concerned class, then that particular test image is said to be most analogous with the concerned training image. It can be perceived that the Euclidean Distance values of Grade-I Test Image-1, and Grade-I Test Image-3 are minimum when compared with Grade-I training image than with Grade-II and Grade-III training image. The distance measure of Grade-I Test Image-2 becomes least for Grade-II training image than with Grade-I and Grade-III training image. Hence, the segmentation is proper for two images and this method is unable to classify a single test image properly. Whereas, the Euclidean Distance measure of Grade-II Test Image-2, and Grade-II Test Image-3 are minimum when compared with Grade-II training image than with Grade-I and Grade-III training image. Whereas, the distance value of Grade-II Test Image-1 is minimum for Grade-I training image than with Grade-II and

Grade-III training image. Consequently, the classification is accurate for two images and it is unsuitable for a test image. Lastly, the Euclidean Distance measures of all the three Grade-III test images, i.e. Grade-III Test Image-1, Grade-III Test Image-2, and Grade-III Test Image-3 are least when compared with Grade-III training image than with Grade-I and Grade-II training image. Therefore, the classification is appropriate for all the test images. Lastly, it can be concluded that the Histogram Euclidean Distance method can successfully classify seven test images out of the total nine test images. For two instances it misclassifies the test image. The percentage accuracy is almost 78% for this method and hence, it may be considered for remedial and preemptive measures in classification related applications. The probable reason for the performance enhancement in comparison to Histogram Intersection method may be consideration of local minima instead of global minima for the overlapping method, prevent introduction of any false minima and thus have high generalization capacity.

Chapter Summary

This chapter describes the techniques for classification of illuminance images using PCA-Eigenface method, Histogram Intersection technique, and Histogram Euclidean Distance method. The positional lux values are captured by an illuminance sensor as and when the remote car moves along the selected indoor space. The acquired data is converted to an image and after that PCA-Eigenface based image processing technique, Histogram Intersection method, and Histogram Euclidean Distance technique are applied to classify the captured illumination image grade and a comparative performance analysis have also been executed. The PCA-Eigenface method was giving the highest accuracy followed by Histogram Euclidean Distance method. The Histogram Intersection technique was giving the least accuracy when the experimental research analysis was executed. The next and the last chapter represent the conclusions extracted from the conducted research work and further, depict some of the future prospects of this study.

Conclusion and Future Scope

6.1 Conclusion

The primary aim of a lighting layout is to provide efficient light for visual phenomenon. On the other hand, non-visual functions integrate and control our organic activities like circadian rhythm, myosis, melatonin secretion, intellectual ability, memory, temper and locomotion, to name a few. The effective usages of light emitting diodes have significant impact on our biological processes and photodynamic therapy instead of metal-halide luminaries or compact fluorescent bulbs to strive for a better human life. A review of biological and health impact on public life caused by artificial light have been represented as an initial study.

The illumination is an important parameter to assess the lighting quality of a situation and precise lux measurement using proper sensor is required prior to its implementation in any practical application. In this study, the estimation of lux values on the acquired dataset using different types of machine learning regression models have been represented. Extensive comparative performance assessment of the evaluating parameters has also been carried out to predict the illuminance values with respect to a pre-calibrated reference meter. The different types of regression analysis are performed on the captured lux sensor dataset to predict the illumination sensor output accurately in terms of a calibrated lux meter prior to its real-time use. The sensor data are computed using different machine learning regression techniques and plotted with respect to a standard lux meter data. The process is initially conducted using an illumination sensor and also by the help of a RGB sensor as both the

sensors can be used for prediction of illuminance. RGB sensor offers the advantage of estimation of CCT values in addition to illuminance prediction and that is why they are more preferable at certain applications. If an illumination sensor is used then the lux values are obtained from the sensor that is interfaced with a microcontroller and simultaneously the values are also captured from a standard lux meter at the client terminal. Now the illuminance data are transmitted from the client end to the server terminal, where, four types of machine learning based regression algorithms are applied for estimation of calibrated sensor values from raw illumination data obtained from the lux sensor. Similarly, when RGB sensor is used, the RGB values are obtained from a sensor that is integrated with a microcontroller and the lux data are obtained from a standard chroma meter at the client end. Now, the RGB data are transmitted in a wireless network and four various types of machine learning regression techniques are applied at the server end for proper estimation of the illuminance values on a real-time captured dataset. Thus, an accurate RGB sensor model is developed that can predict the lux values and are also comparable to a standard lux meter.

Correlated Colour Temperature (CCT) is also an important parameter to determine the quality of lighting in an indoor space. In this study, the calibration of RGB sensor have been presented for estimation of real-time CCT values using four different types of regression techniques similar to that of illuminance estimation. Further, comparative performance assessment has been done on the evaluating parameters with respect to a calibrated chroma meter. The RGB values have been acquired from a sensor interfaced with a microcontroller and the CCT data are simultaneously observed from a calibrated chroma meter at the client terminal. The machine learning regression techniques are applied at the server terminal to find out the CCT values and a comparative performance analysis have been done to find the best possible prediction model that can be compared to a standard meter based on the performance indices to decide on their accuracy.

An IoT based illumination monitoring system has been developed that enables the users to measure lux values at multi-positional indoor space using mobile sensors and store them in a cloud server network. The sensing unit is designed by the integration of an illumination sensor and IR transceiver for position detection with embedded microcontroller having on-chip wifi device placed over the roof of a RF operated car. The car when moves through a selected indoor space gathers positional lux values at certain time interval and stores them on the cloud server through a wireless transceiver system. The stored values are used to generate a lux map that is compared with the benchmark and the result of comparison is considered to be intelligent information for modification of the existing illumination system. A similar set-

up is developed for acquisition of positional RGB sensor values and estimation of illuminance and CCT data therefrom the equations obtained in the machine learning based regression analysis.

Computer vision methods are conventionally used for identification of object boundaries from an image of interest. Extensive performance analysis of computer vision techniques have been carried out for detection of objects present in a room from the acquired real-time lux sensor data. A server-client wireless network is initially set up to capture horizontal lux data of a room using unmanned surface vehicle. The client unit comprises of illuminance sensor and IR transceiver module for capturing the positional lux information of an indoor space. The sensing block is interfaced with a wireless enabled microcontroller and it transmits the sensor values to a sever unit by the help of a wireless router. Now, the obtained values are stored in a computer system that works as a server module. The acquired real-time positional lux data are converted into image and four different computer vision techniques have been used to detect the possible position and object shape at the indoor space. Comparative assessment based on three different types of performance indices have been carried out to find out the most acceptable solution.

In this study, a method to detect similarity level of lux images from a real-time captured dataset using a wireless server-client network arrangement has also been proposed. An illuminance sensor is interfaced with an embedded wireless microcontroller, which is considered to be the client terminal. This entire system is kept at the top of a remote car; while traversing through the selected floor space, it acquires lux values of that place, transmit and save them in a computer system, which is considered as the server terminal. The process is repeated to capture multiple training data and at the server end, each dataset is converted into a grayscale illuminance image, possessing spatial pixel intensity for each instance in pre-processing phase. Now, when a test image arrives, they are compared for resemblance with a training image using PCA-Eigenface method, Histogram Intersection technique, and Histogram Distance method by calculating their pixel proximities. This computation generates a feature value, which can be used as a comparison metric. For an unknown or test image, this feature value is significant enough to compare with a particular training image. A comparative performance evaluation of the aforesaid considered techniques with representation of their accuracy levels have been executed successfully in this research analysis.

Human Centric Lighting is popularly known as lighting for health and better living amongst the lighting designers and researchers. It has a significant impact on individual health,

behavioural and emotional stability at night that suppress melatonin generation rate. This study proposes a new concept called Internet of Human Centric Lighting by which lighting systems can be monitored and administered by smart internet enabled gadgets for stimulating our work efficiency during day-time and relaxation at night to reinforce natural circadian rhythm for a better living environment.

6.1.1 Social Impacts of Study

Careful lighting design with optimum lighting levels can provide us with personal safety against criminal incidents and enable us to enjoy social as well as commercial gatherings securely. Prior to the commencement of any sports, musical, or related activities, if the developed remote car can manoeuvre throughout the entire indoor space then the corresponding positional lighting levels can be properly yet automatically monitored. If the lux levels are found to be within satisfactory limit then one can enjoy the activity thoroughly. The requirement of any hand-held lux meter will certainly abolish and will boost the activity level of the umpires or organizers depending upon the activity. Moreover, if it is required during an on-going activity, the developed system can be utilized for monitoring the locational indoor lux levels. Also, no player or any performer can complain about the illuminance level of any selected indoor space as it is entirely automated. If the indoor light levels are below a certain threshold limit, it may lead to light pollution. Over-exposure to lighting can sometimes reduce our visibility and produces strident shadows. Both over-exposure as well as light pollution in indoor lighting affect the circadian rhythm of a human being and thus may lead to certain deadly diseases, at times.

6.1.2 Economic Impacts of Study

If the indoor space gives optimum security interms of illuminance, then, enthusiasm will be enhanced amongst the people to watch the respective activity live from the indoor arena instead of viewing the telecast through television or any other equivalent platforms. Hence, more spectators will be encouraged to visit the indoor space and it will eventually enhance the revenue and profitability of the organizers. Even, if anyone is watching the activity live from television or any other platform, then, adequate illumination level that is standardized for any sports or other activities must be maintained and that can be monitored easily through the help of the designed model. The standard of telecast will be enriched and it may attract more television rating point (TRP) for the broadcasters; hence their advertisers will increase

and will eventually escalate their profitability at the same time. Moreover, no organizer will be required to arrange costly, hand-held light meters if they possess the developed lux monitoring system within their facility. Also, if the developed illuminance monitoring system provides information that lux level of the designed model is beyond a certain required limit, then, the additional luminaries may be removed. This will keep the lighting levels within satisfactory limits and minimize the project expense at the same time.

6.1.3 Environmental Impacts of Study

The developed prototype is capable of monitoring the positional illuminance level of the selected indoor space. While capturing the indoor lux values if it finds out that at a certain position, the illumination level is quite high, then the corresponding area can be detected and intimation may be provided to the concerned personnel to remove the additional luminaries from that space such that it serves the purpose for which it has been designed. Thus, the designed model can save the wastage of interior electrical energy up to its optimum level. As most of the generated energy is from coal based thermal power plants and considering the present situation of huge scarcity of natural resources it can turn out as a boon. On the other hand, if the developed system intimates about lower illuminance level and there is a possibility of light pollution due to poor lighting design, installation or maintenance then the respective section may be well-informed about it prior to the commencement of any activity and the lighting level can be restored to its required limit. This can also lead to maintain a balance in the ecosystem such that both human and non-human species can stay vigorously within the selected indoor space.

6.2 Future Prospects of Research Work

This section is meant to describe the future prospects of this research study. Initially, a review work has been performed to search the novelties of a number of original research works. However, this task is undertaken to decipher the benefits of an efficient lighting design for the visual impression as well as the biological impact of light at various spectra (e.g., health, wellbeing and alertness) essential for our daily life. Apart from health and alertness, an elegant lighting installation tends to speedy enactment, optimum security, minimization of accidents and lesser absence. These finally results in better productivity as well as working environment. At present, there is massive use of LED lighting technology and the other artificial sources of light have highly been outnumbered. Moreover, LED emits light in

narrow frequency range. There is a need to study the long-term impact on all biological systems to ensure health safety. There is also a need to map detailed emission spectra of all major light sources for better understanding of statistically increasing health problems using specific light sources.

A sensor can experience different conditions and each of them is to be considered in the training dataset before selecting any proper sensor model to improve the quality of lighting. The different methods discussed in this study are standard techniques yet cost-effective and also some of them yield high accuracy. Amongst the available regression models, only four techniques that have been found to be popularly applied in similar studies have been considered for this study and their performance have been found to be satisfactory when it is compared with a calibrated reference meter. Some other methods can also be applied that may give equally good or even better response. The techniques that have been used here are popular for giving satisfactory response even in presence of noise and only random noise has been added to this study to observe the performance of the machine learning regression techniques. Some other types of noise can also be included to test the robustness of the regression model.

The study has been conducted using illumination sensor and RGB sensor only. However, some other accurate as well as multivariable sensors may also be available in the market and can be explored in future. For development of the estimation model, an enhanced training and validation dataset may be utilized for a better response. The selected estimation model can be used in augmented reality, environmental and also in computer vision related applications to understand the applicability of the regression techniques for a better mankind. The experiment was conducted in a dark room that can also be done in presence of natural light and can become a part of our further exploration. These are all being investigated now for accomplishment in our future research study.

At the outset, the designed prototype using wireless transceiver based client-server network configuration yields satisfactory experimental observation in a selected indoor space. The car along with the sensors integrated with wireless microcontroller moves through various locations and in the process it tracks the location and illuminance values continuously and store in a file to maintain the light levels within a benchmark limit. Further, filtering of the acquired lux data is done by any authorized person using Dropbox based IoT cloud server communication medium and the updated file may also be shared for perusal of others. Initially, calibration of lux sensor with the standard lux meter is done in a similar application environment prior to data capturing to eradicate the impact of indoor wall reflectance and

other related factors in the acquired sensor data. However, their individual contributions have not been administered in this research work. For any indoor space, provision should be available for free movement of the remote car for homogeneous data capturing. Furthermore intelligence can be incorporated by generating a physical alarm as and when the illumination values fall below the threshold limit and accordingly inform the maintenance section to take preventive measures and regain the benchmark level. Moreover, using the developed system in all possible applications is presently under investigation. The performance analysis of four different edge detection techniques for obstacle identification using lux sensor data inside an indoor space have also been represented in this study for detecting the possible position and shape of the object. The proposed method is capable of detecting both frontal and hanging stationary obstacles using offline image processing of the acquired illuminance data. However, non-stationary, online obstacle identification techniques are being studied at present that can be a part of our future exploration.

An image comprises of valuable intelligence on a particular event or it can be formulated as an experimental outcome. A similarity between two images cannot always be separable by a human eye. PCA-Eigenface method, Histogram Intersection technique, and Histogram Distance method have been applied in this research analysis for similarity detection between an unknown or test image and a trained image. In the conducted study, it has been observed that if the measured lux boundary values are known, the lux distribution within a contour can be approximated accurately. The generated lux images from the sensor data can be investigated using PCA-Eigenface based similarity detection technique, Histogram Intersection method, and Histogram Distance technique for evaluation of the quality of illuminance. The obtained information may be applied for corrective and preventive measures in classification related applications. Some other techniques may also be applied for similar types of classification related problems with even better accuracy. These are presently being explored and can also become a part of our future course of analysis.

As the concept of Human Centric Lighting system is comparatively new in this part of the world, hence, customer detailed review report may not be available easily. Sometimes, the lesser important points happen to obtain greater importance and it entirely depends upon the application area, type and time of usage. Hence, a new concept called Internet of Smart Lighting or Internet of Human Centric Lighting is proposed. This new concept of lighting installation may enhance the project capital investment by a fraction but definitely reduce the operational expenses with an increase in the environmental impacts. The possible contributions for installation of this type of lighting systems are thoroughly discussed in this

study. Human Centric Lighting system will work well in workplace related to academics, research or places where light is an important parameter to be taken under consideration. This new concept of lighting arrangement will slowly but surely find a space from reputed places to every household in times to come. A review of this concept has been a part of this study, which requires a detailed understanding for development of a hardware model that is not only internet enabled but simultaneously maintains the circadian rhythm of the human being and the non-human species for a better civilization.

In this research analysis, the sensing unit is movable and acquires the illuminance information in a wireless client-server network while the remote car is in motion. The sensing unit that is considered as the client system transmits the positional lux information to the server system under the influence of a wifi router or through a mobile hotspot arrangement. Another system can be developed where more number of sensors can be installed throughout the entire indoor space from where the positional illuminance information will be captured and sorted as per the requirement. The possibility and performance analysis of this type of arrangement may be explored in future. Moreover, this study is limited to monitoring the automated illuminance level of the indoor space only and can be expanded to monitoring the illumination level for the outdoor space as well. Last but not the least, all the measurements in this study have been conducted using sensors that can be replaced by a RGB camera and may be explored as a separate research study.

Chapter Summary

This chapter depicts the conclusions obtained from this research study and highlights the social, economic and environmental aspects of the conducted experimental analysis. This chapter further discusses about the futuristic prospects of the performed research work.

List of References

- [1] A. Banafa, What is next for IOT & IIOT, Enterprise mobility summit, Australia, 2015.
- [2] M. T. Jilani, M. Z. U. Rehman, A. M. Khan, O. Chughtai, M. A. Abbas, M. T. Khan, An implementation of IoT-based microwave sensing system for the evaluation of tissues moisture, *Microelectronics Journal*, Vol. 88, pp. 117–127, 2019, <https://doi.org/10.1016/j.mejo.2018.03.006>.
- [3] V. R. Rao, C. K. Sarkar, D. Nirmal, and M. Kumar, Guest Editorial: Special Section on Nano Devices, Circuits and Systems, *IEEE Transactions on Nanotechnology*, Vol. 16, No. 3, pp. 367, 2017, doi: 10.1109/TNANO.2017.2699898.
- [4] P. Khademagha, M.B.C. Aries, A.L.P. Rosemann, E.J. van Loenen, Implementing non-image-forming effects of light in the built environment: A review on what we need, *Building and Environment*, 108 pp. 263-272, 2016, <http://dx.doi.org/10.1016/j.buildenv.2016.08.035>.
- [5] A. de Vries, J.L. Souman, B. de Ruyter, I. Heynderickx, Y.A.W. de Kort, Lighting up the office: The effect of wall luminance on room appraisal, office workers' performance, and subjective alertness, *Building and Environment*, 142 pp. 534–543, 2018, <https://doi.org/10.1016/j.buildenv.2018.06.046>.
- [6] N. Trivellin, M. Meneghini, M. Ferretti, D. Barbisan, M. Dal Lago, G. Meneghesso, E. Zanoni, Effects and exploitation of Tunable White Light for circadian rhythm and human-centric lighting, *Proc. IEEE 1st International Forum on Research and Technologies for Society and Industry Leveraging a better tomorrow (RTSI)*, pp. 154-156, Italy, 2015, doi: 10.1109/RTSI.2015.7325089.
- [7] J. L. Ecker, O. N. Dumitrescu, K. Y. Wong, N. M. Alam, S.K. Chen, T. LeGates, J. M. Renna, G. T. Prusky, D. M. Berson, S. Hattar, Melanopsin-Expressing Retinal Ganglion-Cell Photoreceptors: Cellular Diversity and Role in Pattern Vision, *Neuron*, Cell Press, Elsevier, pp. 49-60, 2010, doi: 10.1016/j.neuron.2010.05.023.
- [8] M. E. Stabio, S. Sabbah, L. E. Quattrochi, M. C. Ilardi, P. M. Fogerson, M. L. Leyrer, M. T. Kim, I. Kim, M. Schiel, J. M. Renna, K. L. Briggman, D. M. Berson, The M5 Cell: A Color-Opponent Intrinsically Photosensitive Retinal Ganglion Cell, *Neuron*, Cell Press, Elsevier, pp. 150-163, 2018, <https://doi.org/10.1016/j.neuron.2017.12.030>.
- [9] A. E. Allen, R. Storchi, F. P. Martial, R. A. Bedford, R. J. Lucas, Melanopsin Contributions to the Representation of Images in the Early Visual System, *Current*

- Biology 27, Cell Press, Elsevier, pp. 1623-1632,2017, <http://dx.doi.org/10.1016/j.cub.2017.04.046>.
- [10] R. J. Lucas, S. Peirson, D. M. Berson, T. M. Brown, H. M. Cooper, C. A. Czeisler, M. G. Figueiro, P. D. Gamlin, S. W. Lockley, J. B. O'Hagan, L. L. A. Price, I. Provencio, D. J. Skene, G. C. Brainard, Measuring and using light in the melanopsin age, *Trends in Neurosciences*, Vol. 37, No. 1, 2014, doi:10.1016/j.tins.2013.10.004.
- [11] G. S. Lall, V. L. Revell, H. Momiji, J. A. Enezi, C. M. Altimus, A. D. Guler, C. Aguilar, M. A. Cameron, S. Allender, M. W. Hankins, R. J. Lucas, Distinct Contributions of Rod, Cone, and Melanopsin Photoreceptors to Encoding Irradiance, *Neuron* 66, Cell Press, Elsevier, pp. 417–428, 2010, doi: 10.1016/j.neuron.2010.04.037.
- [12] J.A. Enezi, V. Revell, T. Brown, J. Wynne, L. Schlangen, R. Lucas, A “Melanopic” Spectral Efficiency Function Predicts the Sensitivity of Melanopsin Photoreceptors to Polychromatic Lights, *Journal of Biological Rhythms*, Vol. 26 No. 4, pp. 314-323, 2011, doi: 10.1177/0748730411409719.
- [13] T. Palumaa, M. J. Gilhooley, A. Jagannath, M. W. Hankins, S. Hughes, S. N. Peirson, Melanopsin: photoreceptors, physiology and potential, *Current Opinion in Physiology* 5, Elsevier, pp. 68–74, 2018, <https://doi.org/10.1016/j.cophys.2018.08.001>.
- [14] A. S. Prayag, R. P. Najjar, C. Gronfier, Melatonin suppression is exquisitely sensitive to light and primarily driven by melanopsin in humans, *Journal of Pineal Research* 66:e12562, Wiley, 2019, doi: 10.1111/jpi.12562.
- [15] A. S. Prayag, M. Münch, D. Aeschbach, S. L. Chellappa, C. Gronfier, Light Modulation of Human Clocks, *Wake and Sleep, Clocks & Sleep* 1, MDPI, pp. 193–208, 2019, doi:10.3390/clockssleep1010017.
- [16] M.O. Mattsson, T. Jung, A. Proykova, Health effects of artificial light, *Opinion of Scientific Committee on Emerging and Newly Identified Health Risks*, European Union, 2012, doi:10.2772/8624.
- [17] L. Bellia, F. Bisegna, G. Spada, Lighting in indoor environments: Visual and non-visual effects of light sources with different spectral power distributions, *Building and Environment*, Vol. 46, Issue 10, pp. 1984-1992, 2011, <https://doi.org/10.1016/j.buildenv.2011.04.007>.
- [18] S. Das, Lighting and health of building occupants: a case of Indian information technology offices, *Current Science*, Vol. 109, No. 9, pp. 1573-1580, 2015, doi: 10.18520/v109/i9/1573-1580.

- [19] G. Renger, The light reactions of photosynthesis, *Current Science*, Vol. 98, No. 10, pp. 1305-1319, 2010.
- [20] A. Ryer, *The Light Measurement Hand Book*, Technical Publications Dept, International Light Inc, Newburyport, pp. 25-30, ISBN 0-9658356-9-3, USA, 1997, <http://www.intl-light.com/handbook>.
- [21] G. Vandewalle, P. Maquet, D-J. Dijk, Light as a modulator of cognitive brain function, *Trends in Cognitive Sciences*, Vol. 13, Issue 10, pp. 429–438, 2009, <https://doi.org/10.1016/j.tics.2009.07.004>.
- [22] IES RP-5-13: Recommended Practice for Daylighting Buildings, Illuminating Engineering Society, ISBN 978-0-87995-281-5, USA, 2013.
- [23] M. Boubekri, *Daylighting, Architecture and Health, Building Design Strategies*, Architectural Press, Elsevier, ISBN: 978-0-7506-6724-1, USA, 2008.
- [24] F. Sharp, D. Lindsey, J. Dols, J. Coker, The use and environmental impact of daylighting, *Journal of Cleaner Production*, Elsevier, Vol. 85, pp. 462-471, 2014, ISSN 0959-6526, <https://doi.org/10.1016/j.jclepro.2014.03.092>.
- [25] T.W. Davies, J. Bennie, R. Inger, K. J. Gaston, Artificial light alters natural regimes of night-time sky brightness, *Scientific Reports* 3, Article No: 1722, 2013, <https://doi.org/10.1038/srep01722>.
- [26] C.B. Luginbuhl, P.A. Boley, D. R. Davis, The impact of light source spectral power distribution on sky glow, *Journal of Quantitative Spectroscopy and Radiative Transfer*, Vol. 139, pp. 21-26, 2014, <https://doi.org/10.1016/j.jqsrt.2013.12.004>.
- [27] K.J. Gaston, J.P. Duffy, S. Gaston, J. Bennie, T. W. Davis, Human alteration of natural light cycles: causes and ecological consequences, *Oecologia* 176, 917–931, 2014, <https://doi.org/10.1007/s00442-014-3088-2>.
- [28] P. Cinzano, F. Falchi, C. D. Elvidge, The first World Atlas of the artificial night sky brightness, *Monthly Notices of the Royal Astronomical Society*, Vol. 328, Issue 3, pp. 689–707, 2001, <https://doi.org/10.1046/j.13658711.2001.04882.x>.
- [29] F. Hölker, T. Moss, B. Griefahn, W. Kloas, C. C. Voigt, D. Henckel, A. Hänel, P. M. Kappeler, S. Völker, A. Schwoppe, S. Franke, D. Uhrlandt, J. Fischer, R. Klenke, C. Wolter, K. Tockner, The Dark Side of Light: A Transdisciplinary Research Agenda for Light Pollution Policy, *Ecology and Society* 15(4): 13, 2010, <http://www.ecologyandsociety.org/vol15/iss4/art13>.
- [30] R. Haitz, J.Y. Tsao, Solid-state Lighting Why it will succeed, and why it won't be overtaken, *Optik & Photonik*, No. 2, pp. 26–30, 2011, doi:10.1002/opph.201190325.

- [31] C. Cronström, A Demonstration Unit for Human Centric Lighting, Master Thesis, Division of Product Development, Department of Design Sciences, Lund University, 2018.
- [32] G. Benediktsson, Lighting control– possibilities in cost and energy-efficient lighting control techniques, Master Thesis, Division of Industrial Electrical Engineering and Automation, Faculty of Engineering, Lund University, 2009.
- [33] D.M. Berson, F. A. Dunn, M. Takao, Photo transduction by retinal ganglion cells that set the Circadian clock, *Science*, 295(5557):1070-3, 2002, doi: 10.1126/science.1067262.
- [34] K. Y. Wong, F. A. Dunn, D. M. Berson, Photoreceptor Adaptation in Intrinsically Photosensitive Retinal Ganglion Cells, *Neuron*, Vol.48, pp. 1001–1010, Cell Press, Elsevier, 2005, doi: 10.1016/j.neuron.2005.11.016.
- [35] T. M. Brown, C. Gias, M. Hatori, S. R. Keding, M. Semo, P. J. Coffey, J. Gigg, H. D. Piggins, S. Panda, R. J. Lucas, Melanopsin Contributions to Irradiance Coding in the Thalamo-Cortical Visual System, *PLoS Biology* 8(12): e1000558, <https://doi.org/10.1371/journal.pbio.1000558>.
- [36] D.J. Clements-Croome, Y. Kaluarachchi, Assessment of the influence of indoor environment on job stress and productivity of occupants in offices, *Design, Construction and Operation of Healthy Buildings*, American Society of Heating, Refrigerating and Air-Conditioning Engineers (ASHRAE), pp. 67-81, 1998.
- [37] C. A. Czeisler, J. F. Duffy, T. L. Shanahan, E. N. Brown, J. F. Mitchell, D. W. Rimmer, J. M. Ronda, E. J. Silva, J. S. Allan, J. S. Emens, D-J. Dijk, R. E. Kronauer, Stability, Precision, and Near-24-Hour Period of the Human Circadian Pacemaker, *Science*, Vol. 284, pp. 2177-2181, 1999, doi: 10.1126/science.284.5423.2177.
- [38] G. Costa, Shift Work and Health: Current Problems and Preventive Actions, *Safety Health Work*, 1:112-123, eISSN : 2093-7997, 2010, doi: 10.5491/SHAW.2010.1.2.112.
- [39] K.J. Gaston, M.E. Visser, F. Hölker, The biological impacts of artificial light at night: the research challenge, *Philosophical Transactions B*, The Royal Society, 370: 20140133, 2015, <https://doi.org/10.1098/rstb.2014.0133>.
- [40] T.I. Karu, L.V. Pyatibrat, N.I. Afanasyeva, A novel mitochondrial signalling pathway activated by visible-to-near infrared radiation, *Photochemistry and photobiology*, 80(2):366-72, 2004, doi: 10.1562/2004-03-25-RA-123.
- [41] M. Norval, R.M. Lucas, A.P. Cullen, F. R. de Gruijl, J. Longstreth, Y. Takizawa, J. C. van der Leung, The human health effects of ozone depletion and interactions with

- climate change, *Photochemical & Photobiological Sciences*, 10(2):199-225, 2011, doi: 10.1039/c0pp90044c.
- [42] R. Küller, L. Wetterberg, Melatonin, cortisol, EEG, ECG and subjective comfort in healthy humans: Impact of two fluorescent lamp types at two light intensities, *Lighting Research and Technology*, Vol. 25 Issue 2, pp. 71-81, 1993, <https://doi.org/10.1177/096032719302500203>.
- [43] M. Rüter, M.C.M. Gordijn, D.G.M. Beersma, B. de Vries, S. Daan, Time-of-day-dependent effects of bright light exposure on human psychophysiology: comparison of daytime and nighttime exposure, *American Journal of Physiology-Regulatory, Integrative and Comparative Physiology*, 290(5):R1413-20, 2006, doi: 10.1152/ajpregu.00121.2005.
- [44] J. Grunberger, L. Linzmayer, M. Dietzel, B. Saletu, The effect of biologically-active light on the noo- and thymopsyche and on psychophysiological variables in healthy volunteers, *International Journal of Psychophysiology*, 15(1):27-37, 1993, doi: 10.1016/0167-8760(93)90092-4.
- [45] M. Tops, A.D. Tenner, G.J. van den Beld, S. H. A. Begemann, The effect of the length of continuous presence on the preferred illuminance in offices, *Proc. of CIBSE Lighting Conference*, 1998.
- [46] T. Partonen, J. Lonnqvist, Bright light improves vitality and alleviates distress in healthy people, *Journal of Affective Disorders* 57, pp. 55–61, 2000.
- [47] C. Hayes, Research assesses the value of human-centric lighting, *LEDs Magazine*, 2015, downloaded from: <https://www.ledsmagazine.com/smart-lighting-iot/indoor-networks-controls/article/16695929/research-assesses-the-value-of-humancentric-lightingmagazine>.
- [48] T. Katsuura, S. Lee, A review of the studies on nonvisual lighting effects in the field of physiological anthropology 38:2, *Journal of Physiological Anthropology*, 2019, <https://doi.org/10.1186/s40101-018-0190-x>.
- [49] M. Knoop, K. Broszio, A. Diakite, C. Liedtke, M. Niedling, I. Rothert, F. Rudawski & N. Weber, Methods to Describe and Measure Lighting Conditions in Experiments on Non-Image-Forming Aspects, *LEUKOS*, Vol. 15, Nos. 2–3, 163–179, 2019, doi:10.1080/15502724.2018.1518716.
- [50] The Human Centric Lighting Market 2019 to 2024: Global Market Prospects, Impacts & Opportunities, 2019, downloaded from: <https://www.researchandmarkets.com/reports/4790869>.

- [51] Z. Freyberg, R. W. Logan, The Intertwined Roles of Circadian Rhythms and Neuronal Metabolism Fueling Drug Reward and Addiction, *Current Opinion in Physiology* 5:80-89, Elsevier, 2018, doi:10.1016/j.cophys.2018.08.004.
- [52] C. C. Nobis, N. Labrecque, N. Cermakian, From immune homeostasis to inflammation, a question of rhythms, *Current Opinion in Physiology*, Elsevier, Vol. 5, pp. 90-98, 2018, <https://doi.org/10.1016/j.cophys.2018.09.001>.
- [53] A. M. Dugar, What is all this “Human-centric lighting” mumbo-jumbo about, ISLE Newsletter, 2016.
- [54] Smart cities mission, Govt. Of India website, downloaded from <http://smartcities.gov.in/content/innerpage/fund-release.php>.
- [55] Eletimes, LED Lighting Special: Come forth into the light of things, 2018, downloaded from <https://www.eletimes.com/led-lighting-special-come-forth-light-things>.
- [56] Gartner Newsroom, Gartner Says Smart Lighting Has the Potential to Reduce Energy Costs by 90 Percent, 2015, downloaded from: <https://www.gartner.com/en/newsroom/press-releases/2015-07-15-gartner-says-smart-lighting-has-the-potential-to-reduce-energy-costs-by-90-percent>.
- [57] Eletimes, Smart Lighting: Giving new rays to the Smarter Environment, 2018, downloaded from: <https://www.eletimes.com/smart-lighting-giving-new-rays-to-the-smarter-environment>.
- [58] Eletimes, Lighting up India: India’s LED Revolution, 2019, downloaded from: <https://www.eletimes.com/lighting-up-india-indias-led-revolution>.
- [59] S. Chakraborty, Human Centric Lighting to IOT-a paradigm shift in the field of Illumination Engineering, ISLE Newsletter, 2018.
- [60] Inc42 BrandLabs, Smart Cities Should Be Human Centric Says Anne Stenros, Helsinki City’s Chief Design Officer, 2018, downloaded from: <https://inc42.com/features/anne-stenros-smart-city-human-centric/>.
- [61] E. Kiraci, A. Palit, M. Donnelly, A. Attridge, M. A. Williams, Comparison of in-line and off-line measurement systems using a calibrated industry representative artefact for automotive dimensional inspection, *Measurement*, 163 (2020) 108027, 2020, <https://doi.org/10.1016/j.measurement.2020.108027>.
- [62] A. Yilmaz, Artificial neural network modelling of colour temperature variations with different types of armatures and light sources, *Light & Engineering Journal*, Vol. 24 Issue 4, pp. 64-71, 2016.

- [63] K. Samu, B. Thamo, Internet based light quality measurement, *Recent Innovations in Mechatronics (RIIM)*, Vol. 4 No. 1, 2017, doi: 10.17667/riim.2017.1/4.
- [64] Y. Wang, H. Huang, G. Chen, Effects of lighting on ECG, visual performance and psychology of the elderly, *Optik - International Journal for Light and Electron Optics* 203 (2020) 164063, pp. 1-9, 2020, <https://doi.org/10.1016/j.ijleo.2019.164063>.
- [65] J. Lin, X. Ding, C. Hong, Y. Pang, L. Chen, Q. Liu, X. Zhang, H. Xin, X. Wang, Several biological benefits of the low color temperature light-emitting diodes based normal indoor lighting source, *Nature Scientific Reports* (2019) 9:7560, 2019, <https://doi.org/10.1038/s41598-019-43864-6>.
- [66] C. Li, G. Cui, M. Melgosa, X. Ruan, Y. Zhang, L. Ma, K. Xiao, M. R. Luo, Accurate method for computing correlated color temperature, *Optics Express*, pp. 14066-14078, Vol. 24, No. 13, 2016, doi: 10.1364/OE.24.014066.
- [67] Y. Zhu, M. Yang, Y. Yao, X. Xiong, X. Li, G. Zhou, N. Ma, Effects of Illuminance and Correlated Color Temperature on Daytime Cognitive Performance, Subjective Mood, and Alertness in Healthy Adults, *Environment and Behavior*, pp. 1-32, 2017, doi:10.1177/0013916517738077.
- [68] M. Ye, S. Q. Zheng, M. L. Wang, M. R. Luo, The effect of dynamic correlated colour temperature changes on alertness and performance, *Lighting Research & Technology*, 0: 1–12, 2018, doi:10.1177/1477153518755617.
- [69] Lux Sensor SKL 310 datasheet downloaded from http://www.skyeinstruments.info/index_htm_files/LUX%20SENSOR%20v3.pdf.
- [70] F. Marinho, C. M. Carvalho, F. R. Apolinario, L. Paulucci, Measuring light with light dependent resistors: an easy approach for optics experiments, *European Journal of Physics*, Vol. 40, No. 3, 2019.
- [71] Ambient Light Sensors - Circuit and Window Design, Vishay Semiconductors, datasheet downloaded from <https://www.vishay.com/docs/84154/appnotesensors.pdf>.
- [72] Linear Light Sensor LLS05-A datasheet downloaded from https://www.futurlec.com/Datasheet/Sensor/Light_Sensor.pdf
- [73] Light Sensor LS-BTA datasheet downloaded from <https://www.vernier.com/files/manuals/ls-bta/ls-bta.pdf>.
- [74] Light Sensor and High Sensitivity Light Sensor, CI-6504A datasheet downloaded from https://d2n0lz049icia2.cloudfront.net/product_document/Light-Sensor-Manual-CI-6504A-6604.pdf.

- [75] Photometric Sensor SE-202 datasheet downloaded from <https://www.apogeeinstruments.com/content/SE-202-205.pdf>.
- [76] Luminosity Sensor TSL2561 datasheet downloaded from <https://cdn-shop.adafruit.com/datasheets/TSL2561.pdf>.
- [77] Digital Ambient Light Sensor MAX 44004 datasheet downloaded from <https://datasheets.maximintegrated.com/en/ds/MAX44004.pdf>.
- [78] Ambient Light Sensor OPT3001 datasheet downloaded from http://www.ti.com/lit/ds/symlink/opt3001.pdf?ts=1591726815191&ref_url=https://www.google.com/.
- [79] F. Bellocchio, S. Ferrari, M. Lazzaroni, L. Cristaldi, M. Rossi, T. Poli, R. Paolini, Illuminance Prediction through SVM Regression, Proc. IEEE Workshop on Environmental Energy and Structural Monitoring Systems, Italy, 2011, <https://doi.org/10.1109/EESMS.2011.6067051>.
- [80] S. Ferrari, A. Fina, M. Lazzaroni, V. Piuri, L. Cristaldi, M. Faifer, T. Poli, Illuminance Prediction through Statistical Models, Proc. IEEE Workshop on Environmental Energy and Structural Monitoring Systems, Italy, 2012, <https://doi.org/10.1109/EESMS.2012.6348406>.
- [81] S. Ferrari, M. Lazzaroni, V. Piuri, A. Salman, L. Cristaldi, M. Rossi, T. Poli, Illuminance Prediction through Extreme Learning Machines, Proc. IEEE Workshop on Environmental Energy and Structural Monitoring Systems, Italy, 2012, <https://doi.org/10.1109/EESMS.2012.6348407>.
- [82] D. Caicedo, A. Pandharipande, F. M. J. Willems, Illumination gain estimation and tracking in a distributed lighting control system, Proc. 2014 IEEE Conference on Control Applications (CCA), pp. 1650-1655, France, 2014.
- [83] A. M. Lopes, P. Abreu, M. T. Restivo, Analysis and Pattern Identification on Smart Sensors Data, Proc. 2017 4th Experiment at International Conference (exp.at'17), pp. 97-98, Italy, 2012, <https://doi.org/10.1109/EXPAT.2017.7984409>.
- [84] A. Pandharipande, D. Caicedo, X. Wang, Sensor-Driven Wireless Lighting Control: System Solutions and Services for Intelligent Buildings, IEEE Sensors Journal, Vol. 14, No. 12, pp. 4207-4215, 2014.
- [85] D. Caicedo, A. Pandharipande, Distributed Illumination Control With Local Sensing and Actuation in Networked Lighting Systems, IEEE Sensors Journal, Vol. 13, No. 3, pp. 1092-1104, 2013.

- [86] C. Basu, J. J. Caubel, K. Kim, E. Cheng, A. Dhinakaran, A. M. Agogino, R. A. Martin, Sensor-Based Predictive Modeling for Smart Lighting in Grid-Integrated Buildings, *IEEE Sensors Journal*, Vol. 14, No. 12, pp. 4216-4229, 2014.
- [87] S. Borile, A. Pandharipande, D. Caicedo, L. Schenato, A. Cenedese, A Data-Driven Daylight Estimation Approach to Lighting Control, *IEEE Access*, Vol. 5, pp. 21461-21471, 2017, doi: 10.1109/ACCESS.2017.2679807.
- [88] D. Caicedo and A. Pandharipande, Daylight and occupancy adaptive lighting control system: An iterative optimization approach, *Lighting Research & Technology*, 0:1–15, 2015, doi: 10.1177/1477153515587148.
- [89] S. Jain, V. Garg, A review of open loop control strategies for shades, blinds and integrated lighting by use of real-time daylight prediction methods, *Building and Environment*, Vol. 135 (2018), pp. 352-364, 2018, <https://doi.org/10.1016/j.buildenv.2018.03.018>.
- [90] A.T. Ergüzel, A study on the implementation of dimmable street lighting according to vehicle traffic density, *Optik - International Journal for Light and Electron Optics* 184 (2019) pp. 142–152, 2019, <https://doi.org/10.1016/j.ijleo.2018.12.183>.
- [91] I. Pigliautile, S. Casaccia, N. Morresi, M. Arnesano, A. L. Pisello, G. M. Revel, Assessing occupants' personal attributes in relation to human perception of environmental comfort: Measurement procedure and data analysis, *Building and Environment*, Vol. 177, 2020, <https://doi.org/10.1016/j.buildenv.2020.106901>.
- [92] H. Wu, Y. Wu, X. Sun, J. Liu, Combined effects of acoustic, thermal, and illumination on human perception and performance: A review, *Building and Environment*, Vol. 169, 2020, <https://doi.org/10.1016/j.buildenv.2019.106593>.
- [93] A. Mukherjee, P. Goswami, Z. Yan, L. Yang, S. Routray, G. Palai, Distributed gradient descent based cluster head identification in MIMO sensor networks, *Optik - International Journal for Light and Electron Optics* 204 (2020), 164185, 2020, <https://doi.org/10.1016/j.ijleo.2020.164185>.
- [94] H-Y. Chen, A. J-W. Whang, Y-Y. Chen, C-H. Chou, The hybrid lighting system with natural light and LED for tunnel lighting, *Optik- International Journal for Light and Electron Optics*, Vol. 203, 163958, 2020, <https://doi.org/10.1016/j.ijleo.2019.163958>.
- [95] S. S. Patra, R. Ramsisaria, R. Du, T. Wu, B. E. Boor, A machine learning field calibration method for improving the performance of low-cost particle sensors, *Building and Environment*, Vol. 190, 107457, 2021, <https://doi.org/10.1016/j.buildenv.2020.107457>.

- [96] Y. Cho, J. Seo, H. Lee, S. Choi, A. Choi, M. Sung, Y. Hur, Platform design for lifelog-based smart lighting control, *Building and Environment*, Vol. 185, 107267, 2020, <https://doi.org/10.1016/j.buildenv.2020.107267>.
- [97] Y. Gao, H. Li, H. Zhang, G. Cao, J. Zhang, N. Zou, Daylight perceptive lighting and data fusion with artificial neural network, *Optik* 125, Issue 10, pp. 2405–2408, 2014, <http://dx.doi.org/10.1016/j.ijleo.2013.10.084>.
- [98] X. Zhang, S. Yue, R. Gong, Q. Li, Illumination estimation based on a weighted color distribution, *Optik-International Journal for Light and Electron Optics* 185 (2019), pp. 965–971, 2019, <https://doi.org/10.1016/j.ijleo.2019.04.001>.
- [99] C. Xiang, Z. Li-Jun, L. Yan, S. Xing-Lin, L. Hang-Quan, X. Shun, H. Yang, R. Xue-Chang, Development of multi-function digital optoelectronic integrated sensor, *Optik*, Vol. 180, pp. 406–413, 2019, <https://doi.org/10.1016/j.ijleo.2018.11.108>.
- [100] J-S. B. Valencia, F-E. L. Giraldo, J-F. V. Bonilla, Calibration method for Correlated Color Temperature (CCT) measurement using RGB color sensors, *Proc. IEEE Symposium of Signals, Images and Artificial Vision–2013: STSIVA–2013*, Columbia, 2013, doi:10.1109/STSIVA.2013.6644921.
- [101] T. Leikanger, C. Schuss, J. Hakkinen, Calibration of Smartphone Light Sensors with a Near Field Communication Enabled Reference, *Proc. IEEE Sensors, USA*, 2016, doi: 10.1109/ICSENS.2016.7808930.
- [102] L. Breniuc, C-G. Haba, C.-D. Gălățanu, D. Petrișor, R. Herțanu, Correlated Color Temperature Measuring and Adjustment System, *Proc. 11th International Symposium on Advanced Topics In Electrical Engineering*, Romania, 2019, doi:10.1109/ATEE.2019.8724926.
- [103] P. Pierleoni, A. Belli, L. Palma, S. Valenti, S. Raggiunto, L. Incipini, P. Ceregioli, The Scrovegni Chapel Moves Into the Future: An Innovative Internet of Things Solution Brings New Light to Giotto’s Masterpiece, *IEEE Sensors Journal*, Vol. 18 No. 18, pp. 7681–7696, 2018, doi: 10.1109/JSEN.2018.2858543.
- [104] R. Silhavy, P. Silhavy, Z. Prokopova, Analysis and selection of a regression model for the Use Case Points method using a stepwise approach, *The Journal of Systems and Software* 125, pp. 1–14, 2017, <http://dx.doi.org/10.1016/j.jss.2016.11.029>.
- [105] S. Lee, C. Lim, J-H Chang, A new a priori SNR estimator based on multiple linear regression technique for speech enhancement, *Digital Signal Processing*, Vol. 30, pp. 154–164, 2014, <https://doi.org/10.1016/j.dsp.2014.04.001>.

- [106] V. Katkovnik, Multiresolution local polynomial regression: A new approach to pointwise spatial adaptation, *Digital Signal Processing*, Vol. 15, Issue 1, pp. 73-116, 2005, <https://doi.org/10.1016/j.dsp.2004.06.004>.
- [107] G.K. Uyanik, N. Guler, A study on multiple linear regression analysis, *Procedia - Social and Behavioral Sciences* 106, pp. 234–240, 2013, <https://doi.org/10.1016/j.sbspro.2013.12.027>.
- [108] L. Ai, J. Wang, R. Yao, Classification of parkinsonian and essential tremor using empirical mode decomposition and support vector machine, *Digital Signal Processing*, Vol. 21, Issue 4, pp. 543-550, 2011, <https://doi.org/10.1016/j.dsp.2011.01.010>.
- [109] L-H. Ren, Z-F. Ye, Y-P. Zhao, A modeling method for aero-engine by combining stochastic gradient descent with support vector regression, *Aerospace Science and Technology* Vol. 99,105775, pp. 1-11, 2020.
- [110] S. Kavita, S. Varuna, R. Ramya, A Comparative Analysis on Linear Regression and Support Vector Regression, *Proc. 2016 Online International Conference on Green Engineering and Technologies (IC-GET)*, India, 2016, doi:10.1109/GET.2016.7916627.
- [111] S. Peng, Q. Hu, J. Dang, W. Wang, Optimal feasible step-size based working set selection for large scale SVMs training, *Neurocomputing* 407, pp. 366–375, 2020, <https://doi.org/10.1016/j.neucom.2020.05.054>.
- [112] Y. Feng, X. Wu, Y. Hu, Forecasting Research on the Wireless Mesh Network Throughput Based on the Support Vector Machine, *Wireless Personal Communications* 99, 581–593, 2018, <https://doi.org/10.1007/s11277-017-5135-x>.
- [113] M. Petric, A. Neskovic, N. Neskovic, M. Borenovic, Indoor Localization Using Multi-operator Public Land Mobile Networks and Support Vector Machine Learning Algorithms, *Wireless Personal Communications* 104, 1573–1597, 2019, <https://doi.org/10.1007/s11277-018-6099-1>.
- [114] A. Charrada, A. Samet, Fast-Fading Channel Environment Estimation Using Linear Minimum Mean Squares Error-Support Vector Regression, *Wireless Personal Communications* 106, 1897–1913, 2019, <https://doi.org/10.1007/s11277-018-5728-z>.
- [115] A. Djouama, M-S. Lim, F.Y. Ettoumi, Channel Estimation in Long Term Evolution Uplink Using Minimum Mean Square Error-Support Vector Regression, *Wireless Personal Communications* 79, 2291–2304, 2014, <https://doi.org/10.1007/s11277-014-1985-7>.

- [116] O. Kisi, Generalized regression neural networks for evapotranspiration modelling, *Hydrological Sciences Journal* 51:6, pp. 1092-1105, 2006, <https://doi.org/10.1623/hysj.51.6.1092>.
- [117] S. Heddam, Generalized regression neural network (GRNN)-based approach for colored dissolved organic matter (CDOM) retrieval: case study of Connecticut River at Middle Haddam Station, USA, *Environmental Monitoring and Assessment* 186, pp. 7837–7848, 2014, doi: 10.1007/s10661-014-3971-7.
- [118] Ö. Polat, T. Yıldırım, FPGA implementation of a General Regression Neural Network: An embedded pattern classification system, *Digital Signal Processing*, Vol. 20, Issue 3, pp. 881-886, 2010, <https://doi.org/10.1016/j.dsp.2009.10.013>.
- [119] H. Jin, X. Chen, L. Wang, K. Yang, L. Wu, Adaptive Soft Sensor Development Based on Online Ensemble Gaussian Process Regression for Nonlinear Time-Varying Batch Processes, *Industrial & Engineering Chemistry Research* 54, pp. 7320–7345, 2015, doi: 10.1021/acs.iecr.5b01495.
- [120] A. Băltoiu, B. Dumitrescu, Sparse Bayesian learning algorithm for separable dictionaries, *Digital Signal Processing*, Vol. 111, 2021, <https://doi.org/10.1016/j.dsp.2021.102990>.
- [121] V. M. Barthelmes, Y. Heo, V. Fabi, S. P. Corgnati, Exploration of the Bayesian Network framework for modelling window control behaviour, *Building and Environment*, Vol. 126, pp. 318-330, 2017, <https://doi.org/10.1016/j.buildenv.2017.10.011>.
- [122] G. Camps-Valls, J. Verrelst, J. Munoz-Mari, V. Laparra, F. Mateo-Jiménez, J. Gómez-Dans, A Survey on Gaussian Processes for Earth-Observation Data Analysis: A Comprehensive Investigation, *IEEE Geoscience and Remote Sensing Magazine* Vol. 4 Issue 2, pp. 58-78, 2016, doi: 10.1109/MGRS.2015.2510084.
- [123] R. Desai, P. Porob, P. Rebelo, D. R. Edla, A. Bablani, EEG Data Classification for Mental State Analysis Using Wavelet Packet Transform and Gaussian Process Classifier. *Wireless Personal Communications* 115, 2149–2169, 2020, <https://doi.org/10.1007/s11277-020-07675-7>.
- [124] Z. Sun, T. Chen, Y. Tong, M. Zhang, Blind Equalization of Constant Modulus Signals Based on Gaussian Process for Classification, *Wireless Personal Communications* 97, 6005–6018, 2017, <https://doi.org/10.1007/s11277-017-4824-9>.
- [125] R. Durichen, M. A. F. Pimentel, L. Clifton, A. Schweikard, D. A. Clifton, Multitask Gaussian Processes for Multivariate Physiological Time-Series Analysis, *IEEE*

- Transactions on Biomedical Engineering Vol. 62, No. 1, pp. 314-322, 2015, doi: 10.1109/TBME.2014.2351376.
- [126] K. Yang, H. Jin, X. Chen, J. Dai, L. Wang, D. Zhang, Soft sensor development for online quality prediction of industrial batch rubber mixing process using ensemble just-in-time Gaussian process regression models, *Chemometrics and Intelligent Laboratory Systems* 155, pp. 170–182, 2016, <http://dx.doi.org/10.1016/j.chemolab.2016.04.009>.
- [127] B. Yang, H-Y. Chou, T-H. Yang, Color reproduction method by support vector regression for color computer vision, *Optik* 124, pp. 5649–5656, 2013, <http://dx.doi.org/10.1016/j.ijleo.2013.04.036>.
- [128] D. G. Chachlakis, T. Zhou, F. Ahmad, P. P. Markopoulos, Minimum Mean-Squared-Error autocorrelation processing in coprime arrays, *Digital Signal Processing*, Vol. 114, 103034, 2021, <https://doi.org/10.1016/j.dsp.2021.103034>.
- [129] W. Yuchen, W. Xiaohong, L. Jie, Color Appearance Phenomena under High Ambient Illumination, *Optik* Vol. 145, pp. 22-29, 2017, <http://dx.doi.org/10.1016/j.ijleo.2017.06.111>.
- [130] K. Roy, R. N. Das, P. Ambure, R.B. Aher, Be aware of error measures. Further studies on validation of predictive QSAR models, *Chemometrics and Intelligent Laboratory Systems* 152, pp. 18–33, 2016, <http://dx.doi.org/10.1016/j.chemolab.2016.01.008>.
- [131] H. Jin, L. Eklundh, In situ calibration of light sensors for long-term monitoring of vegetation, *IEEE Transactions on Geoscience and Remote Sensing*, Vol. 53, Issue: 6, pp. 3405-3416, 2015, <https://doi.org/10.1109/TGRS.2014.2375381>.
- [132] L. Balzano, R. Nowak, Blind Calibration of Sensor Networks, *Proc. 6th International Symposium on Information Processing in Sensor Networks*, USA, 2007, <https://doi.org/10.1109/IPSN.2007.4379667>.
- [133] Y. Xiang, L. S. Bai, R. Pledrahita, R. P. Dick, Q. Lv, M. Hannigan, L. Shang, Collaborative Calibration and Sensor Placement for Mobile Sensor Networks, *Proc. ACM/IEEE 11th International Conference on Information Processing in Sensor Networks (IPSN)*, China, 2012, <https://doi.org/10.1109/IPSN.2012.6920952>.
- [134] R. T. Rajan, R. V. Schaijk, A. Das, J. Romme, F. Pasveer, Reference-free Calibration in Sensor Networks, *IEEE Sensors Letters*, Vol. 2, Issue: 3, 2018, <https://doi.org/10.1109/LSENS.2018.2866627>.

- [135] ATmega 168 datasheet downloaded from http://ww1.microchip.com/downloads/en/DeviceDoc/Atmel-2545-8-bit-AVR-Microcontroller-ATmega48-88-168_Summary.pdf.
- [136] S. Kumar, P. K. Tiwari, S.B. Chaudhury, An optical triangulation method for non-contact profile measurement, Proc. IEEE International Conference on Industrial Technology, pp. 2878-2883, India, 2006.
- [137] M. Kouider, M. Nadi, D. Kourtiche, Sensors Auto-calibration Method Using Programmable Interface Circuit Front-end, Sensors 3(10), pp. 491-497, 2003, <https://doi.org/10.3390/s31000491>.
- [138] H-Y. Chen, C. Chen, Determination of Optimal Measurement Points for Calibration Equations-Examples by RH Sensors, Sensors 19, 1213,2019, doi: 10.3390/s19051213.
- [139] J-M. Gutierrez-Martinez, A. Castillo-Martinez, J-A. Medina-Merodio, J. Aguado-Delgado, J-J. Martinez-Herraiz, Smartphones as a Light Measurement Tool: Case of Study, Applied Sciences, 7, 616, 2017, doi:10.3390/app7060616.
- [140] P. Valíček, T. Novák, V. Kolář, R. Hrbáč, K. Sokanský, Suggestion of Long-term Measuring of Daylight Contributions in Interiors, Proc. 16th International Scientific Conference on Electric Power Engineering (EPE), Czech Republic, 2015, <https://doi.org/10.1109/EPE.2015.7161154>.
- [141] Ambient Light Sensor BH 1750 FVI, datasheet downloaded from <http://www.mouser.com/ds/2/348/bh1750fvi-e-186247.pdf>.
- [142] Digital Lux Meter, Model No: 1332, datasheet downloaded from <http://www.metravi.com/PDF/1332&1332A.pdf>.
- [143] J-S. Botero, J. Valencia Aguirre, J-F. Vargas Bonilla, Estimation of Light Source Color Rendition with Low-Cost Sensors Using Multilayer Perceptron and Extreme Learning Machine, LEUKOS, 17:3, 280-290, 2021, doi: 10.1080/15502724.2020.1755306.
- [144] Chroma Meter, CL-200A, datasheet downloaded from https://www.konicaminolta.com/instruments/download/catalog/light/pdf/cl200a_catalog_eng.pdf.
- [145] C. Kofod, Indoor Lighting in the Public and Private Service Sectors Guidelines, 2017.
- [146] M. Deru, N. Blair, P. Torcellini, Procedure to Measure Indoor Lighting Energy Performance, Technical Report, National Renewable Energy Laboratory, 2005.
- [147] H-B. Huang, Y-S. Huang, P-C. Huang, H-H. Lin, H-C. Lee, Poster abstract: Managing Road Lighting with a Hitchhiking Sensor System, Proc. 12th ACM/IEEE International

- Conference on Information Processing in Sensor Networks (IPSN'13), pp. 325-326, USA, 2013.
- [148] C. Jing, D. Shu, D. Gu, Design of Streetlight Monitoring and Control System Based on Wireless Sensor Networks, Proc. 2nd IEEE Conference on Industrial Electronics and Applications, 2007.
- [149] P. Satvaya, I. Mondal, S. Mazumdar, Development of an Intelligent Security Lighting System using Wireless Communication Technology, International Journal of Engineering Technology Science and Research (IJETS), Vol. 5, Issue 1, pp. 1695-1701, 2018.
- [150] H-C. Lee, H-B. Huang, A Low-Cost and Noninvasive System for the Measurement and Detection of Faulty Streetlights, IEEE Transactions on Instrumentation and Measurement, Vol. 64, No. 4, pp. 1019-1031, 2015.
- [151] Z. Weng, J. Fang, M. Kong, Y. Cheng, Research on Intelligent Lighting System of LED Based on Wireless Sensor Network Technology, Proc. International Conference on Chemical, Material and Food Engineering (CMFE-2015), 2015.
- [152] N. K. Suryadevara, S. C. Mukhopadhyay, S. Dieter, T. Kelly, S. P. S. Gill, WSN-Based Smart Sensors and Actuator for Power Management in Intelligent Buildings, IEEE/ASME Transactions On Mechatronics, Vol. 20, No. 2, pp. 564-571, 2015.
- [153] N. K. Suryadevara, S. C. Mukhopadhyay, Wireless Sensor Network Based Home Monitoring System for Wellness Determination of Elderly, IEEE Sensors Journal, Vol. 12, No. 6, pp. 1965-1972, 2012.
- [154] I. Vaccari, E. Cambiaso, M. Aiello, Evaluating Security of Low-Power Internet of Things Networks, International Journal of Computing and Digital Systems, Vol. 8, No. 2, 2019, <http://dx.doi.org/10.12785/ijcds/080202>.
- [155] M. Marjani, F. Nasaruddin, A. Gani, A. Karim, I. A. T. Hashem, A. Siddiqa, I. Yaqoob, Big IoT Data Analytics: Architecture, Opportunities, and Open Research Challenges, IEEE Access, Vol. 5, pp. 5247-5261, 2017, doi: 10.1109/ACCESS.2017.2689040.
- [156] Z. Abbas, W. Yoon, A Survey on Energy Conserving Mechanisms for the Internet of Things: Wireless Networking Aspects, Sensors, 15, 24818-24847, 2015, doi:10.3390/s151024818.
- [157] K. Bicakci, D. D. Yavuz, S. Gurkan, TwinCloud: Secure Cloud Sharing Without Explicit Key Management, Proc. IEEE Conference on Communications and Network Security (CNS), 2016, DOI: 10.1109/CNS.2016.7860552.

- [158] Y. Omura, H. Masuda, Y. Mimura, Feasibility investigation of obstacle-avoiding sensors unit without image processing, *Journal of Sensors*, Vol. 2013, Article ID: 643815, pp. 1-11, 2013, <http://dx.doi.org/10.1155/2013/643815>.
- [159] Y. Zhu, B. Yi, T. Guo, A simple outdoor environment obstacle detection method based on information fusion of depth and infrared, *Journal of Robotics*, Vol. 2016, Article ID: 2379685, pp. 1-10, 2016, <http://dx.doi.org/10.1155/2016/2379685>.
- [160] G. Csaba, L. Somlyai, Z. Vamosy, Differences between Kinect and structured lighting sensor in robot navigation, *Proc. 10th IEEE International Symposium on Applied Machine Intelligence and Informatics*, pp. 85-90, Slovakia, 2012.
- [161] H-H. Pham, T-L. Le, N. Vuillerme, Real-time obstacle detection system in indoor environment for the visually impaired using Microsoft Kinect sensor, *Journal of Sensors*, Vol. 2016, Article ID: 3754918, pp. 1-13, 2016, <http://dx.doi.org/10.1155/2016/3754918>.
- [162] M. A. Ansari, D. Kurchaniya, M. Dixit, A comprehensive analysis of image edge detection techniques, *International Journal of Multimedia and Ubiquitous Engineering*, Vol. 12, No. 11, pp. 1-12, 2017, <http://dx.doi.org/10.14257/ijmue.2017.12.11.01>.
- [163] B. Crnokić, S. Rezić, S. Peihar, Comparison of edge detection methods for obstacles detection in a mobile robot environment, *Proc. 27th Daaam International Symposium on Intelligent Manufacturing and Automation*, pp. 235-244, Austria, 2016, doi: 10.2507/27th.daaam.proceedings.035.
- [164] W. Chen, S. Chen, H. Guo, X. Ni, Welding flame detection based on color recognition and progressive probabilistic Hough transform, *Concurrency and Computation Practice and Experience*, Vol. 32, Issue 19, pp. 1-9, 2020, <https://doi.org/10.1002/cpe.5815>.
- [165] L-H. Gong, C. Tian, W-P. Zou, N-R. Zhou, Robust and imperceptible watermarking scheme based on Canny edge detection and SVD in the contourlet domain, *Multimedia Tools and Applications*, Vol. 80, Issue 1, pp. 439-461, 2021, <https://doi.org/10.1007/s11042-020-09677-w>.
- [166] Erwin, T. Yuningsih, Detection of blood vessels in optic disc with Maximum Principal Curvature and Wolf Thresholding Algorithms for vessel segmentation and Prewitt Edge Detection and Circular Hough Transform for optic disc detection, *Iranian Journal of Science and Technology, Transactions of Electrical Engineering*, Vol. 45, No. 2, pp. 435-446, 2021, <https://doi.org/10.1007/s40998-020-00367-9>.

- [167] O. Li, P.-L. Shui, Subpixel blob localization and shape estimation by gradient search in parameter space of anisotropic Gaussian kernels, *Signal Processing*, Vol. 171, No. 107495, pp. 1-15, 2020, <https://doi.org/10.1016/j.sigpro.2020.107495>.
- [168] S. Dhar, M. K. Kundu, Accurate segmentation of complex document image using digital shearlet transform with neutrosophic set as uncertainty handling tool, *Applied Soft Computing*, Vol. 61, pp. 412–426, 2017, <https://doi.org/10.1016/j.asoc.2017.08.005>.
- [169] S. Dhar, M. K. Kundu, Interval type-2 fuzzy set and human vision based multi-scale geometric analysis for text-graphics segmentation, *Multimedia Tools and Applications*, Vol. 78, No. 16, pp. 22939-22957, 2019, <https://doi.org/10.1007/s11042-019-7649-6>.
- [170] J. D. Bodapati, U. Srilakshmi, N. Veeranjanyulu, FERNet: A Deep CNN Architecture for Facial Expression Recognition in the Wild, *Journal of The Institution of Engineers (India): Series B*, Vol. 103, No. 2, pp. 439-448, 2022, <https://doi.org/10.1007/s40031-021-00681-8>.
- [171] N. Sharma, M. Mishra, M. Shrivastava, Colour image segmentation techniques and issues: an approach, *International Journal of Scientific & Technology Research*, Vol. 1, Issue 4, pp. 9-12, 2012.
- [172] J. M. Toivanen, T. Tarvainen, J.M.J. Huttunen, T. Savolainen, A. Pulkkinen, H. R. B. Orlande, J. P. Kaipio, V. Kolehmainen, Thermal tomography utilizing truncated Fourier series approximation of the heat diffusion equation, *International Journal of Heat and Mass Transfer*, Vol. 108, pp. 860-867, 2017, <http://dx.doi.org/10.1016/j.ijheatmasstransfer.2016.12.060>.
- [173] V. Kolehmainen, J. P. Kaipio, H. R. B. Orlande, Reconstruction of thermal conductivity and heat capacity using a tomographic approach, *International Journal of Heat and Mass Transfer*, Vol. 50, Issues 25–26, pp. 5150-5160, 2007.
- [174] M. Çarıkçı, F. Özen, A face recognition system based on Eigenfaces Method, *Procedia Technology*, Vol. 1, pp. 118-123, 2012.
- [175] M. Slavković, D. Jevtić, Face recognition using Eigenface approach, *Serbian Journal of Electrical Engineering*, Vol. 9, No. 1, pp. 121-130, 2012, doi: 10.2298/SJEE1201121S.
- [176] M. Kundu, P. K. Kundu, S. K. Damarla, *Chemometric Monitoring: Product Quality Assessment, Process Fault Detection and Applications*, CRC Press, 2018.
- [177] L. Sirovich, M. Kirby, Low-Dimensional Procedure for the Characterization of Human Faces, *Journal of the Optical Society of America A*, Vol. 4, pp. 519-524, 1987.

- [178] M. Turk, A. Pentland, Eigenfaces for Recognition, *Journal of Cognitive Neuroscience*, Vol. 3, No. 1, pp. 71-86, 1991.
- [179] K. L. Elmore, M. B. Richman, Euclidean distance as a similarity metric for Principal Component Analysis, *Monthly Weather Review*, American Meteorological Society, Vol. 129, pp. 540-549, 2001.
- [180] L. Wang, Y. Zhang, J. Feng, On the Euclidean Distance of images, *IEEE Transactions on Pattern Analysis and Machine Intelligence*, Vol. 27, No. 8, pp. 1334-1339, 2005.
- [181] W. J. Krzanowski, Between-groups comparison of principal components, *Journal of American Statistical Association*, Vol. 74, pp. 703-707, 1979.
- [182] N. A. Putri, A. P. U. Siahaan, F. Wadly, Muslim, Image similarity test using Eigenface calculation, *International Journal of Scientific Research in Science and Technology*, Vol. 3, Issue 6, pp. 510-514, 2017.
- [183] K. Yang, C. Shahabi, A PCA-based Similarity measure for Multivariate time series, *Proc. 2nd ACM international workshop on Multimedia databases*, pp. 65-74, USA, 2004, <https://doi.org/10.1145/1032604.1032616>.
- [184] A. D. Calvillo, R. A. Vazquez, J. Ambrosio A. Waltier, Face Recognition Using Histogram Oriented Gradients, *Intelligent Computing Systems, Proc. 1st International Symposium Proceedings (ISICS 2016)*, Vol. 297, 2016, https://doi.org/10.1007/978-3-319-30447-2_11.
- [185] P. Carcagni, M. D. Coco, M. Leo, C. Distanto, Facial expression recognition and histograms of oriented gradients: a comprehensive study, *SpringerPlus* 4:645, 2015, doi: 10.1186/s40064-015-1427-3.
- [186] H-C. Kim, D. Kim, S. Y. Bang, Face recognition using the mixture-of-eigenfaces method, *Pattern Recognition Letters*, Vol. 23, Issue 13, pp. 1549–1558, 2002, [https://doi.org/10.1016/S0167-8655\(02\)00119-8](https://doi.org/10.1016/S0167-8655(02)00119-8).
- [187] H-C. Kim, D. Kim, S. Y. Bang, S-Y. Lee, Face recognition using the second-order mixture-of-eigenfaces method, *Pattern Recognition*, Vol. 37, Issue 2, pp. 337–349, 2004, [https://doi.org/10.1016/S0031-3203\(03\)00227-9](https://doi.org/10.1016/S0031-3203(03)00227-9).
- [188] O. Chapelle, P. Haffner, V. Vapnik, SVMs for Histogram Based Image Classification, *IEEE Transactions on Neural Networks*, 1999.
- [189] M. Blachnik, J. Laaksonen, Image Classification by Histogram Features Created with Learning Vector Quantization, *Proc. International Conference on Artificial Neural Networks-ICANN 2008, Lecture Notes in Computer Science book series*, Vol. 5163, pp. 827-836, 2008, https://doi.org/10.1007/978-3-540-87536-9_85.

- [190] W. Voravuthikunchai, B. Crémilleux, F. Jurie, Histograms of Pattern Sets for Image Classification and Object Recognition, Proc. 2014 IEEE Conference on Computer Vision and Pattern Recognition, pp. 224-231, USA, 2014, doi: 10.1109/CVPR.2014.36.
- [191] M. H. A. Hijazi, F. Coenen, Y. Zheng, Image Classification Using Histograms and Time Series Analysis: A Study of Age-Related Macular Degeneration Screening in Retinal Image Data, Proc. Industrial Conference on Data Mining (ICDM 2010), Advances in Data Mining. Applications and Theoretical Aspects, Lecture Notes in Computer Science, pp. 197–209, Vol. 6171, 2010, https://doi.org/10.1007/978-3-642-14400-4_16.
- [192] A. F. Abate, S. Barra, L. Gallo, F. Narducci, Kurtosis and skewness at pixel level as input for SOM networks to iris recognition on mobile devices, Pattern Recognition Letters 91, pp. 37–43, 2017, <https://doi.org/10.1016/j.patrec.2017.02.002>.
- [193] A.A. Tamimi, O.N. A. Al-Allaf, M.A. Alia, Eigen Faces and Principle Component Analysis for Face Recognition Systems: A Comparative Study, International Journal of Computers & Technology, pp. 5650-5660, Vol. 14, No. 4, 2015.
- [194] N. Pandey; P. K. Yadav; K.P. Arjun, Face Recognition System Using Computational Algorithms, IEEE 2nd International Conference on Advance Computing and Innovative Technologies in Engineering (ICACITE), India, 2022, <https://doi.org/10.1109/ICACITE53722.2022.9823568>.
- [195] C. Annubaha, A. P. Widodo, K. Adi, Implementation of eigenface method and support vector machine for face recognition absence information system, Indonesian Journal of Electrical Engineering and Computer Science, pp. 1624~1633, Vol. 26, No. 3, 2022, <https://doi.org/10.11591/ijeecs.v26.i3.pp1624-1633>.
- [196] H. Choi, J. Park, Y-M. Yang, A Novel Quick-Response Eigenface Analysis Scheme for Brain–Computer Interfaces, Sensors 2022, 22, 5860. <https://doi.org/10.3390/s22155860>.

